Florian Wieser, BSc

# Development of procedures to improve the quality of 13C-enriched internal standards typically used in metabolome analysis.

**MASTER'S THESIS**

to achieve the university degree of

Diplom-Ingenieur

Master's degree programme: Biomedical Engineering

submitted to

**Graz University of Technology**

Supervisor

Dipl.-Ing. Dr.nat.techn. Univ.-Doz. Mario Klimacek

Institute of Biotechnology and Biochemical Engineering

Graz, September 2019

## AFFIDAVIT

I declare that I have authored this thesis independently, that I have not used other than the declared sources/resources, and that I have explicitly indicated all material which has been quoted either literally or by content from the sources used. The text document uploaded to TUGRAZonline is identical to the present master‘s thesis.

Date

Signature

# Abstract

Analysis of intracellular metabolites constitutes an important tool used in all human- and bio-sciences to study cellular metabolims at molecular level. Metabolomic studies are commonly performed using chromatographic separation methods coupled to mass-spectrometry analytics. A crucial prerequisite to obtain accurate and reliable "intracellular data" is internal standardization. Typically, a mixture of compounds labelled with a stable isotope like $^{13}C$ is used as internal standard. In the past internal standards were produced commonly by *in vivo* labelling of various organisms. Nevertheless, commercially available products are still rare and expensive. Furthermore, these products do not cover the entire spectrum of metabolites and the stable isotope labelling of several components still remains incomplete.

To this end, in this master thesis three approaches were investigated: To increase the portion of completely labelled compounds, the production of the internal standard in *Scheffersomyces stipitis* was performed in serial cultivations. In order to keep possible $^{12}C$-contaminations as low as possible, unlabelled vitamins and trace elements were replaced by a self-made yeast extract. Additionally, co-cultivation with labelled sodium carbonate was performed to further increase the labelling of metabolites of $CO_2$-consuming pathways. Furthermore, matrix effects were reduced for more reliable mass spectrometry analysis.

A subsequently performed targeted metabolomics study showed that particularly several vitamins and metabolite storage pools are entirely labelled applying the introduced approaches.



**Keywords**: Metabolomics, internal standardization, liquid chromatography - mass spectrometry, $^{13}C$-labelled yeast extract, *Scheffersomyces stipitis*.

# Kurzfassung

Die Analyse intrazellulärer Metabolite stellt ein wichtiges Werkzeug der Human- und Biowissenschaften dar und ermöglicht es den Metabolismus direkt auf molekularer Ebene zu erforschen. Metabolomische Studien werden üblicherweise anhand von Chromatografie gekoppelter Massenspektrometrie durchgeführt. Eine wesentliche Vorraussetzung um genaue und zuverlässige "intrazelluläre Daten" zu erhalten, ist die interne Standardisierung. Als interner Standard wird üblicherweise eine mit stabilen Isotopen (z.B. $^{13}C$) markierte Mixtur aus den zu analysierenden Komponenten verwendet. In der Vergangenheit wurden interne Standards häufig mittels *in vivo* Markierung diverser Organismen hergestellt. Kommerziell erhältliche Produkte sind allerdings immer noch selten und zudem teuer in der Anschaffung. Weiters decken die Produkte nicht das vollständige Spektrum an Metaboliten ab und die Markierung vieler Komponenten ist noch immer unvollständig.

Aus diesem Grund wurden in dieser Masterarbeit die drei folgenden Ansätze untersucht: Um den Anteil komplett durchmarkierter Metabolite zu erhöhen, wurde die Herstellung des internen Standards in *Scheffersomyces stipitis* seriell durchgeführt. Zu dem Zweck mögliche $^{12}C$-Kontaminationen gering zu halten, wurden unmarkierte Vitamine und Spurenelemente durch einen selbst hergestellten Hefeextrakt ersetzt. Zusätzlich wurde eine Co-Kultivierung mit markiertem Natriumcarbonat durchgeführt, um die Markierung der Metabolite aus den $CO_2$-konsumiernden Stoffwechselwegen zu erhöhen. Weiters wurde die Zuverlässigkeit der massenspektroskopischen Analytik durch Reduktion von Matrixeffekten erhöht.

In einer darauffolgenden metabolomischen Studie konnte gezeigt werden, dass sich die genannten Ansätze speziell zur Durchmarkierung bestimmter Vitamine und einiger Metabolitspeicher eignet.

**Schlüsselwörter**: Metabolomik, interne Standardisierung, Flüssigkeitschromatography-Massenspektrometrie, $^{13}C$-markierter Hefeextrakt, *Scheffersomyces stipitis*.

# Acknowledgement

First and foremost, I want to thank my thesis advisor Priv.-Doz. Dipl.-Ing. Dr.nat.techn. Mario Klimacek for providing me this topic, for the excellent supervision and the continuous support during my time in the lab and the writing process of this master thesis. The door to Prof. Klimaceks office was always open whenever questions about my research arose, he kept motivating me with helpful remarks, engagement and profound knowledge.

I would also like to thank Univ.-Prof. Dipl.-Ing. Dr.techn. Bernd Nidetzky, who provided me an opportunity to make my master thesis at the Institute of Biotechnology and Biochemical Engineering (I.B.B.) at Graz University of Technology.

Special thanks also goes to Joanneum Research Forschungsgesellschaft mbH Graz, which enabled this work by giving me access to their laboratory and research facilities. Herby I want also to thank Dipl.-Ing. Elmar Zügner and Dipl.-Ing. Gert Trausinger of the Health department for conducting the LC/MS measurement and their helpful support.

I would also like to extend my gratitude to Wirtschaftskammer Steiermark for honouring me with one of their research fellowships.

Furthermore, I would like to thank the following people for their support:

Adnan Fojnica for the many amusing hours we have spent in the lab and the friendship gained.

Karin Longus and Margaretha Schiller for their help and assistance in the laboratory.

All the members of the I.B.B. for their helpful support and the great working atmosphere.

Finally, I want to express sincerest thanks to my family, for enabling me to study and providing me with unfailing support through my entire life.

# List of abbreviations

## Miscellaneous

| | |
|---|---|
| $^{13}$C-ER | $^{13}$C-enrichment |
| ACP | Acyl carrier protein |
| ANOVA | Analysis of variances |
| BEF | Baffled Erlenmeyer flask |
| $dH_2O$ | Distilled water |
| EC | Enrichment culture |
| EDTA | Ethylenediaminetetraacetic acid |
| ES | Extraction solution |
| ESI | Electrospray ionization |
| fMM | Final mineral medium |
| HPLC | High performance liquid chromatography |
| I.B.B. | Institute for Biotechnology and Biochemical Engineering |
| LC-MS | Liquid chromatography-mass spectrometry |
| MC | Main-culture |
| MM | Mineral medium |
| MS | Mass spectrometry |
| NMR | Nuclear magnetic resonance |
| $OD_{600}$ | Optical density at 600 nm |
| $OD_{850}$ | Optical density at 850 nm |
| PC | Pre-culture |
| PEG3350 | Polyethylene glycol 3350 |
| PEG8000 | Polyethylene glycol 8000 |
| PEG20000 | Polyethylene glycol 20000 |
| PRPP | Phosphoribosyl pyrophosphate |
| QC | Quality control |
| RSE | Relative standard error |
| rpm | Rounds per minute |
| QS | Quenching solution |
| SFA | Serial fermentation approach |
| SIL | Stable-isotope-labelled |
| SMYE | Self-made yeast extract |
| S. stipitis | Scheffersomyces stipitis |
| TCA | Tricarboxylic acid cycle |
| TE | Trace elements |
| YPD | Yeast peptone dextrose |

## Metabolites

| | |
|---|---|
| AMP | Adenosine monophosphate |
| CoA | Coenzyme A |
| GMP | Guanosine monophosphate |
| IMP | Inosine monophosphate |
| NAD+ | Nicotinamide adenine dinucleotide+ |
| NADH | Nicotinamide adenine dinucleotide |
| PI | Phosphatidylinositol |
| UMP | Uridine monophosphate |

# Table of Contents

# 1 Introduction

## 1.1 Metabolomics

Metabolomics is an upcoming scientific field which attempts to systematically identify and quantify endogenous metabolites from biological samples. Metabolites represent a diverse group of intermediate products of metabolism and include small molecules (<1.5 kD) like peptides, amino acids, nucleic acids, carbohydrates, organic acids, vitamins, polyphenols, alkaloids as well as inorganic species [1]. The sum of all metabolites present in a cell is defined as the metabolome. These metabolites are participants in metabolic reactions and are required for maintenance, growth and normal function of the cell [2, 3]. Depending on the organism, the size of the metabolome varies widely between a few hundreds up to thousands of molecules. While it was estimated that a *S. cerevisiae* cell contains approximately 600 metabolites [4], for example, cells of higher organisms like plants include already about 200.000 metabolites [5]. Additionally, the concentrations of the respective metabolites of the metabolome vary considerably (7-9 magnitude, pM-mM) [6].
After genomics, proteomics and transcriptomics, metabolomics is the latest of the omics technologies. While the genome, proteome and transcriptome are connected directly to gene expression, the metabolome offers additionally an instant snapshot of the cells physiological condition. The metabolome provides information which is directly linked to the phenotype, molecular physiology and function of cells (depicted by Figure 1).

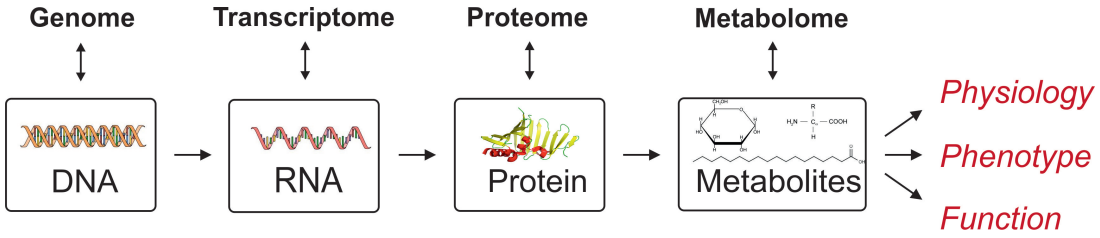


**Figure 1:** The role of metabolomics and its context to the other omics technologies.

Hence, metabolomics has become a powerful tool for a broad range of applications in various fields of human- and bio-sciences, including biotechnology, medical sciences, predictive modeling of plant, animal and microbial systems as well as food sciences [7].
Depeding on the number of adressed metabolites, a distinction is made between a targeted and an untargeted metabolomics experiment. While earlier studies have focused on the measurement of pre-selected specific groups of compounds (targeted metabolomics), the rise of nuclear magnetic resonance (NMR) spectroscopy or mass spectrometry (MS) based methodologies have enabled untargeted metabolomics, which intends to capture all measureable compounds, including chemical unknowns (meta- bolic fingerprinting, metabolic footprinting) [8].
Additionally, metabolome studies can be cateogrized in metabolite profiling and quantitative metabolomics. Metabolite profiling deals about measuring the fingerprint of biochem-

ical perturbations caused by environment, deseases or drugs [9]. It has also been successfully applied in the description of cell phenotypes and the identification of biomarkers for different strains, tissues and growth conditions. In contrast, quantitative metabolomics is able to determine dynamic metabolite pool sizes and has become therefore increasingly important in the elucidation of *in vivo* reaction kinetics, metabolic modeling and fluxome analysis [10].
One subdomain of metabolomics is the rather new field of fluxomics, where metabolic network models are established by combining the information of quantified metabolic fluxes with typical contraints like uptake and excretion rates, reaction reversibilities and maximum flux capacities. Determinatin of fluxes has proven to be useful for the determination of enzyme functions, the identification of regulatory mechanisms in response to environmental perturbations and as a tool in metabolic engineering. Recently these models also consider thermodynamic information. Here statements on the feasibility of reaction fluxes or flux distributions can be made based on calculating changes in Gibbs energy using metabolite concentrations [11].

## 1.2 Practical applications of metabolomics

In the following, prominent examples of various scientific disciplines where metabolomics has been successfully applied will be described.
In biotechnology, most of the microbial-produced products are secondary products of metabolism, which means that they are not linked directly to the primary metabolism neither to the growth rate. Though, the primary central carbon metabolism provides precursors, cofactors as well as ATP - all essential for the formation of secondary products. Hence, the understanding of the primary cellular metabolism and its *in vivo* regulation are crucial to overcome bottlenecks of microbial cell factories. Thus, metabolomics data could help to develop strategies to manipulate the metabolism of microbial cell factories for increased product yields [12].
In medical sciences, metabolomics in combination with pattern recognition techniques are consulted to monitor metabolic changes in subjects related to diseases. Thereby new biomarkers specific for the respective desease can be discovered and developed. Furthermore, implications of medical interventions can be investigated directly on a molecular level. Thus, metabolomics has become a future promising tool for the prognosis, the diagnosis and for a better understanding of pathophysiological processes in diseases with an heterogenous nature like cancer [13].
Metabolomics has also bee successfully applied to plants and animals. While microbes are the richest overall source of metabolites, plants are the source of the most complex individual mixtures and therefore also valuable organisms for metabolic engineering [14]. The deeper understanding of plant physiology and biology will contribute to develop better crops with improvements in yield and quality [15]. In animal metabolomics, studies

with several model organisms including zebra fish, fruit fly and nematode have given a wealth of novel information on physiological, developmental and pathological processes, which can be applied to research in other organisms [7].
Improvements in methodology and data handling will lead to an even broader range of applications and will hence contribute to a comprehensive understanding of systems biology.

## 1.3 Analytical platforms for metabolomics

Metabolome analysis remains still challenging because unlike the genome or transcriptome, the analytical platforms have to deal with a highly diverse group of various metabolites [16]. Though, there was a rise of metabolomic studies in recent years, which was mainly fueled by the development of sensitive high-throughput methods like MS [17]. Todays modern high-tech analytical protocols include mainly chromatographic separation methods like gas chromatography (GC), high performance liquid chromatography (HPLC), ultra performance liquid chromatography or capillary electrophoresis, coupled to analytical techniques like NMR or MS [1, 12]. While NMR is non-destructive and has the potential to determine real-time metabolite concentrations of living cells, nonththeless, MS-based approaches are more common due to the high sensitivity and the possibility to detect a much broader range of metabolites in one run [18]. These techniques have the potential to analyse tens to hundreds of metabolites in biological samples within minutes [1, 19]. Nevertheless, due to the physical and chemical diversity of the metabolome, still no single analytical platform has been developed to detect all metabolites within a biological sample [1]. Comprehensive metabolomic studies require therefore the parallel application of different analytical platforms e.g. GC-MS, HPLC-MS and NMR [1, 16]. The choice of a methodology represents always a compromise between chemical selectivity, sensitivity and measuring speed and is therefore strongly depending on the application [20].

### 1.3.1 LC coupled to MS

Due to its applicability to a broad range of metabolite classes and its high sensitivity, liquid chromatography coupled to mass spectrometry (LC-MS) constitutes todays most widely applied analytical protocol [21, 22]. In constrast to GC-MS, LC-MS benefits from a simpler sample preparation as no metabolite derivatization is required [6]. LC-MS includes separation of analytes by LC, followed by ionisation driven by electrospray ionisation (ESI) or less common, atmospheric pressure chemical ionisation (APCI) and subsequent detection and identification by MS [6]. The phase chemistry and dimension of the LC column greatly influences the nature of metabolites that can be investigated and will affect also the resolution and sensitivity of the measurement [6, 22]. ESI can be performed either in positive or negative ionization mode. Since metabolites are generally detected in only one mode, metabolite coverage can be considerably increased if the experiment is performed in

both modes. In general, derivatization of samples is not required, but can help – depending on the sample – to increase the chromatographic resolution and sensitivity or to make previously non-ionizable metabolites ionizable for ESI [6]. Tandem MS is characterized by the rapid, sensitive and selective qualitative and quantitative measurement of numerous metabolites. Its main advantage over NMR-based techniques constitutes its sensitivity for various analytes even at low concentration levels (μM) [1, 6, 23]. In the mass analyzer itself, the ionized analytes will produce specific peak patterns (fingerprints), which allow the identification of metabolites [23]. It should be characterized by a high accuracy, resolution and acquisition speed for untargeted metabolomic studies. These techniques include time-of flight and fourier transform-based MS using orbitrap. In targeted metabolomic studies, mass analyzers with high sensitivity and dynamic range like quadrupole platforms or tandem platforms as quadrupole-TOF, are of interest [21]. For global metabolomic studies LC-ESI/MS has proven to be appropriate for the quantification of metabolites of primary metabolic pathways, like phosphorylated carbon compounds [24].

### 1.3.2 Current limitations of LC-ESI/MS

Although LC-ESI/MS is superior over other analytics for comprehensive studies, its accuracy and especially reliability within or between different measurements is still limited. These inacuracies are known to be caused primilary by ion suppression or enhancement in the electrospay ionization source [6, 25, 26]. For ion suppression or enhancement itself, various interactions between the analytes of interest and the co-eluting sample matrix are held responsible – the so-called matrix effects. These effects have been traced to mechanisms including the competition between analyte and matrix, or even between two co-eluting analytes for charges. Another mechanism constitutes the viscosity or surface tension modification of the electrospray droplets by components of the matrix or by co-eluting analytes. Since a standard is not affected by a matrix, the analyte of interest and the standard will hence give different responses [25, 27]. An evaluation of ion suppression effects necessitates extensive standard addition protocols for each component and is thus, critically impairing the applicability of LC-ESI/MS [24]. To overcome these and other problems with environmental changes of the LC/MS system (mobile phase gradient flow, column efficiency deterioration, temperature fluctuation, mass detector noise etc.) isotope-labelled internal standards are routinely used nowadays [28]. A detailed description of internal standardization will be given later in Section 1.5.
Furthermore, it was found out that high amounts of divalent salts arising from the sample matrix, mainly phosphate and sulfate, can lead to non-linearty of calibration curves and therefore adversely impact the accuracy of analysis. This consideration constitutes a superposition of ion suppression and space charge effects inside the orbitrap, as Lu et al. supposed [29]. Also in a previous study at the Institute of Biotechnology and Biochemical Engineering (I.B.B.) with the same analytics applied was encountered with this issue

and highlighted the resulting non-linearity. In one of these studies the concentrations of anorganic salts were lowered either from the start, by lowering the amounts of salty compounds in the cultivation medium, or by introducing an additional washing step during the sample preparation [30].

## 1.4 Workflow of LC/MS based metabolomic studies

A workflow of a typical metabolome study is depicted in Figure 2: At first samples are transferred at a predefined physiological state to a quenching solution (QS) in order to freeze the level of metabolites by inactivating enzyme activities and chemical reactions. Metabolites are obtained from the inside of the cell using one of several cell extraction methods. Extracted metabolites are then subjected to LC-MS analysis and resultant signals are assigned qualitatively (mass and retention time for compound identity) and quantitatively (signal strength, integrated peak area or peak height) to corresponding metatoblites. Eventually, the obtained LC-MS data set is then processed and analyzed by applying appropriate (driven by the objective of the study) univariate and multivariate statistics. In the following common steps of the sample preparation, their alternatives as well as their downsides will be elucidated in more detail.

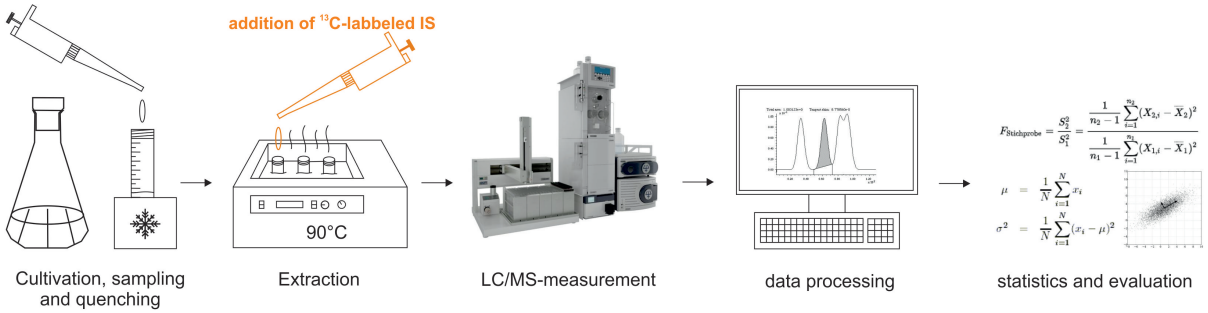


**Figure 2:** The major steps of present metabolome studies using LC/MS based techniques. Online source of MS image: www.gilson.com.

### 1.4.1 Sampling

In a metabolomics experiment, the process of sampling aims at gathering a picture or a snapshot of the metabolomic state at the level of intracellular metabolites at a specific point of time. Both, the time and the method of sampling can have a substantial influence at the reproducibility of analytical samples [6]. The sampling time is defined as the time necessary to transfer the cells from their culture environment into the quenching solution. Keeping this time as low as possible is crucial, since the metabolome can change very rapidly in response to altered environmental conditions such as $pO_2$ and temperature fluctuations, osmotic stress, nutrition depletion or exposion to light [31, 32].

### 1.4.2 Quenching

Quenching is a substantial step that aims at inactivating enzymes and maintain the metabolite levels in the cell as good as possible. Hence, queching in combination with the former sampling process should be performed as fast as possible [33]. Todays most widely applied quenching methods for micro organisms comprise fast and direct sampling into liquid nitrogen (–196 °C) [34], 60 % (v/v) methanol solution (–40 °C) [35] and glycerol-saline (–23 °C) [36]. Due to its efficiency, the usage of cold methanol as quenching solution (QS) represents so far the gold-standard. However, studies with different methanol concentrations have shown that the membrane of yeasts and bacterial cells are actually vulnerable to cold methanol solution and leakage of intracellular metabolites may occur [36, 37]. To overcome this issue, Canelas et al. suggested the usage of a 100 % methanol solution. They reported this method produces significantly less leakage of intracellular compounds [17]. The same leakage can arise by using liquid nitrogen, due to the formation of ice crystals [33]. So far, no quenching method offers a perfect metabolite coverage without occurrence of any leakage. Therefore, the method must be chosen with respect to the cellular system and culture medium deployed and of course, depending on the nature of the analytes of interest [33].
Previous studies at the I.B.B. were based on a protocol (pure methanol, –80 °C) according to Canelas et al. [17]. The application of methanol suffers from the requirement of big amounts of poisonous methanol and the rather elaborate and expensive disposal of the same. Hence, in the course of a project conducted at the I.B.B., ice-cold buffered physiological salt solution was tested as an alternative. As this study did not indicate a decrease of analysis accuracy, also in this thesis saline will be deployed as QS.

### 1.4.3 Extraction

The ideal extraction method has three crucial requirements: Firstly, the extraction has to be complete, i.e. all metabolite pools have to be accessible for the subsequent analysis. Secondly, enzymes must be entirely inactivated in order to impede possible metabolite conversions during extraction and thirdly, metabolites should not be degraded by the extraction process itself [17]. Furthermore, care must be taken to keep matrix effects as low as possible with the applied extraction solution (ES). The most prominent extraction methods were evaluated in 2009 by Canelas et al., which include ES like hot water [37], boiling ethanol [38], chloroform/methanol [39], freeze-thawing in methanol [40] and acidic acetonitrile/methanol [41]. In a metabolite extraction study with *S. cerevisiae* they found the best performance for boiling ethanol and chloroform/methanol, both with high efficacies and excellent metabolite recoveries. The usage of hot water as ES led to an overestimation of several metabolite pools, freeze-thawing in methanol does not ensure complete enzyme inactivation and acenotrile-methanol was inferior due to yet unknown reasons [17].

### 1.4.4 Problems regarding the steps of the sample preparation

Because of the instability of a broad range of intracellular metabolites and severe conditions applied during the steps of the sample preparation (e.g. high temperature and acidity), metabolite degradation and subsequently metabolite loss can occur. Hence, time-consuming sample processing procedures with elaborate recovery determination of each metabolite of interest would be necessary. Additionally, steps of the sample preparation include multiple manual handling steps, which are prone to operator-to-operator and run-to-run variations [24]. To compensate for metabolite losses during the steps of the sample preparation, as well as the afore-mentioned matrix effects and other issues which impair the ioniziation efficiency of the MS, stable isotope-labelled (SIL) internal standards are commonly applied.

## 1.5 Internal standardization

In general, internal standardization constitutes a method to improve the accuracy of quantitative analysis. An internal standard is a chemical substance that shows similar behaviour as the analyte of interest and is – in contrast to an external standard – added in a constant amount directly to the samples (depicted orange in Figure 2), the blank and the calibration standards [42]. Despite the required high similarity between the IS and the analyte of interest, still both must be distinguishable in at least one way by the methodology (mass in MS) [43]. In metabolomics, the chemical and physical properties of the metabolites and the internal standard are almost identical and differ only in mass. Hence both are believed to be effected analogous by the steps of the sample preparation and matrix effects.

The ratio of the analyte of interest to the internal standard constitutes the basis for accurate metabolite quantification: Since it is assumed, that both components are effected in the same way by the whole analytical process, the signal ratio of the analyte and the internal standard should remain constant – regardless what may have occured along the steps of the sample preparation [28, 42]. This ratio can then be applied to obtain the analyte concentration from a calibration curve: The general calibration function for internal stadardization is depicted in equation 1. The slope $b_1$ and offset $b_0$ must be determined in advance experimentally. As the applied concentration of internal standard is known, the resulting analyte to internal standard ratio allows to calculate the analyte concentration of interest (see equation 2).

In contrast to external standardization, with the application of internal standardization each metabolite concentration is quantified relatively to the concentration of the internal standard. Hence, the afore-mentioned drawbacks of LC-ESI/MS and metabolite loss during the steps of the sample preparation are inherently eliminated [43].

$$\boxed{\frac{A_a}{A_{IS}} = b_0 + b_1 \frac{c_a}{c_{IS}}} \tag{1}$$

$$\boxed{c_a = \frac{c_{IS} \cdot (\frac{A_a}{A_{IS}} - b_0)}{b_1}} \tag{2}$$

| | | |
|---|---|---|
| $A_a$ | *Peak area of analyte* | [1] |
| $A_{IS}$ | *Peak area of internal standard* | [1] |
| $c_a$ | *Concentration of analyte* | $[\frac{g}{L}]$ |
| $c_{IS}$ | *Concentration of internal standard* | $[\frac{g}{L}]$ |
| $b_0$ | *Offset of calibration function* | [1] |
| $b_1$ | *Slope (sensitivity)* | [1] |

### 1.5.1 SIL internal standards

In metabolome studies SIL internal standards are more and more often applied and have the potential to become the gold standard [44]. Stable isotopes mimic the physical and chemical properties of the related metabolites of interest almost perfectly, but differ in mass due to a difference in the number of neutrons and can therefore be distinguished by MS [18, 43, 45]. Generally applicable isotopes include $^{13}$C, $^{15}$N, $^{34}$S, $^{2}$H and $^{18}$O. While $^{15}$N and $^{34}$S are well suited for investigations of nitrogen and sulfur-containing compounds and their bio-transformation in living systems, $^{2}$H and $^{18}$O are seldomly used, since they are easily exchanged by hydrogen and oxygen of the surrounding water [25]. Carbon on the contrary, occurs naturally as a component in every metabolite and can easily be supplied by pure carbon sources to synthetic defined media for microbes or in the form of carbon dioxide to photosynthetic organisms [16]. This and the chromatographical perfect co-elution of $^{13}$C-labelled metabolites and their non-labelled analogues, have helped $^{13}$C to become by far the most frequently applied isotope in comprehensive metabolomic studies [25]. Different types of $^{13}$C-glucose in terms of which C atoms are labelled within the glucose molecule, exist. While for studies that require extensive labelling uniformly labelled $^{13}$C is suggested, for detailed analysis of central carbon metabolism e.g. $^{13}$C-1,2-glucose may be more appropriate [18].

### 1.5.2 Current production of SIL internal standards

Since spiking each $^{13}$C-labelled component solely is laborious and expensive, the production of SIL internal standards for all-embracing quantification studies is recently achieved by *in vivo* labelling of micro organisms as yeast or bacteria and plants [16]. This idea was

originally introduced by Mashego et al. by feeding *S. cerevisiae* with uniformly labelled $^{13}$C-glucose in chemostat culture. They demonstrated that 80 percent of metabolites are already completely labelled after one hour. This approach was further improved by Wu et al., where they overcame the loss of expensive $^{13}$C-glucose by application of fed-batch culture and furthermore increased accuracy of results [24, 43]. However, provision of fully labelled carbon sources is only reasonable in cells which can be cultivated in simple fully defined media. In general, cells for the production of SIL internal standards should ideally come from the same species as the samples of interest to ensure a matching metabolite coverage [18]. The organism is then cultivated to - theoretically - hundred percent $^{13}$C-enrichment ($^{13}$C-ER) of all metabolites [16, 43].
Since common vitamin stocks contain unlabelled components, Wu et al. restricted the vitamin supplementation to vitamins that are essential for growth in yeast (0.05 g/L biotin, 1 g/L thiamine [24]). However, this restriction might alter metabolite concentrations of vitamin depending pathways and could therefore decrease the quality of a resulting SIL internal standard. Another experimental problem constitutes the naturally $^{12}$C-$CO_2$ content of the air, which could introduce $^{12}$C carbon in metabolites by carboxylation reactions. Wu and Mashego et al. addressed this problem by filtering the air with KOH solution [24] or silica and NaOH [43].
However, although this constitutes so far the most promising approach for accurate metabolome quantification, it still suffers from several issues: Firstly, as Mashego et al. reported, the short labelling period of 4 h ($\sim$ 2 generations) has led to an insufficient replacement of unlabelled metabolites in certain metabolite pools (particularly adenine and pyridine nucleotides). The authors traced this back to the relatively slow turnover of metabolite storage pools. Even though, it is possible to correct the insufficient labelling afterwards mathematically, it increases the computational effort and the applied substraction increases error of results [43]. Secondly, the commercial availability of $^{13}$C-labelled metabolit extracts is still limited and purchase is associated with high costs [25, 43]. And thirdly, the metabolite coverage is still incomplete - available internal standards do not cover the full spectrum of target metabolites. An online research found just two companies (ISOtopic solutions[1], Vienna; Isolife[2], Wageningen (NL)) which are specialised in the production and marketing of comprehensive SIL internal standards for metabolome quantification. The internal standards of ISOtopic solutions cover, according to their own statements, hundreds of metabolites. They sell 15 mg of labelled *Pichia pastoris* dry cell extract for 600 euro. Isolife, which are specialized on the production of internal standards on plant basis, offer 0.1 g of labelled broccoli flower cell extract for 1060 euro.
To overcome the remaining drawbacks of internal standards, as well as the afore-mentioned limitations of the LC/MS analysis and the steps of the sample preparation, a protocol based on serial fermentation was established in this thesis.

[1] www.isotopic-solutions.com
[2] www.isolife.nl

## 1.6 Outline of this master thesis

With respect to the limitations of currently commercially available internal standards, the following major goals were defined: Firstly, the $^{13}$C-ER per metabolite should be increased. Secondly, the spectrum of labelled metabolites should be extended. And thirdly, the production process of internal standards should be made cheaper. Furthermore, the protocol for keeping divalent salts and ions arising from the sample matrix introduced by Trausinger et al. should be improved and adapted for cultivation in Erlenmeyer flasks.

In order to achieve the four stated goals the following sub-objectives were defined:

- Growth characterization of *P. stipitis*.
- Improvement of the medium composition for the purpose of serial fermentation.
- Reduction of salts in the sample matrix for LC-ESI/MS.
- Establishment of a serial fermentation working routine, including quenching, extraction and lyophilization in terms of handling and time management.
- Twofold execution of the SFA with three sub-experiments each for a duration over ten days.
- Analysis of gathered samples at Joanneum Research Health using LC-ESI/MS.
- Data processing including outlier-handling, trend correction and normalization steps.
- Data analysis based on appropriate uni and multivariate statistics and final evaluation of the stated hypothesis.

Three hypothesis were stated, which shall on the one hand, increase the $^{13}$C-ER of each metabolite and on the other hand, lead to a broader metabolite coverage:

1.) In contrast to earlier approaches for *in vivo* $^{13}$C-labelling of micro organisms, in this thesis the cultivations will be performed serially. The deployed yeast strain *Scheffersomyces stipitis* will be cultivated on $^{13}$C-labelled glucose substrate to a defined cell density. The resulting (partial) $^{13}$C-labelled cells will then be used as inoculum for a new cultivation on $^{13}$C-labelled glucose substrate. By repeating this procedure for several cycles it is attempted to dilute remaining $^{12}$C-components out.

2.) Unlabelled vitamins and trace elements (TE) will be replaced by a self-made yeast extract (SMYE). This substitution should minimize $^{12}$C-contaminations from the cultivation medium itself and hence additionally support the $^{13}$C-ER of metabolites.

3.) The further addition of $^{13}$C-labelled $Na_2CO_3$ should help to increase the $^{13}$-labelling of metabolites of the $CO_2$-consuming pathways and compete with naturally $^{12}$C-$CO_2$ arising from the air.

The principle of this serial fermentation approach (SFA) including all three hypothesis is depicted in Figure 3: The substitution of vitamins and TE by a SMYE in combination with a serial fermentation on $^{13}$C-labelled glucose substrate should, in theory, dilute out remaining sources of $^{12}$C-contamination and provide biosynthesis of $^{13}$C-labelled metabolites. The SMYE will be produced from the culture to be labelled and fed back in the next cycle of serial fermentation, each time being more enriched with $^{13}$C. For inoculation of the next cycle, the afore labelled cells will be consulted and should therefore be successively further $^{13}$C-ER.

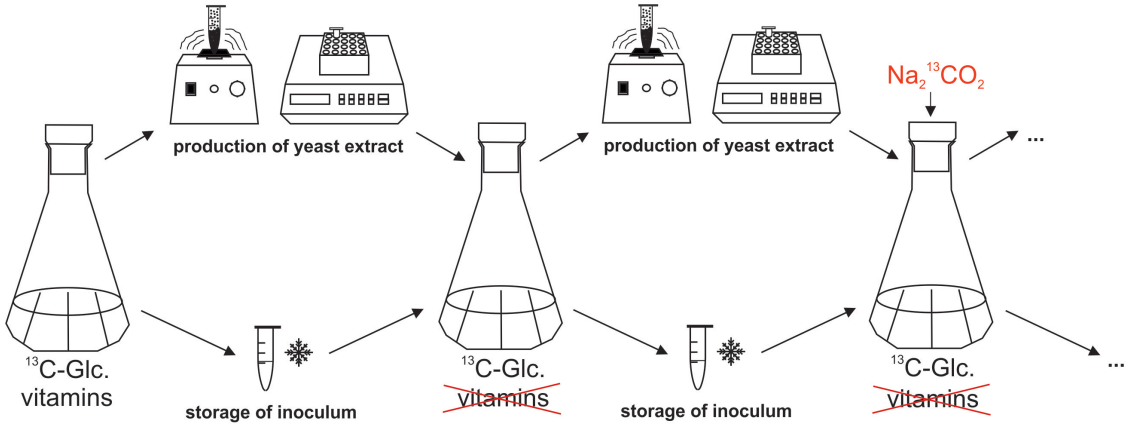


**Figure 3:** The basic strategy of the SFA: Remaining $^{12}$C-fractions are diluted out by fermenting in serial cultivations (hypothesis 1), where vitamins and trace elements are substituted by a SMYE (hypothesis 2). The addition of $^{13}$C-$Na_2CO_3$ (depicted in red) should further increase the $^{13}$C-ER of $CO_2$-consuming pathways (hypothesis 3).

Like in earlier studies on the I.B.B. [30], the analysis of intracellular metabolites will be performed using LC-ESI/MS analytics. In contrast to these studies, where fermentations were carried out in biofermentors, in this thesis all cultivations will be performed in Erlenmeyer flasks. Due to the inability of automated pH-adjustment in Erlenmeyer flasks the above-mentioned measures to reduce the concentration of divalent salts in the sample matrix by Trausinger et al. will be further investigated and adapted for the purpose of serial fermentation in Erlenmeyer flasks.

### 1.6.1 *Scheffersomyces stipitis*

The SFA will be implemented using the yeast strain *S. stipitis*. In the previous studies, conducted by Mashego et al. and Wu et al., the well investigated model organism *S. cerevisiae* was applied for this purpose. In addition to $^{13}$C-glucose, *S. cerevisiae* is also able to incorporate $^{13}$C carbon by utilizing $^{13}$C-ethanol as a substrate (crabtree effect). However, a preliminary study at the I.B.B. rejected the usage of *S. cerevisiae* due to the slow growth rate during ethanol consumption phase, which would highly complicate the experimental time management when fermenting serially.
*S. stipitis* on the other hand, is crabtree negative and known for its high growth rates, making it therefore to an appropriate strain for the purpose of serial fermentation.

# 2 Materials

## 2.1 Instruments and equipment

**Centrifugation**

| | |
|---|---|
| Centrifuge 5804R | Eppendorf AG (Hamburg, Germany) |
| Centrifuge 5810R | Eppendorf AG (Hamburg, Germany) |
| Centrifuge Jouan BR4i | Thermo Fisher Scientific (Waltham, USA) |
| Centrifuge tube 50 mL, 15 mL, 1.5 mL | SARSTEDT AG & Co. (Nürnbrecht, Germany) |
| Centrifuge tube 50 mL, 15 mL | Greiner Bio-One GmbH (Frickenhausen, Germany) |

**Cultivation**

| | |
|---|---|
| Erlenmeyer flask, baffled, 1000 ml, 300 ml | Schott DURAN Produktions GmbH & Co. KG (Main, Germany) |
| Shaker RC-406 | INFORS HT (Bottmingen, Switzerland) |
| Shaking incubator GFL 3033 | GFL Gesellschaft für Labortechnk GmbH & Co. (Burgwedel, Germany) |
| Petri dishes 92x16 mm | SARSTEDT AG & Co. (Nürnbrecht, Germany) |
| Petri dishes 55x15 mm | Carl Roth GmbH +Co. KG (Karlsruhe, Germany) |

**Filters**

| | |
|---|---|
| Polyamide filter Sartolon®, 0.2 µm | Satorius AG (Göttingen, Germany) |
| Syringe filter Minisart®, 0.2 µm | Satorius AG (Göttingen, Germany) |

| | |
|---|---|
| **HPLC/MS system**<br>- HPLC Dionex Ultimate 3000<br>- Autosampler WPS-3000<br>- Solvent rack SRD-3600<br>- Pump LGP-3600 (LPG-3000)<br>- Flow manager FLM-3300<br>- X-calibur software, version 2.2 SP1 | Thermo Fisher Scientific (Waltham, USA) |
| Pre-column KrudCatcher™ULTRA HPLC In-Line Filter, 0.5 µm Depth Filter x0.004 in ID | Phenomenex Inc. (Torrance, USA) |
| Column Atlantis T3C18, 3 µM, 100 A, 150x 2.1 mm | Waters Corporation (Milford, USA) |
| HPLC vials, 200 µL, TopSert TPX-Short Thread Vial, 32x11.6 | VWR (West Chester, USA) |
| Heated electrospray ionization source (HESI) | Thermo Fisher Scientific (Waltham, USA) |
| Mass spectrometer Exactive™ | Thermo Fisher Scientific (Waltham, USA) |

**Pipettes**

| | |
|---|---|
| PeqPETTE, 5 mL | PEQLAB Biotechnologie GmbH |
| Pipette tips, 5 mL | PEQLAB Biotechnologie GmbH |
| Pipette Pipetman neo, 20 µL,200 µL, 1000 µL | Gilson, Inc. (Middleton, USA) |
| Pipette tips, 200 µL, 1000 µL | Greiner, Bio-One GmbH (Frickenhausen, Germany) |

**pH-measurement**

| | |
|---|---|
| pH meter 691 | Metrohm (Herisau, Switzerland) |

**Spectrophotometry**

| | |
|---|---|
| Semi-micro cuvettes, 1.6 mL, layer thickness 10 mm | SARSTEDT AG & Co. (Nürnbrecht, Germany) |
| Spectrophotometer DU800 | Beckman Coulter Inc. (Fullerton, USA) |
| WPA CO8000 Biowave Cell Density Meter | Biochrom (Cambridge, UK) |

**Miscellaneous**

| | |
|---|---|
| −20 °C freezer VF-29 | ELIN GmbH & Co. KG (Linz, Austria) |
| −70 °C freezer Revco ULT1786 | GS Laboratory Equipment (Asheville, USA) |
| −70 °C freezer Herafreeze HFU686 | Heraeus Holding GmbH (Hanau, Germany) |
| Analytical scale A 210P | Satorius AG (Göttingen, Germany) |
| Biological Safety Cabinet EF-A4 | Clean Air Techniek B.V. (Woerden, Netherlands) |
| Dry freezer Alpha 1-4 | Martin Christ Gefriertrocknungsanlagen GmbH (Osterode am Harz, Germany) |
| Glass beads 0.5 mm | Carl Roth GmbH +Co. KG (Karlsruhe, Germany) |
| Paraffine band Parafilm® | Carl Roth GmbH +Co. KG (Karlsruhe, Germany) |
| Table autoclave CertoClav CV-EL | CertoClav Sterilizer GmbH (Traun, Austria) |
| Thermomixer compact | Eppendorf AG (Hamburg, Germany) |
| Thermomixer comfort | Eppendorf AG (Hamburg, Germany) |
| Vortex shaker REAX top | Heidolph Instruments GmbH & Co. KG (Schwabach, Deutschland) |
| Waterbath type 1083, $\leq$ 99 °C | GFL Gesellschaft für Labortechnk GmbH & Co. (Burgwedel, Germany) |

## 2.2 Chemicals

**Table 1:** List of chemicals used.

| | |
|---|---|
| Acetic acid, ≥ 99.0 % | Sigma-Aldrich (St. Louis, USA) |
| Agar-Agar | Carl Roth GmbH +Co. KG (Karlsruhe, Germany) |
| Ammonium acetate, ≥ 98.0 % | MERCK (Darmstadt, Germany) |
| Ammonium molybdate tetrahydrate | Sigma-Aldrich (St. Louis, USA) |
| Biotin, ≥ 99.0 % | Sigma-Aldrich (St. Louis, USA) |
| Calcium pantothenate | MERCK (Darmstadt, Germany) |
| Ethanol, ≥ 99.8 % | VWR (West Chester, USA) |
| Ethanol, ≥ 96.0 % | LACTAN (Graz, Austria) |
| Glucose monohydrate, ≥ 99.5 % | Carl Roth GmbH +Co. KG (Karlsruhe, Germany) |
| Glucose $^{13}C_6$, ≥ 99.0 % | Sigma-Aldrich (St. Louis, USA) |
| Glycerol, ≥ 99.5 % | Carl Roth GmbH +Co. KG (Karlsruhe, Germany) |
| Hydrochloric acid | Carl Roth GmbH +Co. KG (Karlsruhe, Germany) |
| Liquid $N_2$ | Air Liquide Austria GmbH (Graz, Austria) |
| Magnesium sulphate heptahydrate, ≥ 99.0 % | Carl Roth GmbH +Co. KG (Karlsruhe, Germany) |
| Peptone ex caseine | Carl Roth GmbH +Co. KG (Karlsruhe, Germany) |
| Polyethylene glycol 3350 | Merk Schuchard OHG (Hohenbrunn, Germany) |
| Polyethylene glycol 8000 | Sigma-Aldrich (St. Louis, USA) |
| Polyethylene glycol 20000 | Sigma-Aldrich (St. Louis, USA) |
| Potassium dihydrogen phosphate, ≥ 99.0 % | Carl Roth GmbH +Co. KG (Karlsruhe, Germany) |
| Sodium ascorbic acid, ≥ 99.0 % | Carl Roth GmbH +Co. KG (Karlsruhe, Germany) |
| Sodium carbonate, ≥ 99.5 % | Sigma-Aldrich (St. Louis, USA) |
| Sodium carbonate $^{13}C$, ≥ 99 % | Sigma-Aldrich (St. Louis, USA) |
| Sodium chloride, ≥ 99.5 % | Carl Roth GmbH +Co. KG (Karlsruhe, Germany) |
| Sodium hydroxide, ≥ 99.0 % | Carl Roth GmbH +Co. KG (Karlsruhe, Germany) |
| Thiamine | Sigma-Aldrich (St. Louis, USA) |
| Trace element solution, 1000x | Supplied by I.B.B. / made according to [46] |
| Vitamin solution, 1000x | Supplied by I.B.B. / made according to [46] |
| Water Chromasolv Plus for HPLC | Honeywell International Inc. (New Jersey, USA) |
| Yeast extract | Carl Roth GmbH +Co. KG (Karlsruhe, Germany) |
| Zinc acetate, ≥ 99.0 % | Carl Roth GmbH +Co. KG (Karlsruhe, Germany) |

## 2.3 Reagents

### 2.3.1 Physiological salt solution

Physiological salt solution was prepared at a concentration of 0.9 % (*v/v*) by dissolving NaCl in distilled water ($dH_2O$). If necessary, the solution was sterilized by autoclaving for 20 min at 121 °C and 1 bar.

### 2.3.2 Phosphate assay

In Table 2 compositions of the two reagents used for phosphate assay are depicted. Both were adjusted to pH 5.0 by addition of HCl. Reagents A and B were than combined at a ratio of 1:5 prior to usage.

**Table 2:** Composition of reagents used for the phosphate assay, prepared according to Saheki et al. [47].

| Component | Reagent A | Reagent B |
|---|---|---|
| | c [mM] | |
| Ammonium molybdate tetrahydrate | 15.0 | – |
| Sodium ascorbic acid | – | 504.8 |
| Zink acetate | 100.0 | – |

Abbreviations: c, concentration.

### 2.3.3 Quenching and Extraction

A 50 mM ammonium acetate QS was prepared with $dH_2O$ and adjusted to pH 7.0 using ammonia. The ES was prepared by mixing a 15 mM aqueous ammonium acetate solution with ethanol (≥ 99.8 %) in a ratio of 1:4. pH was adjusted to 7.5 by addition of acetic acid.

### 2.3.4 Storage compound solutions for long-term storage of *S. cerevisiae*

All storage compound solutions were prepared by mixing the respective storage compound (glycerol (Gly), polyethylene glycol (PEG3350, PEG8000 and PEG20000) with $dH_2O$ to a final concentration of 60 % (*v/v*).

## 2.4 Yeast strain

*S. stipitis*
CBS 6054 Supplied by I.B.B.

## 2.5 Media

### 2.5.1 Yeast peptone dextrose medium

Table 3 contains the composition of Yeast Peptone Dextrose (YPD) media, used for the preparation of conventional (YPD1) and $^{13}$C-enriched (YPD2) YPD agar plates. Solution B was adjusted to pH 5.7 with 1 M HCl before sterilization. Solutions A and B were autoclaved separately for 20 min at 121 °C and 1 bar and combined afterwards when temperature decreased to about 40 °C. Approximately 5 mL and 20 mL of the final mixture were then poured immediately into small or big petri dishes, respectively.

**Table 3:** Composition of YPD media.

| Solution | Component | YPD1 c [g/L][a] | YPD2 c [g/L][a] |
|---|---|---|---|
| A | D-Glucose-$^{12}$C($^{13}$C)[b] | 5.0 | 5.0 |
| B | Agar-agar | 15.0 | 15.0 |
| | Peptone | 20.0 | 20.0 |
| | Yeast extract | 10.0 | 10.0 |

[a] Values refer to final concentrations. [b] Unlabelled and labelled D-Glucose were used in the preliminary studies and the SFA, respectively. Abbreviations: c, concentration.

### 2.5.2 Mineral media

In this section, compositions of all mineral media (MM) applied in this master thesis are depicted. For each, solutions A and B were autoclaved separately for 20 min at 121 °C and 1 bar. Solution B was adjusted to pH 5.7 with 1 M KOH right before autoclaving. Solutions A and B were combined to the final concentration prior to inoculation. Components of solution C (except the SMYE) were sterilized by sterile filtration. A sterile SMYE was prepared by different methods (see Section 3.1.5). All components of solution C were added just before inoculation.

Table 4 includes all mineral media applied in the preliminary studies of the SFA for improving the medium composition. Media used for different experiments are separated by dashed lines. Note that MMa5, MMa6, MMb3 are identical with MMb1, MMb5 and MMc1, respectively, but for the sake of clarity and clear allocation to the respective experiment, redundant medium compositions are depicted. For the same reasons all control medium compositions (MMa+, MMb+, MMc+, MMd+, MMa−, MMb−, MMc−, MMd−) are depicted in Table 4.

**Table 4:** Compositions of mineral media used in the preliminary studies for improving the medium composition. Abbreviations in this table refer to: Glc, D-Glucose; MKP, monopotassium phosphate ($KH_2PO_4$); MgS, magnesium sulfate heptahydrate ($MgSO_4 \cdot {}_7H_2O$); AmS, ammonium sulfate ($[NH_4]_2SO_4$); AmC, ammonium chloride ($NH_4Cl$); TE, trace elements; SoC, sodium carbonate ($Na_2CO_3$); vit, vitamins; SMYE, self-made yeast extract; c, concentration.

| Object of invest. | Medium name | Glc | MKP | MgS | AmS | AmC[f] | TE[b] | SoC | vit[b] | SMYE[b] |
|---|---|---|---|---|---|---|---|---|---|---|
| | | c [g/L][a] | | | | | | | | |
| | Solution: | A | B | | | | | C | | |
| | MMS | 20.0 | 14.1 | 0.50 | 5.0 | - | 0.1% | – | 0.1% | – |
| YE concentration and method of preparation | MMa1 | 5.0 | 14.1 | 0.50 | 5.0 | – | 0.1% | – | – | 0.25%[c] |
| | MMa2 | 5.0 | 14.1 | 0.50 | 5.0 | – | 0.1% | – | – | 0.5%[c] |
| | MMa3 | 5.0 | 14.1 | 0.50 | 5.0 | – | 0.1% | – | – | 1.0%[c] |
| | MMa4 | 5.0 | 14.1 | 0.50 | 5.0 | – | 0.1% | – | – | $1.\dot{6}\%$[c] |
| | MMa5 | 5.0 | 14.1 | 0.50 | 5.0 | – | 0.1% | – | – | $3.\dot{3}\%$[c] |
| | MMa6 | 5.0 | 14.1 | 0.50 | 5.0 | – | 0.1% | – | – | $6.\dot{6}\%$[c] |
| | MMa+ | 5.0 | 14.1 | 0.50 | 5.0 | – | 0.1% | – | 0.1% | – |
| | MMa– | 5.0 | 14.1 | 0.50 | 5.0 | – | – | – | – | – |
| Omission of magnesium and trace elements | MMb1 | 5.0 | 14.1 | 0.50 | 5.0 | – | 0.1% | – | – | $3.\dot{3}\%$[d] |
| | MMb2 | 5.0 | 14.1 | – | 5.0 | – | 0.1% | – | – | $3.\dot{3}\%$[d] |
| | MMb3 | 5.0 | 14.1 | 0.50 | 5.0 | – | – | – | – | $3.\dot{3}\%$[d] |
| | MMb4 | 5.0 | 14.1 | – | 5.0 | – | – | – | – | $3.\dot{3}\%$[d] |
| | MMb5 | 5.0 | 14.1 | 0.50 | 5.0 | – | 0.1% | – | – | $6.\dot{6}\%$[d] |
| | MMb6 | 5.0 | 14.1 | – | 5.0 | – | 0.1% | – | – | $6.\dot{6}\%$[d] |
| | MMb7 | 5.0 | 14.1 | 0.50 | 5.0 | – | – | – | – | $6.\dot{6}\%$[d] |
| | MMb8 | 5.0 | 14.1 | – | 5.0 | – | – | – | – | $6.\dot{6}\%$[d] |
| | MMb+ | 5.0 | 14.1 | 0.50 | 5.0 | – | 0.1% | – | 0.1% | – |
| | MMb– | 5.0 | 14.1 | 0.50 | 5.0 | – | – | – | – | – |
| Magnesium concentrations | MMc1 | 5.0 | 14.1 | 0.50 | 5.0 | – | – | – | – | $3.\dot{3}\%$[d] |
| | MMc2 | 5.0 | 14.1 | 0.10 | 5.0 | – | – | – | – | $3.\dot{3}\%$[d] |
| | MMc3 | 5.0 | 14.1 | 0.05 | 5.0 | – | – | – | – | $3.\dot{3}\%$[d] |
| | MMc+ | 5.0 | 14.1 | 0.50 | 5.0 | – | 0.1% | – | 0.1% | – |
| | MMc– | 5.0 | 14.1 | 0.50 | 5.0 | – | – | – | – | – |
| Substitution of N-source | MMd1 | 5.0 | 14.1 | 0.50 | – | 4.05 | – | – | – | $3.\dot{3}\%$[de] |
| | MMd2 | 5.0 | 14.1 | 0.10 | – | 4.05 | – | – | – | $3.\dot{3}\%$[de] |
| | MMd3 | 5.0 | 14.1 | 0.05 | – | 4.05 | – | – | – | $3.\dot{3}\%$[de] |
| | MMd+ | 5.0 | 14.1 | 0.50 | 5.0 | – | 0.1% | – | 0.1% | – |
| | MMd– | 5.0 | 14.1 | 0.50 | 5.0 | – | – | – | – | – |
| Addition of $Na_2CO_3$ | MMe1 | 5.0 | 14.1 | 0.05 | – | 4.05 | – | 1.0 | – | $3.\dot{3}\%$[de] |
| | MMe2 | 5.0 | 14.1 | 0.05 | – | 4.05 | – | 0.1 | – | $3.\dot{3}\%$[de] |
| | MMe+ | 5.0 | 14.1 | 0.05 | – | 4.05 | 0.1% | – | 0.1% | $3.\dot{3}\%$[de] |
| | MMe– | 5.0 | 14.1 | 0.05 | – | 4.05 | – | – | – | – |

[a] Values refer to final concentrations. [b] Values refer to (*v*/*v*). [c] Prepared either by incubating at 99 °C (30 or 60 min) or autoclaving at 121 °C for 20 min (see Section 3.1.5). [d] Prepared by autoclaving. [e] Clarified by centrifugation. [f] g/L were calculated to reach the same molarity as for AmS.

Table 5 contains all mineral media compositions used for the preliminary studies of the SFA.

**Table 5:** Composition of mineral media for the preliminary studies of the SFA.

| Sol. | Component | MMs1 | MMs2 | MMs3 | MMs4 | MMs5 | MMs6 | MMs7 |
|---|---|---|---|---|---|---|---|---|
| | | c [g/L][a] | | | | | | |
| A | D-Glucose | 5.0 | 5.0 | 5.0 | 5.0 | 5.0 | 5.0 | 5.0 |
| B | $KH_2PO_4$ | 14.1 | 14.1 | 14.1 | 14.1 | 14.1 | 14.1 | 14.1 |
| | $MgSO_4 \cdot 7\,H_2O$ | 0.50 | 0.05 | 0.05 | 0.50 | 0.50 | 0.50 | 0.50 |
| | $[NH_4]Cl$ | 4.05 | 4.05 | 4.05 | 4.05 | 4.05 | 4.05 | 4.05 |
| | TE[b] | 0.1% | – | 0.1% | 0.1% | 0.1% | 0.1% | 0.1% |
| C | $Na_2CO_3$[c] | – | – | – | – | – | – | – |
| | Biotin | – | – | – | – | – | – | 0.05 |
| | Pantothenic acid | – | – | – | 0.001 | – | – | – |
| | Thiamine | – | – | – | – | 0.001 | – | – |
| | Vitamins[b] | 0.1% | – | – | – | – | – | – |
| | Yeast extract[bd] | – | 3.3̇%[c] | 3.3̇%[c] | 3.3̇%[c] | 3.3̇%[c] | 3.3̇%[d] | 3.3̇%[d] |

[a] Values refer to final concentrations. [b] Values refer to (*v/v*). [c] Clarified by centrifugation and prepared by autoclaving method. [d]Clarified by centrifugation and prepared by bead beating (see Section 3.1.5). Abbreviations: c, concentration.

In Table 6 the final mineral media (fMM) composition used for the implementation of the SFA is depicted.

**Table 6:** Composition of final fMM for the SFA. Note that either unlabelled $^{12}C$-$Na_2CO_3$ or labelled $^{13}C$-$Na_2CO_3$ was utilized for the two runs of the SFA.

| Sol. | Component | MMf1 | MMf2 | MMf3 | MMf4 | MMf5 | MMf6 |
|---|---|---|---|---|---|---|---|
| | | Concentration [g/L][a] | | | | | |
| A | D-Glucose-$^{13}C_6$ | 5.0 | 5.0 | 5.0 | 5.0 | 5.0 | 5.0 |
| B | $KH_2PO_4$ | 14.1 | 14.1 | 14.1 | 14.1 | 14.1 | 14.1 |
| | $MgSO_4 \cdot 7\,H_2O$ | 0.05 | 0.05 | 0.05 | 0.05 | 0.05 | 0.05 |
| | $[NH_4]Cl$ | 4.05 | 4.05 | 4.05 | 4.05 | 4.05 | 4.05 |
| | TE[b] | – | – | – | – | – | – |
| C | Biotin | – | – | – | 0.05 | 0.05 | 0.05 |
| | $Na_2CO_3$-$^{12}C(^{13}C)$[c] | – | 0.1 | 1.0 | – | 0.1 | 1.0 |
| | Vitamins[b] | 0.1% | 0.1% | 0.1% | – | – | – |
| | Yeast extract[bd] | – | – | – | 3.3̇% | 3.3̇% | 3.3̇% |

[a] Values refer to final concentrations. [b] Values refer to (*v/v*). [c] Unlabelled and labelled $Na_2CO_3$ were used in the first and the second run of the SFA, respectively. [d] Clarified by centrifugation and prepared by bead beating (see Section 3.1.5).

Compositions of trace element and vitamin stock solution are shown in Table 7 and 8, respectively.

**Table 7:** Trace element stock solution (1000x) [46].

| Component | Concentr. [mg/L][a] |
|---|---|
| $CaCl_2 \cdot 6\,H_2O$ | 4.50 |
| $CoCl_2 \cdot 6\,H_2O$ | 0.30 |
| $CuSO_4 \cdot 5\,H_2O$ | 0.30 |
| $FeSO_4 \cdot 7\,H_2O$ | 3.00 |
| $H_3BO_3$ | 1.00 |
| KI | 0.10 |
| $MnCl_2 \cdot 2\,H_2O$ | 0.84 |
| $Na_2EDTA$ | 15.00 |
| $Na_2MoO_4 \cdot 2\,H_2O$ | 0.40 |
| $ZnSO_4 \cdot 7\,H_2O$ | 4.50 |

[a]Values refer to final concentrations.

**Table 8:** Vitamin stock solution (1000x) [46].

| Component | Concentr. [mg/L][a] |
|---|---|
| Ca-Pantothenate | 1.00 |
| D-Biotin | 0.05 |
| *m*-Inositol | 25.00 |
| Niacin | 1.00 |
| *p*-Aminobenzoate | 0.20 |
| Pyridoxine-HCl | 1.00 |
| Thiamine-HCl | 1.00 |

[a]Values refer to final concentrations.

# 3 Methods

## 3.1 Cultivations of the preliminary studies

If not mentioned otherwise, all fermentations were performed in a shaking incubator at a temperature of 30 °C and a shaking frequency of rounds per minute (rpm).

### 3.1.1 Pre-cultures

30 µL of yeast glyercol stock solution were streaked out on YPD agar plates (see Section 2.5.1) and incubated upside down at 30 °C in the incubator-warm room for at least 24 h. A loop full of cells of the overgrown YPD plates was then used to inoculate 30 mL of culture medium (MMS). Pre-cultures (PC) were prepared twofold in 300 mL baffled Erlenmeyer flasks (BEF) and were incubated overnight.

### 3.1.2 Main-cultures

Main-cultures (MC) were prepared in doubles and inoculated with cells obtained from PC to an initial optical density at 600 nm ($OD_{600}$) of 0.01. Cultivations were performed in 1000 mL BEF with 100 mL of MMS and incubated overnight. To separate cells from culture medium, 50 mL of cell broth were centrifuged in 50 mL sterile falcon tubes for 5 min at 4 °C and 5000 rpm. The supernatant was discarded and the pellet was washed three times with 40 mL of cold (4 °C) sterile physiological salt solution. The same centrifugation conditions were applied. Afterwards, cells were re-suspended to an $OD_{600}$ of 10 by addition of sterile saline. This cell suspension was then used as inoculum for the experimental cultures and for the preparation of yeast extract (see Section 3.1.5).

### 3.1.3 Production of glycerol stocks

300 µL of MC (MMS) with an $OD_{600}$ of 16.5 (~17 h incubation time) were pipetted into a sterile Eppendorf tube and mixed with 100 µL of sterile glyercol solution (60 %, v/v). Subsequently, the Eppendorf tubes were vortexed, incubated in a thermocycler for 1 h at 30 °C and 500 rpm, shock-frozen in liquid nitrogen and stored in the −70 °C freezer.

### 3.1.4 Cultivations for testing different media compositions

With these experiments the following factors were tested: The SMYE preparation method, the concentration and clarification of the SMYE, the omission of magnesium and TE, as well as the concentration of magnesium and sodium carbonate. All investigated media compositions can be found in Table 4, Section 2.5.2. Experiments were performed in 300 mL BEF with a working volume of 30 mL. Flasks were inoculated with washed cells of MC to an initial $OD_{600}$ of 0.01. In the experiments for testing different magnesium

and sodium carbonate concentrations, all experimental flasks were prepared in doubles. In order to determine the growth rate $\mu$ of *S. stipitis* in response to the altered media composition, samples for $OD_{600}$ measurement were taken at least every 2 h over a minimum time span of 8 h (see Section 3.3.1).
If unclarified SMYE was added to the medium, the resulting $OD_{600}$ of the samples was corrected for the $OD_{600}$ of the SMYE itself by applying equation 3.

$$\boxed{OD_{corr.} = \frac{OD_{600,\,SMYE} \cdot V_{SMYE}}{V_{work.}}} \tag{3}$$

| | | |
|---|---|---|
| $OD_{corr.}$ | *Corrected* $OD_{600}$ | [1] |
| $OD_{600,\,SMYE}$ | $OD_{600}$ *of SMYE* | [1] |
| $V_{SMYE}$ | *Volume of SMYE added to the cultivation* | $[mL]$ |
| $V_{work.}$ | *Working volume* | $[mL]$ |

### 3.1.5 Preparation of yeast extract

In total, three different approaches to produce a SMYE were investigated. In the first approach, the prepared cell suspension (see Section 3.1.2) was transferred into Eppendorf tubes and then boiled for either 30 min or 60 min in a thermomixer at 99 °C and 400 rpm. In the second approach, the cell suspension was autoclaved for 20 min at 121 °C and 1 bar in a table autoclave. For the third approach, a combination of heat inactivation and bead beating was used: 500 µL or 1000 µL of cell suspension were transferred into Eppendorf tubes containing 500 mg of untreated glass beads with 500 µm in diameter. Afterwards the Eppendorf tubes were vortexed thoroughly for 30 sec followed by 1 min incubation in the thermomixer at 70 °C and 1400 rpm. This procedure was repeated five times resulting in a total processing time of 7.5 min.
In most cases the SMYE was additionally clarified by centrifugation (1.5 mL Eppendorf tubes, 5 min, 4 °C and 14 000 rpm). Both, the clarified and unclarified yeast extracts were transferred into new Eppendorf tubes and stored in the −20 °C freezer until usage. The effectiveness of sterilization was tested by pipetting 5 µL of yeast extract onto an YPD agar plate and subsequent incubation for at least 24 h. A positive control was made by spotting 5 µL of raw cell broth onto the same agar plate.
The cell suspension subjected to a cell extract procedure was always concentrated to $OD_{600}$ of ~10 prior to usage (except for experiment in Section 4.1.1, $OD_{600}$ ~5).

### 3.1.6 Preliminary studies for the SFA

Prior to the main serial fermentation experiment, several studies with $^{12}$C-glucose were carried out, to test whether *S. stipitis* can be cultivated in serial batches without affecting the growth rate. These studies were performed in accordance with the concept of the SFA (see Figure 4 in Section 3.2): After an initial stage (left box), cells of MC were washed and concentrated to an $OD_{600}$ of 10. One part of this cell-suspension was then used for the preparation of yeast extract (5), while the other part was stored in meantime (7) to serve later as inoculum for the enrichment culture (EC). The enrichment culture was carried out without any vitamins but with the clarified SMYE (6) and inoculated to an initial $OD_{600}$ of 0.01 (8). EC was cultivated to a final $OD_{600}$ of 3.0–3.5, the cells harvested again and the process repeated (9).

Since the first attempt to perform a serial fermentation over several cycles gave only sufficient growth rates for the first cycle of serial fermentation (see Section 4.2.2), additionally, the following measures were tried chronologically to retain a constant growth rate over more than 1 cycle: Addition of pantothenic acid and thiamine, preparation of SMYE using the bead beating method and the addition of biotin.
An overview of these studies, including the respective applied media, is provided by Table 9. A detailed description of the media compositions can be found in Table 5, Section 2.5.2. ECs of experiment 2 and 3 were prepared in doubles. Working volume of ECs was 30 mL in 300 mL BEF, except for experiment 1 where it was 10 mL (pre-study for reducing the cultivation volume). In order to determine the growth rate, samples for $OD_{600}$ measurement were taken at least every 2 h.

**Table 9:** Experiments carried out to study the effect of several measures on the growth rate along a serial fermentation.

| # | Object of investigation | Applied media | SMYE PM | Cycle |
|---|---|---|---|---|
| 1 | Serial fermentation over more than 2 cycles | MMs2/MMs3 | Autoclaving | 2 |
| 2 | Addition of pantothenic acid and thiamine | MMs1/MMs4/MMs5 | Autoclaving | 2 |
| 3 | SMYE preparation by bead beating | MMs1/MMs6/MMs7 | Bead beating | 2 |
| 4 | Serial fermentation over more than 2 cycles | MMs7 | Bead beating | 4 |

Abbreviations: PM, preparation method of SMYE.

Furthermore, a study was carried out where the culture volume and the frequency of the shaking incubator were adapted for the purpose of serial fermentation. The working volume was reduced in order to spend less expensive $^{13}$C-labelled substrate. Additionally, it was tried to increase the shaking frequency to compensate a possible decrease of the growth rate due to the reduced cultivation volume. Working volumina of 15 mL and 20 mL were examined at a shaking frequency of 120 rpm and a working volume of 10 mL at a shaking frequency of 160 rpm. As a reference a cultivation was performed in 30 mL (MMs7) cultivation medium. Experiments were carried out in duplicates. Again $OD_{600}$

was measured at least every hour for 2 cycles of serial fermentation in order to detect changes in the growth rate.

#### 3.1.6.1 Storage of inoculum for EC

A study was carried out to determine the best storage condition for the inoculum during the preparation of the SMYE. 200 µL cell suspension obtained from MC ($OD_{600}$ ~10) were transferred into a sterile Eppendorf tube containing 800 µL sterile physiological salt solution. The tube was vortexed subsequently. A second inoculum was prepared in the same way but additionally 2.2 mg of sterile-filtrated glucose were added. For preparation of the third inoculum, 2 mL of cell suspension were transferred into a sterile 50 mL falcon tube and centrifuged for 8 min at 5000 rpm and 0 °C, afterwards the supernatant was discarded. The remaining cell pellet and the two Eppendorf tubes were then stored in the cooling room at 4 °C. After 17 h the cell-pellet was re-suspended with 10 mL of sterile physiological salt solution. All three prepared inocula were vortexed right before application. Six ECs (MMe1, Table 4) were inoculated to an initial $OD_{600}$ of 0.01 with one of the three prepared inocula, each in duplicates. $OD_{600}$ was then measured hourly in order to observe the growth behaviour of the yeast.

#### 3.1.6.2 Long-term storage of $^{13}$C-labelled cells

Another experiment was carried out to investigate the most suitable storage compound for the final $^{13}$C-enriched cells after performing the serial fermentation. 300 µL of MC ($OD_{600}$ ~5.6) were transferred into a sterile Eppendorf tube containing 100 µL of one of four storage compound solutions (glycerol, PEG3350, PEG8000 and PEG20000, see Section 2.3.4). For each storage compound five replicates were prepared. The Eppendorf tubes were then incubated for 1 h at 30 °C and 400 rpm in the thermomixer. Additionally, 300 µL of MC were transferred into sterile Eppendorf tubes in five replicates, centrifuged for 5 min (4 °C, 13 000 rpm) and the supernatant discarded in order to obtain just the cell pellets. Afterwards all yeast stocks and cell pellets were shock frozen by immersion into liquid nitrogen and stored in the −70 °C freezer. After one day, one month, four months and six months out of each yeast stock five dilutions (1:10, 1:100, 1:1000, 1:10000, 1:100000) were prepared and 3 µL of each dilution were spotted onto a single agar plate. Note that the cell pellet was re-suspended with 300 µL of sterile physiological salt solution prior to the preparation of the dilutions. The agar plate was then incubated upside down in the incubator-warm room for at least 24 h.

## 3.2 Serial fermentation approach

All fermentations of the SFA were performed with a working volume of 20 mL in 300 mL BEF. Media applied are shown in Table 6 in Section 2.5.2. Cells were cultivated in a shaker incubator with a temperature of 30 °C and a shaking frequency of 120 rpm. $OD_{600}$ was measured to control cell growth.

### 3.2.1 Workflow

Basically the SFA can be subdivided into two stages: A starting phase for initial $^{13}$C-ER and an iterative phase for further $^{13}$C-ER (compare with Figure 4). The initial phase constitutes the standard method how $^{13}$C-labelled internal standards were prepared so far. The MC can therefore be seen as reference to evaluate the effectiveness of the serial fermentation. A YPD2 agar plate (see Section 2.5, Table 3) was inoculated with 30 µL of yeast glycerol stock solution. The petri dish was incubated upside down at 30 °C in the incubator-warm room for two days. A loop full of cells of the overgrown YPD plate was then used to inoculate one PC prepared with fMM1. PC was incubated for 9 h to a final $OD_{600}$ of 1.26 (0.82 for the second run). In addition to $^{13}$C-labelled glucose, two series were carried out at two different concentrations of $^{13}$C-labelled $Na_2CO_3$ (0.1 and 1 g/L). Cells from PC were used to inoculate a MC to an initial $OD_{600}$ of 0.01 (Table 6, fMM1-fMM3). MC was cultivated overnight to a final $OD_{600}$ of about 3.0-3.5.

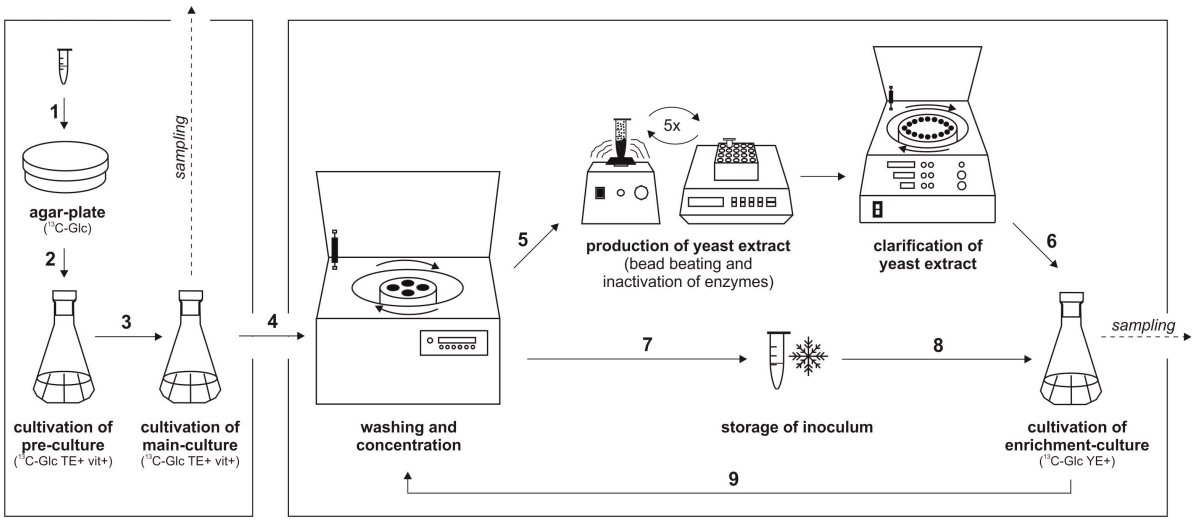


**Figure 4:** Workflow of the SFA. Abbreviations: $^{13}$C-Glc, $^{13}$C-glucose; vit, vitamins; TE, trace elements; YE, yeast extract; Left box - initial stage involving a three-step enrichment of $^{13}$C labelling under otherwise standard mineral medium conditions (TE+, vit+). Right box - iterative cycle for further $^{13}$C-ER. Numbers refer to: 1 Inoculation of agar-plate with glycerol stock solution; 2 Inoculation of PC; 3 Inoculation of MC; 4, 9 Transfer of cell-suspension into 50 mL falcon; 5 Transfer of cell-suspension into Eppendorf tubes containing glass beads; 6 Addition of SMYE; 7 Transfer of cell-suspension into Eppendorf tube (inoculum); 8 Inoculation of enrichment culture.

Cells were then harvested, washed, concentrated and a SMYE was produced utilizing bead beating method (exactly as described in Section 3.1.5). Additionally, 1 mL of the

washed and re-suspended cells was transferred into a sterile Eppendorf tube and stored for maximum 8 h in the cooling room at 4 °C and was then used as inoculum for the ECs. After a time span ranging from 2-7 h an EC was inoculated to an initial $OD_{600}$ of 0.01. Cultivations of the ECs were performed in fMM4-fMM6 containing $SMYE_{bb}$ and biotin (but not vitamins) for 10-23 h to a final $OD_{600}$ of 3.0-3.5. The iterative phase was repeated six times for both runs (see Table 10).

The experiment was repeated but using $^{13}C$-$Na_2CO_3$ instead of unlabelled $^{12}C$-$Na_2CO_3$ (see Section 2.5.2, Table 6). In Table 10 experimental plans for both runs of the SFA are depicted.

**Table 10:** Experimental plan for the two runs of the SFA. Grey cells indicate the cycles of the serial fermentation where LC-ESI/MS samples were taken. Abbreviations refer to: TE - Trace elements.

| Cycle | Culture | TE/ vitamins | $SMYE_{bb}$ | $OD_{600}$ | | First run $^{12}C$-$Na_2CO_3$ c [g/L][a] | | | Second run $^{13}C$-$Na_2CO_3$ c [g/L][a] | | |
|---|---|---|---|---|---|---|---|---|---|---|---|
| | | | | initial | harvest | | | | | | |
| – | agar plate | + | – | – | – | – | – | – | – | – | – |
| – | PC | + | – | – | ~1 | – | – | – | – | – | – |
| 0 (Ref.) | MC | + | – | 0.01 | 3-3.5 | 0.0 | 0.1 | 1.0 | 0.0 | 0.1 | 1.0 |
| 1 | EC1 | – | + | 0.01 | 3-3.5 | 0.0 | 0.1 | 1.0 | 0.0 | 0.1 | 1.0 |
| 2 | EC2 | – | + | 0.01 | 3-3.5 | 0.0 | 0.1 | 1.0 | 0.0 | 0.1 | 1.0 |
| 3 | EC3 | – | + | 0.01 | 3-3.5 | 0.0 | 0.1 | 1.0 | 0.0 | 0.1 | 1.0 |
| 4 | EC4 | – | + | 0.01 | 3-3.5 | 0.0 | 0.1 | 1.0 | 0.0 | 0.1 | 1.0 |
| 5 | EC5 | – | + | 0.01 | 3-3.5 | 0.0 | 0.1 | 1.0 | 0.0 | 0.1 | 1.0 |
| 6 | EC6 | – | + | 0.01 | 3-3.5 | 0.0 | 0.1 | 1.0 | 0.0 | 0.1 | 1.0 |
| 7 | EC7 | – | + | 0.01 | 3-3.5 | 0.0 | 0.1 | 1.0 | 0.0 | 0.1 | 1.0 |

[a] Values refer to final medium concentrations. Abbreviations: c, concentration; Ref., reference.

## 3.3 Analytics

### 3.3.1 Determination of $OD_{600}$

Cell density was measured spectrophotometrically at 600 nm with a Biowave Cell Density Meter against physiological salt solution as a blank. Samples were diluted with physiological salt solution if necessary.
In earlier studies and in some experiments of this thesis Beckman Coulter photometer DU800 was used. Since both applied photometers give different $OD_{600}$ values at the same cell density, all $OD_{600}$ values that were measured with the Biowave Cell Density meter were converted to $OD_{600}$ Beckman values for comparability.

### 3.3.2 Calculation of the conversion factor between Biowave cell Density Meter and Beckman Coulter photometer DU800

Since two different types of photometers were used in this master thesis, an experiment was carried out to determine the conversion factor between both. For this purpose, a cell suspension was harvested from MC ($OD_{600} \sim 16.5$) and nine dilutions ranging from 1:25-1:2500 were prepared with saline in cuvettes, each in duplicates. Subsequently the $OD_{600}$ of each dilution was measured with both photometers. The resulting $OD_{600}$ values of the Biowave Cell Density Meter were then plotted against those of the Beckman Coulter photometer DU800 and Microsoft Excel's LINEST function was applied (equation 4). The slope represents the conversion factor between the two applied photometers.

$$\boxed{OD_{Bio} = cf \cdot OD_{Beck}} \tag{4}$$

| | | |
|---|---|---|
| $OD_{Bio}$ | *$OD_{600}$ of Biowave Cell Density Meter* | [1] |
| $OD_{Beck}$ | *$OD_{600}$ of Beckman Coulter photometer DU800* | [1] |
| $cf$ | *Conversion factor* | [1] |

### 3.3.3 Calculation of generations

Generations of *S. stipitis* during the SFA were determined by dividing the cultivation time of each cycle by the doubling time. The mathematical relation is provided by equation 5.

$$\boxed{Gen. = \frac{\Delta t}{\frac{ln(2)}{\mu}}} \tag{5}$$

| | | |
|---|---|---|
| $Gen.$ | *Number of generations of S. stipitis during 1 cycle of the SFA.* | [1] |
| $\Delta t$ | *Total cultivation time of 1 cycle of the SFA.* | $[h]$ |
| $\mu$ | *Growth rate* | $[\frac{1}{s}]$ |

### 3.3.4 Reduction of phosphate concentration in LC-ESI/MS replicates

From earlier metabolomic studies on the I.B.B. it is known that phosphate and other salts arising from the sample matrix can impair the ionization efficiency of the MS [30, 48]. To this end, in these studies the initial phosphate concentration in the fermentor was lowered, to have uncritical phosphate concentrations ($\leq 1$ mM, [30]) in the final LC-ESI/MS replicates. Since the pH adjustment in shaking flasks is elaborate and could come along with $^{12}$C-contaminations, in this thesis it was attempted to lower the the phosphate amount by introducing an additional washing-step during the quenching procedure.
A quenching experiment was simulated, in order to test if an additional washing-step would lead to uncritical final phosphate concentrations in the LC-ESI/MS replicates. 1 mL of cell suspension ($OD_{600} \sim 3$) containing a predefined amount of phosphate (0.25, 1.5, 4 and 14.1 g/L) were quenched in 4 mL of ice-cold QS. The quenched cells were then separated by centrifugation (5 min, at 5000 rpm and 0 °C) and after decanting the supernatant as quantitatively as possible, the cell pellet was washed two times with 40 mL saline under the same centrifugation conditions. After discarding the supernatant again, the tubes were spun in order to collect residual liquids. The liquids were pipetted into Eppendorf tubes and weighted on an analytical scale to achieve information about the leftover volume (density assumed: 1 mL $dH_2O$ ~1 g) and taken as samples.
Samples for phosphate determination were taken before quenching (reference), after quenching and after the washing-step, each in duplicates. Each was centrifuged (5 min at 13 000 rpm and 0 °C) and the supernatant stored in the −20 °C freezer.

For determinition of the phosphate concentrations of the samples, an assay was performed according to Saheki et al. [47]. Applied reagents were prepared as described in Section 2.3). For quantification, eleven standards in the range of 1-1500 µM $KH_2PO_4$ were prepared. 20 µL of vortexed samples were transferred to cuvettes containing 480 µL of the final reaction mixture. The cuvettes were vortexed subsequently and incubated for 15 min at room temperature. Afterwards the color change was detected photometrically at 850 nm ($OD_{850}$). As a reference 20 µL $dH_2O$ in 480 µL reaction mix was used.
A standard calibration curve was established by plotting the $OD_{850}$ values obtained for each standard against its phosphate concentration. The slope of the resulting calibration curve was used to calculate the phosphate concentration of each sample (Equation 6).

$$\boxed{OD_{850} = \Delta \cdot c_{Pi} + OD_{850,0}} \tag{6}$$

| | | |
|---|---|---|
| $OD_{850}$ | *Optical density at* 850 nm | [1] |
| $c_{Pi}$ | *Phosphate concentration* | $[\mu M]$ |
| $\Delta$ | *Slope of the calibration curve* | $[\frac{1}{\mu M}]$ |
| $OD_{850}$ | *Offset of optical density at* 850 nm | [1] |

### 3.3.5 Sample preparation for HPLC-MS measurement

The sample preparation includes all steps from sampling to the ready-to use metabolite extracts for LC-ESI/MS measurement. A simplified scheme of the whole workflow is depicted in Figure 5: Samples are quenched and washed subsequently in order to dilute out remaining salts, especially phosphate, arising from the sample matrix. Metabolites are then extracted by application of heat and ethanol and dried by lyophilization afterwards. Each step will be described in detail in the following.

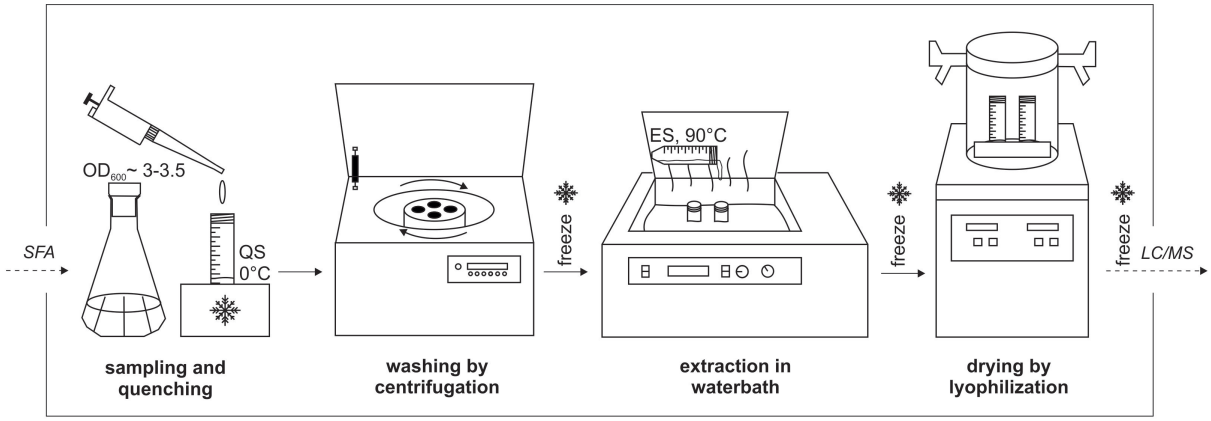


**Figure 5:** Scheme of the workflow of the sample preparation. Abbreviations refer to: ES - Extraction solution. QS - Quenching solution. Snowflakes indicate freezing at −70 °C.

#### Sampling and quenching

In total, sampling was performed two times during the first and three times during the second run of the SFA. Samples were withdrawn from MCs and ECs (indicated by dashed arrows in Figure 4, Section 4), each in quadruplicates.

About 1 mL of cell suspension with an final $OD_{600}$ of 3.0-3.5 was pipetted fastly and directly (without touching the tube wall) into 50 mL falcon tubes containing 4 mL of ice-cold QS (prepared as described in Section 2.3.3). Note that the sampling volume was adapted depending on the $OD_{600}$ value to ensure approximately the same amount of biomass in all samples ($3\ OD_{600} \mathrel{\widehat{=}} 1$ mL, for lower $OD_{600}$ values higher volumes were sampled and vice versa).

The tube was screwed quickly, followed immediately by short but thoroughly vortexing. Subsequently the samples were centrifuged for 2 min at 5000 rpm in the pre-cooled centrifuge (0 °C). The supernatant was discarded, the falcon tubes were refilled with 40 mL of ice-cold saline, vortexed and centrifuged for another 2 min under the same conditions. After discarding the supernatant again, the remaining cell pellet was shock-frozen using liquid nitrogen and stored in the −70 °C freezer.

### Extraction

A 15 mL falcon tube containing 3.5 mL of ES (prepared as described in Section 2.3.3) was pre-heated for 20 min in a water bath to a final temperature of 90 °C. The frozen cell-pellet stored in a 50 mL falcon tube was taken out of the −70 °C freezer, positioned in the water bath and opened subsequently. The hot ES was then immediately poured over the cell pellet (again care was taken not to hit the wall tube), the tube screwed quickly and vortexed short and thoroughly. The falcon was incubated in the water bath again for 3 min, interrupted after 1 min and 2 min by short but thoroughly vortexing. Afterwards the extracted cell lysate was stored on ice while extracting the next sample. Then both cell lysates were centrifuged for 3 min at 5000 rpm and 0 °C. The supernatants were transferred as quantitative as possible into new 50 mL falcon tubes and stored in the −70 °C freezer again.

### Evaporation of extracted LC-ESI/MS samples

Lyophilization was applied in order to dry the extracted metabolites. Prior to lyophilization, samples were stored for 1 h in liquid nitrogen for pre-cooling. The falcon tubes were unscrewed and covered with perforated paraffin band in order to prevent possible contaminations originating from the lyophilisation device. Then the sealed falcon tubes were stored in the lyophilisation device overnight at a temperature of −40 °C and a pressure of maximum 1 mbar.
The dried cell lysate was re-suspended with 300 µL of HPLC grade water. Metabolite residues sticking on the wall tube were scraped off using a plastic spatula when necessary. Subsequently the suspension was transferred as quantitative as possible into an Eppendorf tube, shock frozen with liquid nitrogen and stored in the −70 °C freezer again.

## 3.3.6 LC-ESI/MS measurement at JOANNEUM RESEARCH

LC-ESI/MS measurement was carried out at Joanneum Researchs Health institute with a HPLC-MS system from Thermo Fisher Scientific™. A Dionex Ultimate 3000 HPLC setup with a KrudCatcher™ ULTRA HPLC in-line filter as a pre-column and an Atlantis T3 C18 as analytical column was used for compound separation. MS was performed using an Exactive™ Orbitrap system (for setup details see Section 2.1).
A reversed-phase ion-pairing HPLC method (adapted from Buescher et al. (2010) [49]) in combination with tributylamine as ion-pairing agent [48] was used for metabolite separation. A 40 min gradient, consisting of 2-propanol as eluent A and an aqueous phase (5 % methanol (*v/v*), 10 mM tributylamine, 15 mM acetic acid, pH 4.95) as eluent B, respectively, was applied. The injection volume was 10 µL, while the injection loop was 20 µL. Ionization of metabolites was carried out in negative mode using heated electrospray ionization (HESI). The online detection of analytes was performed using a full scan of all masses between 70 and 1100 m/z with a resolution of 50000 (at 200 m/z).

The 60 replicates in total were randomized globally and measured in three batches. Additionally, a 50 µM $^{13}$C-glucose standard was prepared with $dH_2O$. Pure $dH_2O$ was used as a blank. LC-ESI/MS samples were stored on dry ice during the transportation to Joanneum Research.
Immediately after thawing, all replicates were centrifuged at 13 300 rpm for 5 min. 100 µL of the resulting supernatant were transferred into HPLC vials with 200 µL inserts. A quality control (QC) was prepared by pooling 50 µL of each of the centrifuged replicates. If necessary, air bubbles were removed by knocking slightly against the vials. In Figure 6 the injection sequence for the HPLC-MS measurement is depicted: Blanks and QCs were always followed by four randomized samples. At last the $^{13}$C-glucose standard was injected.

| BL1 | QC1 | S1 | S2 | S3 | S4 | BL2 | QC2 | S5 | S6 | ... | S24 | BL13 | QC13 | $^{13}$C-Glc |
|---|---|---|---|---|---|---|---|---|---|---|---|---|---|---|

**Figure 6:** Injection sequence of HPLC-MS measurement for one batch. Abbreviations: BL, blank; QC, quality control; S, sample; $^{13}$C-Glc, $^{13}$C-labelled glucose standard.

### 3.3.7 Data Processing

Except for the peak integration, all steps of the data processing were performed in Microsoft Excel 2016. Graphs shown in this master thesis were made with SigmaPlot v10.0.

#### Peak integration

Peak detection and integration was performed using a JAVA-based program called PeakScout (version 3.0.7, provided by Joanneum Research). A compound list (also provided by Joanneum Research), containing 880 common metabolites known to be present in yeast or human, was used to scan the 93 replicates in total (including blanks, QCs and glucose standards). Peak integration was performed for each batch separately, the resulting three datasets were then freed from negative or zero values and merged afterwards.

#### Blankload detection and filtering

For each metabolite, areas of the QCs were compared with the areas of the blanks in order to detect and subsequently exclude metabolites which are prone to high blank loading from further calculation. Blank loading terms a metabolite-specific phenomenon where corresponding metabolite signals are also found in blanks by the MS system.
Metabolites which met both of the following criteria were excluded from further calculations:

(i) $\frac{\overline{QC}}{\overline{Blank}} < 1.5$

(ii) ttest with $\alpha = 0.05$

With the first criterion it was checked if the signals of the QCs are in average at least 1.5-fold higher than the signals of the blanks. Secondly, a ttest was applied in order to detect a significant difference between the signals of the QCs and blanks, respectively.

### Outlier removal

Each sample was determined by averaging four replicates. Prior to the calculation of average, the fourfold determination was checked for outliers. An algorithm for an effective automated outlier detection and removal was introduced: First of all, relative standard errors (RSE) between each of the four replicates were calculated. The two replicates which formed the lowest RSE were then assumed to display the true signal value best. The two remaining replicates were defined as outliers, if the RSE between them and the two accepted replicates was higher than 0.3. Note that some samples were determined by less than four replicates, since some of them had to be excluded due to the bad quality of the LC-ESI/MS measurement (see Section 4.3.3). If there were three replicates, the same principle as described above was applied. For two replicates just an average was formed.

### Calculation of $^{13}$C-ER

The $^{13}$C-ER per metabolite was calculated according to equation 7, which inherently normalizes the $^{13}$C-ER to take a value between 0 and 1. For an easier data interpretation, values were converted to percent by multiplying the $^{13}$C-ER by 100.

$$\boxed{{}^{13}C\text{-}ER = \frac{A_{^{13}C}}{A_{^{13}C} + A_{^{12}C}}} \tag{7}$$

| | | |
|---|---|---|
| $^{13}C\text{-}ER$ | *$^{13}$C-ER per metabolite* | [1] |
| $A_{^{13}C}$ | *Signal area of $^{13}$C-labelled metabolite* | [1] |
| $A_{^{12}C}$ | *Signal area of unlabelled metabolite* | [1] |

### Calculation of partial labelling

In order to calculate the patterns of partial labelling of each metabolite, equation 8 was applied: The signal area of an isotopologue of a specific metabolite, is divided by the sum of all other found isotopological signal areas to achieve the fraction in percent.

$$\boxed{\textit{fraction isotopologue } m_x = \frac{A_{m_x}}{\sum_{i=0}^{n} A_{m_i}}} \tag{8}$$

| | | |
|---|---|---|
| $m_x$ | *Fraction of isotopologue* | [%] |
| $A_{m_x}$ | *Signal area of metabolite m with x $^{13}$C-labelled C-atoms* | [1] |
| $A_{m_i}$ | *Signal area of metabolite m with i $^{13}$C-labelled C-atoms* | [1] |

### Trend correction and normalization

For the determination of absolute metabolite levels, it was assumed that signal areas originating from different batches are comparable as long as their QCs are comparable, since LC-ESI/MS samples were randomized globally and QCs were prepared by pooling batch-wise all replicates. In order to make the three batches comparable, each batch was corrected for linear or exponential time trends, respectively, and normalized subsequently. A linear trend can arise by a linear signal reduction over time caused by the LC-ESI/MS methodology. Exponential trends can occur due to natural metabolite degradation with the rather long analysis time of samples in the autosampler (maximum 13 h) during the LC-ESI/MS measurement. Both trends are metabolite-specific.
For the implementation of the trend correction, Pearson correlation coefficients were calculated for each metabolite from a QC area versus time and logarithmized QC area versus time plot. Depending on which correlation coefficient gave the higher result, metabolites were classified to have a linear or exponential trend. Possible trends were then corrected by subtracting the offset of the respective signal of QC caused by the trend, from the original signal area from the QC (see equation 9). In case of exponential trends signal areas of QCs were logarithmized prior to trend correction and transformed back afterwards. If the RSE over all QCs could be reduced by this method, trend correction was also applied to the samples.

$$\boxed{QC_{i,\,tc} = QC_i - \Delta \cdot t} \tag{9}$$

| | | |
|---|---|---|
| $QC_{i,\,tc}$ | *Signal of QC i, after trend correction* | [1] |
| $QC_i$ | *Signal of QC i, before trend correction* | [1] |
| $\Delta$ | *Slope of linear or exponential trend, respectively* | $[\frac{1}{min}]$ |
| $t$ | *Timepoint of measurement* | $[min]$ |

Trend corrected signals were normalized by application of equation 10: For each metabolite, all signal areas were divided by the average of all metabolite-specific QCs originating from this batch. The resulting data sets obtained from trend correction and normalization were merged afterwards.

$$\boxed{A_{i,\,norm} = \frac{A_i}{\overline{QC}}} \tag{10}$$

| | | |
|---|---|---|
| $A_{i,\,norm}$ | *Signal area of metabolite i, after normalization* | [1] |
| $A_i$ | *Signal area of metabolite i, before normalization* | [1] |
| $\overline{QC}$ | *Average of QCs* | [1] |

### 3.3.8 Data evaluation

#### 3.3.8.1 $^{13}$C-ER as a function of the number of fermentation cycles

Each experiment (no addition of $Na_2CO_3$, addition of 0.1 g/L and addition of 1 g/L $Na_2CO_3$) consisted of three samples - one reference sample taken at cycle 0 and two additional samples taken at cycle 3 and 7, respectively. Figure 7 shows a scheme of the strategy for the evaluation of the $^{13}$C-ER depending on the number of fermentation cycles: First of all, metabolites of multiple determined samples (reference samples of cycle 0, samples of cycle 7 without addition of $^{13}$C-$Na_2CO_3$) were checked for reproducibility by analysis of variances (ANOVA) with a level of significance $\alpha$=0.1. Metabolites were excluded from further analysis, if significant differences were observed by ANOVA. The reference sample C0 was determined sixfold in total - for each experiment once (see Table 10, Section 3.2). One determination was excluded in advance, since it was formed by just one replicate originating from bad quality batch 1 (indicated by dashed line in Figure 7). Additionally, sample C7 in the experiments without addition of any $Na_2CO_3$ was determined in both runs of the SFA.

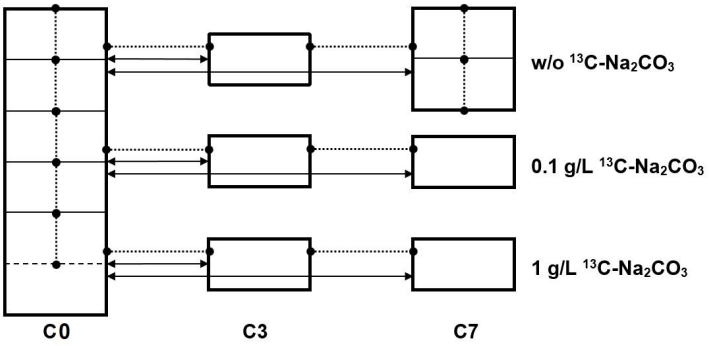


**Figure 7:** Overview of statistical tests applied for evaluating the $^{13}$C-ER as a function of fermentation cycles. Each box represents one sample. Reference sample C0 and sample C7 of the experiment without $^{13}$C-$Na_2CO_3$ addition were determined by 5 and 2 sub-samples (thin-lined boxes). Dotted connections indicate application of ANOVA. Solid arrows represent comparisons by LSD test. Dashed line - excluded sample.

In the next step, another ANOVA ($\alpha$=0.1) was applied between C0, C3 and C7 of each experiment, in order to determine differences in the $^{13}$C-ER. When the samples did not differ significantly from each other, the respective metabolite was excluded from further calculations, since no effects in the $^{13}$C-ER with increasing number of fermentation cycles could be expected.

Effects in the $^{13}$C-ER as a function of fermentation cycles itself, were detected by application of a a-priori- and post-hoc-tests. Samples taken at cycle 3 and 7, respectively, were compared with the reference sample taken at cycle 0 using Scheffe- and LSD test (indicated by solid arrows in Figure 7). The deployed level of significance $\alpha$ was 0.1 for both tests. Note that all effects presented in this thesis were determined by LSD (Least Significant Difference) test, but checked for plausibility with Scheffe test.

#### 3.3.8.2 Effect of $^{13}$C-$Na_2CO_3$ addition on the $^{13}$C-ER

In Figure 8 the basic strategy for evaluating the effects on the $^{13}$C-ER by addition of $^{13}$C-$Na_2CO_3$ is depicted. Samples C7 of the experiments with addition of 0.1 g/L and 1 g/L $^{12}$C-$Na_2CO_3$ were compared to those from the experiments with addition of 0.1 g/L and 1 g/L $^{13}$C-$Na_2CO_3$, respectively.

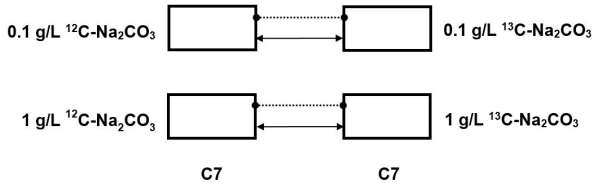


**Figure 8:** Overview of statistical tests applied samples of cycle 7 for the evaluation of the effect of the $^{13}$C-$Na_2CO_3$ addition. Solid boxes represent samples of cycle 7. Dotted connections indicates application of ANOVA. Solid arrows refer to a comparison by LSD-test.

In analogy to the data evaluation of the $^{13}$C-ER as a function of the number of fermentation cycles, first the metabolite-specific $^{13}$C-ER of the samples was compared for differences by applying ANOVA ($\alpha$=0.1). For those metabolites where differences were found, Scheffe- and LSD test ($\alpha$=0.1) were used in order to determine an increase or decrease of the $^{13}$C-ER depending on the addition of $^{13}$C-$Na_2CO_3$.

# 4 Results

## 4.1 Experiments for improving the medium composition

Several experiments were carried out in order to improve the medium composition for the purpose of serial fermentation. In these studies the influences of altered media compositions on the growth rate of *S. stipitis* were examined. For a description of the methodology see Section 3.1.4. A list of all investigated media compositions can be found in Section 2.5.2, Table 4. Corresponding $OD_{600}$ measurement series for the calculation of the growth rates can be found in the excel file `supplemental material_preliminary studies.xlsx`.

### 4.1.1 Influence of SMYE concentration and preparation methods on the growth rate

Two studies were carried out in order to investigate the growth rate of *S. stipitis*, if vitamins are replaced by a SMYE. In the first study, ECs were inoculated to an initial $OD_{600}$ of 0.25 and growth was observed for 9 hours (see Table 11). ECs of the second study were inoculated to an $OD_{600}$ of 0.01 to increase the number of generations (see Tab-

**Table 11:** Growth rate $\mu$ in response to different concentrations of SMYE prepared with different methods. Time span of observation: 0 to 9 h. The quoted uncertainty corresponds to the standard deviation.

| Media | SMYE c [%][a] | SMYE PM | $\mu$ ($R^2 \geq 0.963$) [1/h] |
|---|---|---|---|
| MMa1 | | boil. 30' | 0.332 ± 0.014 |
| MMa1 | 0.25% | boil. 60' | 0.295 ± 0.010 |
| MMa1 | | auto. 20' | 0.304 ± 0.014 |
| MMa2 | | boil. 30' | 0.315 ± 0.016 |
| MMa2 | 0.5% | boil. 60' | 0.336 ± 0.014 |
| MMa2 | | auto. 20' | 0.313 ± 0.014 |
| MMa3 | | boil. 30' | 0.336 ± 0.008 |
| MMa3 | 1.0% | boil. 60' | 0.378 ± 0.005 |
| MMa3 | | auto. 20' | 0.356 ± 0.013 |
| MMa5 | | boil. 30' | 0.424 ± 0.021 |
| MMa5 | 3.3̇% | boil. 60' | 0.428 ± 0.027 |
| MMa5 | | auto. 20' | 0.363 ± 0.014 |
| MMa+ | – | – | 0.413 ± 0.015 |
| MMa– | – | – | 0.292 ± 0.012 |

[a] Values refer to (*v/v*). Abbreviations: c, concentration of SMYE; p. meth., preparation method of SMYE.

**Table 12:** Growth rate $\mu$ in response to different concentrations of SMYE prepared with different methods. Time span of observation: 13 to 21 h. The quoted uncertainty corresponds to the standard deviation.

| Media | SMYE c [%][a] | SMYE PM | $\mu$ ($R^2 \geq 0.916$) [1/h] |
|---|---|---|---|
| MMa4 | | boil. 30' | 0.375 ± 0.038 |
| MMa4 | 1.6̇% | boil. 60' | 0.304 ± 0.013 |
| MMa4 | | auto. 20' | 0.294 ± 0.018 |
| MMa5 | | boil. 30' | 0.304 ± 0.019 |
| MMa5 | 3.3̇% | boil. 60' | 0.293 ± 0.016 |
| MMa5 | | auto. 20' | 0.325 ± 0.019 |
| MMa6 | | boil. 30' | 0.406 ± 0.023 |
| MMa6 | 6.6̇% | boil. 60' | 0.603 ± 0.020 |
| MMa6 | | auto. 20' | 0.422 ± 0.033 |
| MMa+ | – | – | 0.488 ± 0.013 |
| MMa– | – | – | 0.153 ± 0.023 |

[a] Values refer to (*v/v*). Abbreviations: c, concentration of SMYE; PM, preparation method of SMYE.

le 12). Here the growth rate was observed after overnight cultivation, when ECs were already cultivated for 13 hours. In both studies different concentrations of SMYE (ranging from 0.25 to 6.6 %, *v/v*) prepared by different methods were tested. A consideration of the growth rates depicted in Tables 11 and 12 reveals, that the growth rate increased if higher concentrations of SMYE were applied to the medium. In contrast, the method of preparation of the SMYE did not influence the growth rate.
In Figure 18 findings for the first 9 hours of growth are illustrated: Except for the negative control (closed triangles down), growth rates (represented by the slopes) did not differ significantly from each other and remained in the range of the positive control prepared with vitamins. In panel (B) the relationship between the growth rate and the concentration of SMYE for autoclaving method is exemplified. The highest growth rate was found for a concentration of 3.3̇% (v/v) SMYE, virtually in the range of the positive control. However, in later experiments all three methods of preparation were rejected and bead beating in combination with heat inactivation was introduced (see Section 4.2.2).

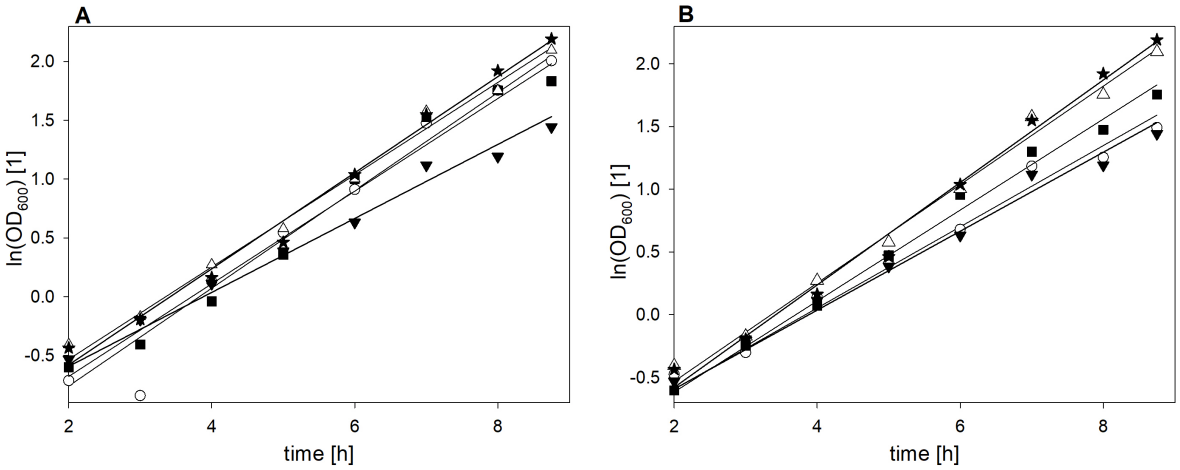


**Figure 9:** Growth rate $\mu$ during the first 9 hours of observation. (A) Growth rates depending on different SMYE production methods and with a fixed SMYE concentration of 3.3̇% (*v/v*). Open circles - boiling for 30 min. Closed squares - boiling for 60 min. Open triangles - autoclaving for 20 min. Closed stars - positive control. Closed triangles down - negative control. (B) Growth rates depending on different concentrations of SMYE prepared by autoclaving for 20 min. Open circles - 0.25% (*v/v*). Closed squares - 1.0% (*v/v*). Open triangles up - 3.3̇% (*v/v*). Closed stars - positive control. Closed triangles down - negative control.

### 4.1.2 Influence of omission of magnesium, TE or both on the growth rate

The growth rate in response to the omission of either TE, magnesium or both, were examined (depicted in Tables 13 and 14). Measures were tested for two different concentrations of SMYE (3.3 % and 6.6 % (*v/v*)) prepared by two distinct preparation methods (autoclaving for 20 minutes in Table 13, boiling for 60 minutes in Table 14).
The omission of TE reduced the growth rate, but not drastically. In contrast, the omission of magnesium decreased the growth rate almost by a factor of 2 in comparison

**Table 13:** Growth rates $\mu$ depending on the omission of TE and/or magnesium. SMYE was prepared by autoclaving. The quoted uncertainty corresponds to the standard deviation.

| Media | SMYE c [%][a] | TE | Mg | $\mu$ ($R^2 \geq 0.921$) [1/h] |
|---|---|---|---|---|
| MMb1 | 3.3̇% | + | + | 0.433 ± 0.020 |
| MMb2 | | + | – | 0.261 ± 0.034 |
| MMb3 | | – | + | 0.387 ± 0.016 |
| MMb4 | | – | – | 0.268 ± 0.014 |
| MMb5 | 6.6̇% | + | + | 0.430 ± 0.023 |
| MMb6 | | + | – | 0.260 ± 0.012 |
| MMb7 | | – | + | 0.416 ± 0.016 |
| MMb8 | | – | – | 0.344 ± 0.031 |
| MMb+ | – | + | + | 0.424 ± 0.036 |
| MMb– | – | – | + | 0.046 ± 0.016 |

[a] Values refer to (*v/v*). Abbreviations: c, concentration of SMYE; TE, trace elements; Mg, magnesium sulfate heptahydrate ($MgSO_4 \cdot 7\,H_2O$).

**Table 14:** Growth rates $\mu$ depending on the omission of TE and/or magnesium. SMYE was prepared by boiling for 60 min. The quoted uncertainty corresponds to the standard deviation.

| Media | SMYE c [%][a] | TE | Mg | $\mu$ ($R^2 \geq 0.890$) [1/h] |
|---|---|---|---|---|
| MMb1 | 3.3̇% | + | + | 0.333 ± 0.016 |
| MMb2 | | + | – | 0.196 ± 0.028 |
| MMb3 | | – | + | 0.317 ± 0.013 |
| MMb4 | | – | – | 0.202 ± 0.018 |
| MMb5 | 6.6̇% | + | + | 0.424 ± 0.013 |
| MMb6 | | + | – | 0.297 ± 0.029 |
| MMb7 | | – | + | 0.403 ± 0.017 |
| MMb8 | | – | – | 0.203 ± 0.024 |
| MMb+ | – | + | + | 0.424 ± 0.036 |
| MMb– | – | – | + | 0.046 ± 0.016 |

[a] Values refer to (*v/v*). Abbreviations: c, concentration of SMYE; TE, trace elements; Mg, magnesium sulfate heptahydrate ($MgSO_4 \cdot 7\,H_2O$).

to the positive control (compare square symbols with closed stars in Figure 10). In contrast, cultures with magnesium added (circles), had a growth rate approximately in the range of those from the positive control. Once again it was shown, that the application of higher concentrations of SMYE slightly increases the growth rate, while the preparation of SMYE does not affect the growth rate.

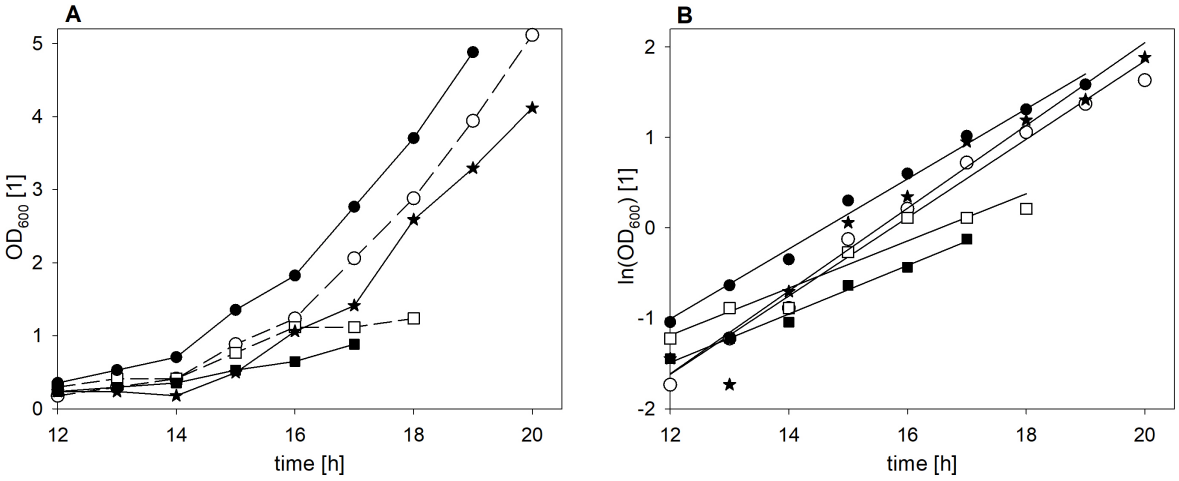


**Figure 10:** Growth curves (A) and logarithmized growth curves (B) in response to the omission of TE and magnesium for a SMYE concentration of 3.3̇% (*v/v*) prepared by autoclaving method. Open circles - TE and magnesium added. Open squares - TE added, magnesium omitted. Closed circles - TE omitted, magnesium added. Closed squares - TE and magnesium omitted. Closed stars - positive control.

### 4.1.3 Clarification of $SMYE_{aut}$ and influence of magnesium concentration on the growth rate

The results of the previous experiment stated that magnesium can not be omitted entirely. Hence, an experiment was performed to analyze how magnesium concentrations applied in the range of 0.01 to 0.5 g/L affect the growth rate of *S. stipitis* (see Table 15).
Obtained $OD_{600}$ data of previous experiments were offset-corrected by subtracting the $OD_{600}$ of the $SYME_{aut}$ itself from the measured values (see Section 3.1.4). In general, subtractions are known to decrease accuracy of results significantly. Therefore it was examined, if a clarification of the $SYME_{aut}$ would contribute to reduce the error of $OD_{600}$ measurements. In order to test the effectiveness of clarification, a reference experiment was carried out (see Table 16) differing only in the lowest magnesium concentration (0.01 vs 0.05 g/L) and of course, the additional clarification step of the yeast extract by centrifugation. For a detailed description of the SMYE preparation see Section 3.1.5. In both experiments experimental flasks were prepared in doubles and media contained SMYE (3.3 %, *v/v*) prepared by autoclaving method, but no TE.
Additionally, media differed in the salts of their nitrogen sources ($[NH_4]_2SO_4$ for Table 15 and $NH_4Cl$ for Table 16). This substitution was not studied in more detail, as an influence on the growth rate was already rejected in previous studies on the I.B.B. [30].

**Table 15:** Growth rate $\mu$ depending on different magnesium concentrations. SMYE was prepared by autoclaving, but not clarified. The quoted uncertainty corresponds to the standard deviation.

| Media | SMYE-clarific. | Mg c [g/L] | $\mu$ ($R^2 \geq 0.924$) [1/h] |
|---|---|---|---|
| MMc1 | - | 0.50 | 0.323 ± 0.016 |
| MMc1 | - | 0.50 | 0.327 ± 0.039 |
| MMc2 | - | 0.10 | 0.329 ± 0.042 |
| MMc2 | - | 0.10 | 0.344 ± 0.011 |
| MMc3 | - | 0.05 | 0.328 ± 0.013 |
| MMc3 | - | 0.05 | 0.317 ± 0.011 |
| MMc+ | - | 0.50 | 0.309 ± 0.025 |
| MMc– | - | 0.50 | 0.122 ± 0.017 |

Abbreviations: Mg, magnesium sulfate heptahydrate ($MgSO_4 \cdot 7\,H_2O$); c, magnesium concentration.

**Table 16:** Growth rate $\mu$ depending on magnesium concentrations. SMYE was prepared by autoclaving and additionally clarified. The quoted uncertainty corresponds to the standard deviation.

| Media | SMYE-clarific. | Mg c [g/L] | $\mu$ ($R^2 \geq 0.992$) [1/h] |
|---|---|---|---|
| MMd1 | + | 0.50 | 0.355 ± 0.009 |
| MMd1 | + | 0.50 | 0.362 ± 0.004 |
| MMd2 | + | 0.10 | 0.374 ± 0.003 |
| MMd2 | + | 0.10 | 0.360 ± 0.010 |
| MMd3 | + | 0.01 | 0.370 ± 0.004 |
| MMd3 | + | 0.01 | 0.362 ± 0.003 |
| MMd+ | - | 0.50 | 0.320 ± 0.018 |
| MMd– | - | 0.50 | 0.177 ± 0.006 |

Abbreviations: Mg, magnesium sulfate heptahydrate ($MgSO_4 \cdot 7\,H_2O$); c, magnesium concentration.

Figure 11 illustrates the findings by depicting the growth rate in response to different magnesium concentrations, one time with unclarified (A) and one time with clarified $SYME_{aut}$ (B). In both experiments, the growth rate was not influenced in the observed range of magnesium concentrations (0.01-0.50 g/L). In contrast, clarification of the $SYME_{aut}$ showed

a clear effect: Beside the reduction of offset and scattering, linearity of calculated regressions was significantly improved ($R^2$ 0.973 vs. 0.992; compare panels (A) and (B) in Figure 11). Due to the benefits, SYME was clarified in all further experiments.

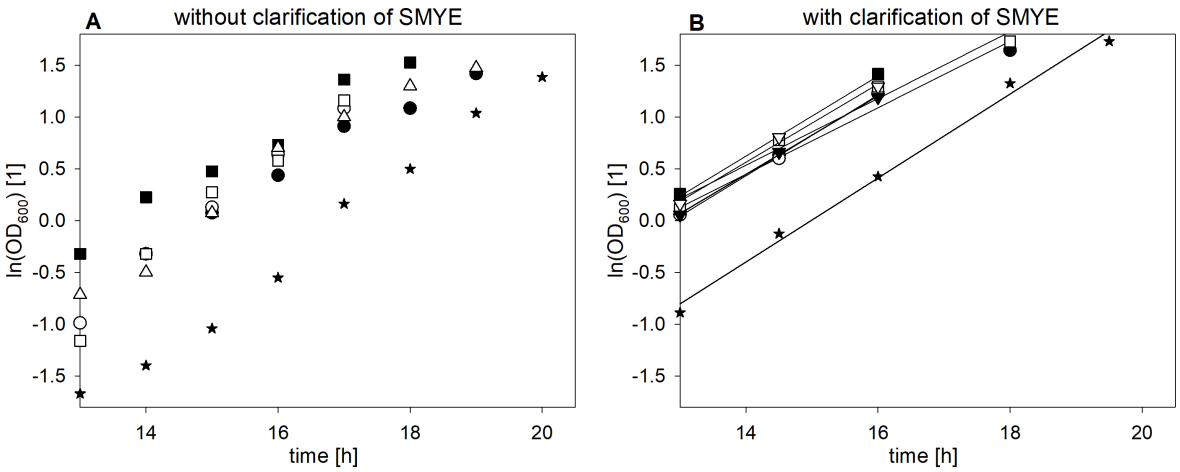


**Figure 11:** Growth rates for different magnesium concentrations and unclarified (A) or clarified (B) SMYE. Open and closed circles - 0.5 g/L, open and closed squares - 0.1 g/L, open and closed triangles up - 0.05 g/L, open and closed triangles down - 0.01 g/L magnesium concentration.

### 4.1.4 Influence of $Na_2CO_3$ addition and inoculum storage condition on the growth rate

Experiments were carried out to identify whether (i) the addition of $Na_2CO_3$ (0.1 and 1 g/L were studied) and/or (ii) the storage conditions of the inoculum (see scheme 4 in Section 3.2) affect the growth rate of *S. stipitis*. Growth rates were determined from the first 8 hours and within the time span of 9-17 hours of cultivation. Results are summarized

**Table 17:** Growth rate $\mu$ determined for two different concentrations of $Na_2CO_3$. Observed hours of growth: 0-8h. The quoted uncertainty corresponds to the standard deviation.

| Media | Source of inoculum | $Na_2CO_3$ c [g/L] | $\mu$ ($R^2 \geq 0.979$) [1/h] |
|---|---|---|---|
| MMe1 | FR | 0.10 | 0.363 ± 0.010 |
| MMe1 | PC(CR) | 0.10 | 0.351 ± 0.016 |
| MMe2 | FR | 1.00 | 0.362 ± 0.009 |
| MMe2 | PC(CR) | 1.00 | 0.334 ± 0.017 |
| MMe+ | FR | – | 0.322 ± 0.016 |
| MMe– | FR | – | 0.183 ± 0.019 |

Abbreviations: c, $Na_2CO_3$ concentration. FR, freshly washed cells. CR, cooling room.

**Table 18:** Growth rate $\mu$ determined for two different concentrations of $Na_2CO_3$. Observed hours of growth: 9-17h. The quoted uncertainty corresponds to the standard deviation.

| Media | Source of inoculum | $Na_2CO_3$ c [g/L] | $\mu$ ($R^2 \geq 0.987$) [1/h] |
|---|---|---|---|
| MMe1 | PC | 0.10 | 0.419 ± 0.021 |
| MMe1 | PC | 0.10 | 0.425 ± 0.013 |
| MMe2 | PC | 1.00 | 0.436 ± 0.008 |
| MMe2 | – | 1.00 | not determined |
| MMe+ | PC | – | 0.387 ± 0.012 |
| MMe– | PC | – | 0.087 ± 0.008 |

Abbreviations: c, $Na_2CO_3$ concentration. FR, freshly washed cells. CR, cooling room.

in Tables 17 and 18. Duplicates in Table 17 were inoculated by two different sources. Each, one time by freshly washed cells (40 mL sodium chloride, centrifugation conditions: 4000 rpm for 5 min at 4 °C) originating from the experiment in Table 18 and one time by washed cells which have been stored overnight in the cooling room (concentrated to $OD_{600}$~10). SMYE was prepared by autoclaving method, TE were omitted.

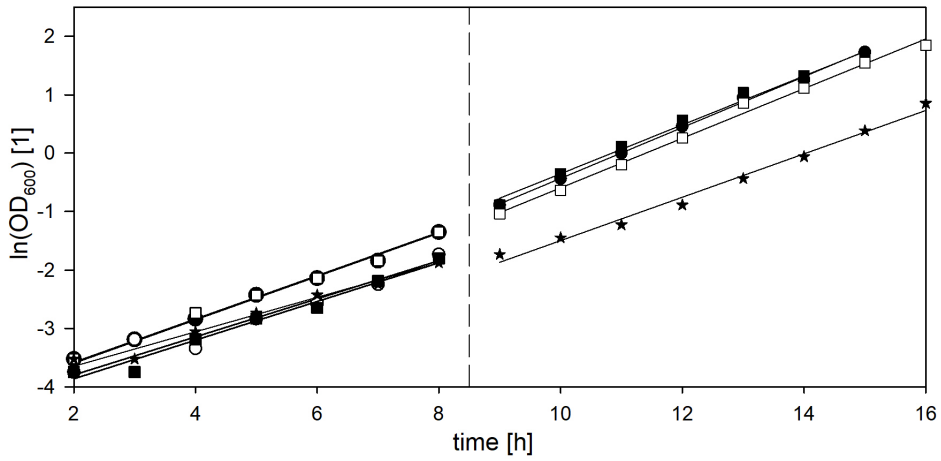


**Figure 12:** Growth rates for different $Na_2CO_3$ concentrations. Open and closed circles - 1 g/L $Na_2CO_3$. Open and closed squares - 0.1 g/L $Na_2CO_3$. Closed stars - Positive control. Note that data separated by the dashed line originates from different experiments. In the left panel closed circles and squares were inoculated with fresh cells, open ones with cells stored in the cooling room.

In Figure 12 both growth curves (determined for the first 8 hours and for the time span within 9-17 hours) were fit together. In both experiments the addition of $Na_2CO_3$ resulted in a small increase of growth rate (compare growth rates of experimental cultivations with those from the positive controls). In contrast, increasing the $Na_2CO_3$ concentration to 1 g/L did not significantly increase the growth rate. A trend to higher growth rates in the later growth stage has been detected, which was already observed with previous experiments.

Growth rates obtained from cultures inoculated with cells stored in the cooling room were slightly lower than those obtained with freshly prepared cells (see Table 17), but still sufficient enough to provide a working serial fermentation routine. An additional study was carried out to investigate the inoculum storage in more detail. With these studies different preparation methods to store the inocula (see next Section 4.2.1) were tested.

## 4.2 Preliminary studies for the SFA

This chapter includes all studies carried out to establish a working routine for a serial fermentation. Additionally, results of experiments which are directly related with the implementation of the SFA (storage of inoculum or final $^{13}$C-enriched cells, phosphate reduction of samples) will be presented. For an in-depth description of the corresponding methodology see Sections 3.1.6 and 3.2. A complete data set of $OD_{600}$ measurements obtained while performing these studies can be found in the supplementary excel sheet `supplemental material_preliminary studies`.

### 4.2.1 Testing of several inoculum storage conditions

During the serial fermentation, between the steps of harvesting the cell suspension and the inoculation of the next cultures, the prepared inocula had to be stored appropriately. A study was conducted in which cells prepared as described in Section 3.1.6.1 were stored overnight at 4 °C (cooling room) suspended either in saline, in saline with glucose or as sole cell pellet. Each inoculum was prepared and tested in duplicates. In Table 19 obtained growth rates are depicted. Figure 13 summarizes the results: While the storage as concentrated cell suspension ($OD_{600} \sim 10$, suspended in NaCl 0.9 %) and storage as pure cell pellet gave similar growth rates (circles and triangles), storage as concentrated cell suspension with sugar gave significant lower growth

**Table 19:** Growth rate $\mu$ determined for inocula stored with different conditions. The quoted uncertainty corresponds to the standard deviation. Determined $R^2$ were greater than 0.944 except for susp. + glc (0.548 and 0.854).

| Media | Storage of inoculum | $\mu$ ($R^2 \geq 0.944$) [1/h] |
|---|---|---|
| MMd2 | suspension | 0.276 ± 0.019 |
| MMd2 | suspension | 0.254 ± 0.024 |
| MMd2 | susp. + glc | 0.087 ± 0.032 |
| MMd2 | susp. + glc | 0.155 ± 0.026 |
| MMd2 | pellet | 0.276 ± 0.025 |
| MMd2 | pellet | 0.250 ± 0.025 |

Abbreviations: glc., cell suspension with glucose.

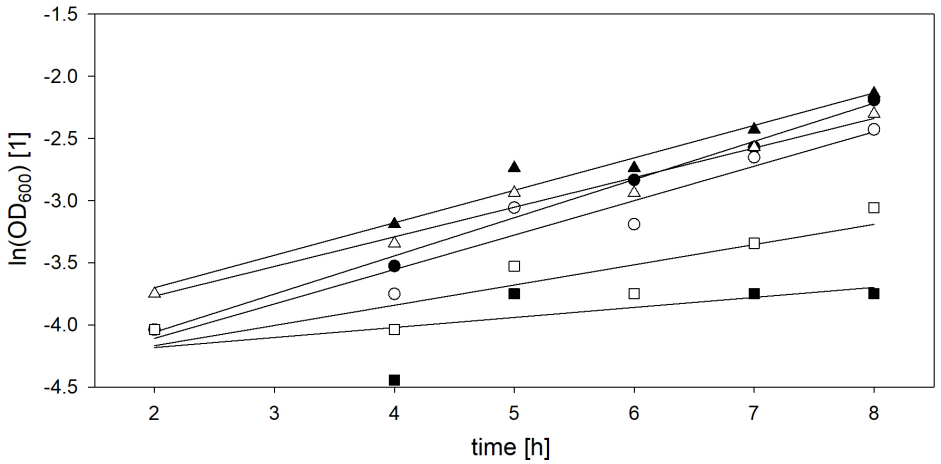


**Figure 13:** Growth rate in response to inocula stored at different conditions. Open and closed circles - stored as cell suspension. Open and closed squares - stored as cell suspension with glucose. Open and closed triangles - stored as sole cell pellet.

rates (squares). Compared to the other investigated storage conditions, growth rate was almost only half as high. However, based on these results cells were stored as suspension in 0.9 % saline at an $OD_{600}$ of ~10, as this preparation requires minimal effort and provides sufficient growth rates.

### 4.2.2 Establishment of a working routine for a serial fermentation

Several further studies were carried out to establish a serial fermentation with sufficient cell growth ($\mu \geq 0.25$), that allows performance of 1 cycle of serial fermentation within 24 hours. Results of these studies will be presented chronologically in this section and are summarized in Table 20.

The first attempt to perform a serial fermentation over several cycles, where vitamins are substituted by $SMYE_{aut}$, always resulted in a drastic loss of growth after cycle 1. In Figure 15 (panel A) this outcome is illustrated: Compared to the first cycle of serial fermentation (closed symbols), growth rates of the second cycle were reduced by a factor of 2-3 (open symbols). For both cycles of serial fermentation, duplicate cultivations were performed, each, prepared one time with and one time without TE. TE omission gave controversial results. While during cycle 1, cultures prepared with TE had a significant higher growth rate, it was the opposite case for cycle 2 (compare growth rates in Table 20 or circles and squares in panel A).
In the next study it was tempted to retain a constant growth rate over more cycles by adding thiamine or pantothenic acid, since these vitamins are known to be degraded when exposed to heat [50, 51, 52]. However, still a reduction of growth occurred for both conditions (panel B; circles for pantothenic acid, squares in for thiamine) after the first cycle (open symbols), while the positive control (stars) maintained its growth rate over both cycles. However, addition of pantothenic acid and thiamine did again result in a similar 2.5-fold reduced growth rate for cells cultivated in the second cycle. It was assumed, that the preparation of SMYE by autoclaving method might be too harmful for essential vitamins, since high heat and pressure are applied. Therefore, the more gentle method of bead beating was investigated. $SMYE_{bb}$ was prepared as described in Section 3.1.5. Two cultivations were performed in parallel, differing only in the applied bead beating volume of 0.5 or 1 mL. Considering the growth rate, this method gave a SMYE of at least the same quality as with autoclaving or boil-


**Figure 14:** Sterility control for SMYE. Top - SMYE; Bottom - positive control.

ing method (compare growth rates of cycle 1 in Table 20). But when considering the experimental effort, bead beating has proven to be by far superior: In contrast to the other SMYE preparation methods tested in this thesis (autoclaving, boiling), bead beating can be performed within several minutes ($\leq 8$ minutes). Furthermore, as the other tested SMYE preparation methods, it provides a yeast extract of hundred percent sterility (see Figure 14). Nevertheless, the bead beating method could not provide a SMYE which enables a serial fermentation for more than one cylce (compare open and closed symbols in Figure 18, panel C). During cycle 2, after 19 hours of cultivation biotin was added, since biotin is also known to be a vitamin crucial for yeast growth [24]. Figure 15, panel C (open symbols after dashed line) illustrates, that after addition of biotin *S. stipitis* could recover to growth rates similar to those observed in cycle 1 within two hours.

**Table 20:** Effects of SMYE preparation method as well as vitamin addition on the growth rate $\mu$ of *S. stipitis* during several cycles of serial fermentation. Dashed lines separate experiments which were carried out jointly. Individual experiments are separated by dashed lines. The depicted uncertainty refers to the standard deviation.

| Media | Cycle | PM | BB volume [mL] | Trace elements | Vitamins added | $\mu$ [1/h] |
|---|---|---|---|---|---|---|
| MMs2 | 1 | autoclaving | – | – | – | 0.258 ± 0.012 |
| MMs3 | 1 | autoclaving | – | + | – | 0.302 ± 0.009 |
| MMs2 | 2 | autoclaving | – | – | – | 0.127 ± 0.000 |
| MMs3 | 2 | autoclaving | – | + | – | 0.106 ± 0.007 |
| MMs4 | 1 | autoclaving | – | + | Pa | 0.372 ± 0.000 |
| MMs5 | 1 | autoclaving | – | + | Th | 0.365 ± 0.000 |
| MMs1 | 1 | – | – | + | V | 0.337 ± 0.018 |
| MMs4 | 2 | autoclaving | – | + | Pa | 0.132 ± 0.009 |
| MMs5 | 2 | autoclaving | – | + | Th | 0.146 ± 0.012 |
| MMs1 | 2 | – | – | + | V | 0.368 ± 0.003 |
| MMs6 | 1 | bead beating | 0.5 | + | – | 0.395 ± 0.000 |
| MMs6 | 1 | bead beating | 1.0 | + | – | 0.380 ± 0.000 |
| MMs1 | 1 | – | – | + | – | 0.351 ± 0.002 |
| MMs6 | 2 | bead beating | 0.5 | + | – | 0.053 ± 0.000 |
| MMs6 | 2 | bead beating | 1.0 | + | – | 0.122 ± 0.000 |
| MMs1 | 2 | – | – | + | – | 0.308 ± 0.026 |
| MMs7 | 2 | bead beating | 0.5 | + | B | 0.322 ± 0.000 |
| MMs7 | 2 | bead beating | 1.0 | + | B | 0.490 ± 0.074 |
| MMs7 | 1 | bead beating | 0.5 | + | B | 0.384 ± 0.000 |
| MMs7 | 2 | bead beating | 0.5 | + | B | 0.378 ± 0.000 |
| MMs7 | 3 | bead beating | 0.5 | + | B | 0.368 ± 0.000 |
| MMs7 | 4 | bead beating | 0.5 | + | B | 0.366 ± 0.000 |

Abbreviations: BB, bead beating. PM, SMYE method of preparation. Pa, pantothenic acid. Th, thiamine. V, vitamin stock solution. B, biotine.

The effectiveness of biotin addition was proven in another serial fermentation experiment. Results are shown in Figure 15, panel D: Using this medium composition (MMs7) *S. stipitis* could be cultivated at a constant growth rate for 4 cycles without a significant decrease of growth rate.

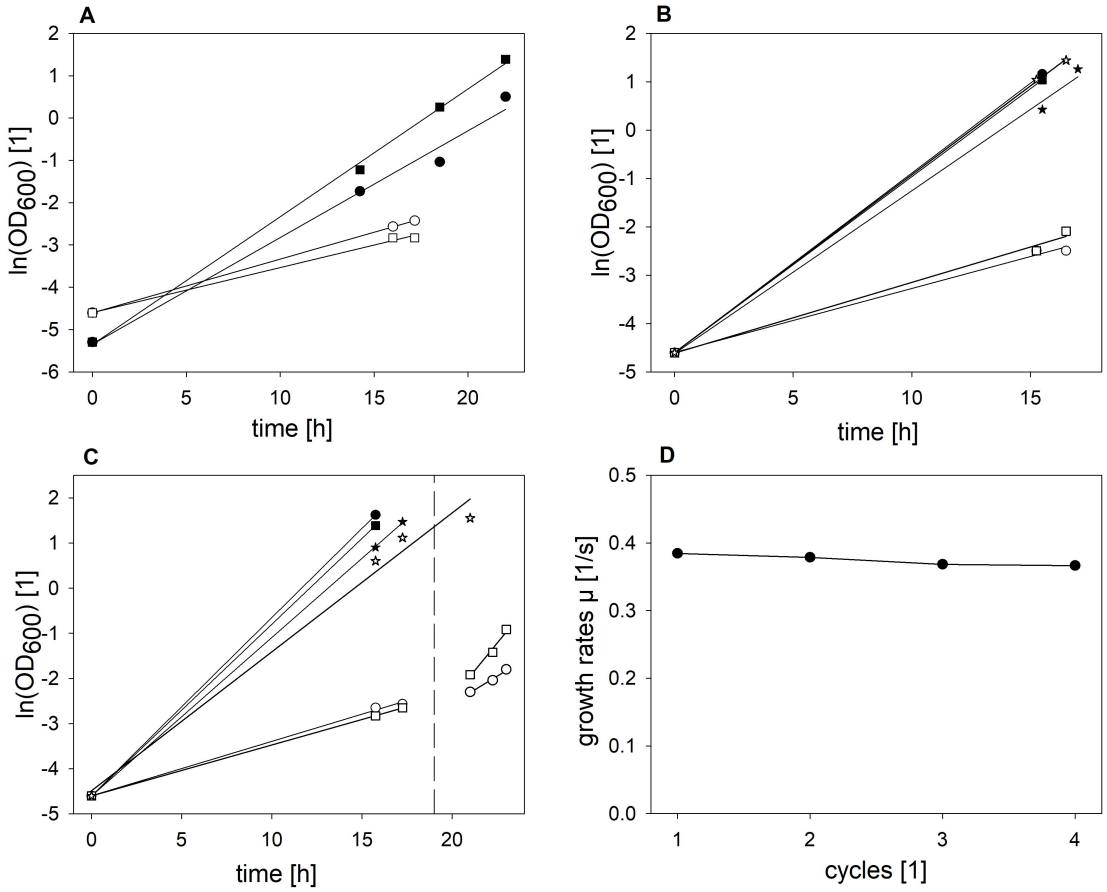


**Figure 15:** Growth rate $\mu$ depicted for two or more cycles of serial fermentation. Within each panel, a different strategy for establishing a serial fermentation routine is illustrated. Except for (D), closed symbols refer to cycle 1 and open symbols to cycle 2. Stars refer to positive controls. (A) Circles - without TE; Squares - with TE. (B) Circles - pantothenic acid; Squares - thiamine. (C) Circles - bead beating volume 0.5 mL; Squares - bead beating volume 1 mL. The dashed line in panel C indicates the moment of biotin addition to the experimental flasks of cycle 2.

### 4.2.3 Adaption of the cultivation conditions for the needs of SFA

Two experiments were carried out to adjust the working volume and shaking frequency for the purpose of serial fermentation. The cultivation volume was lowered in order to waste less expensive $^{13}$C-labelled glucose substrate, but still providing enough cell suspension for the preparation of SMYE, to serve as inoculum, to supervize the SFA with $OD_{600}$ measurements and for sampling, if neccessary. It was a attempted to compensate for possible negative effects of the lowered cultivation volume with an increased shaking frequency. Different working volumes (10, 15, 20 and 30 mL) were tested at distinct shaking frequencies (120 and 160 rpm), each in duplicates. The growth rate was used as

read-out parameter. In Tables 21 and 22, respectively, results of the experiments with a shaking frequency of 120 rpm and 160 rpm are depicted. Both experiments were performed for two cycles of serial fermentation.

**Table 21:** Growth rate $\mu$ determined for three different cultivation volumes at a shaking frequency of 120 rpm. The quoted uncertainty corresponds to the standard deviation.

| Medium | Cycle | CV [mL] | $\mu$ ($R^2 \geq 0.999$) [1/h] |
|---|---|---|---|
| MMs7 | 1 | 15 | 0.380 ± 0.008 |
| MMs7 | 1 | 15 | 0.353 ± 0.009 |
| MMs7 | 1 | 20 | 0.404 ± 0.000 |
| MMs7 | 1 | 20 | 0.405 ± 0.000 |
| MMs7 | 1 | 30 | 0.418 ± 0.000 |
| MMs7 | 2 | 15 | 0.351 ± 0.003 |
| MMs7 | 2 | 15 | 0.336 ± 0.004 |
| MMs7 | 2 | 20 | 0.370 ± 0.003 |
| MMs7 | 2 | 20 | 0.364 ± 0.000 |
| MMs7 | 2 | 30 | 0.389 ± 0.005 |

Abbreviations: CV, cultivation volume.

**Table 22:** Growth rate $\mu$ determined for two different cultivation volumes at a shaking frequency of 160 rpm. The quoted uncertainty corresponds to the standard deviation.

| Medium | Cycle | CV [mL] | $\mu$ ($R^2 \geq 0.998$) [1/h] |
|---|---|---|---|
| MMs7 | 1 | 10 | 0.324 ± 0.008 |
| MMs7 | 1 | 10 | 0.332 ± 0.003 |
| MMs7 | 1 | 30 | 0.370 ± 0.000 |
| MMs7 | 1 | 30 | 0.395 ± 0.000 |
| MMs7 | 2 | 10 | 0.279 ± 0.006 |
| MMs7 | 2 | 10 | 0.332 ± 0.005 |
| MMs7 | 2 | 30 | 0.375 ± 0.000 |
| MMs7 | 2 | 30 | 0.355 ± 0.000 |

Abbreviations: CV, cultivation volume.

In Figure 16 results of both studies (panel A - 120 rpm; panel B - 160 rpm) are presented. In both experiments the growth rate had the tendency to be higher for larger cultivation volumes. In contrast, enhancing the shaking frequency by 40 rpm did not significantly increase the growth rate. Furthermore, a decrease of growth rate after cycle 1 was observed.

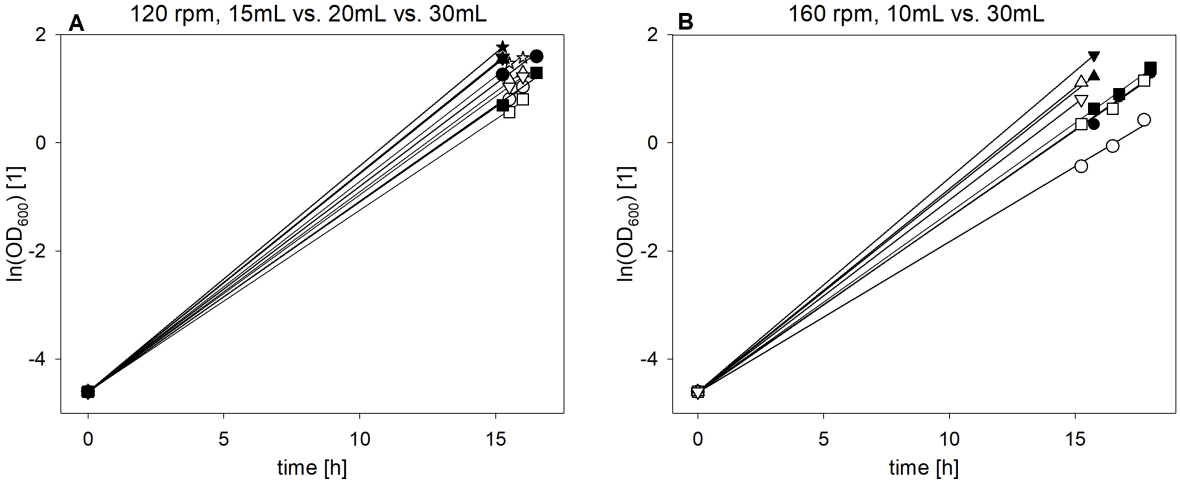


**Figure 16:** Growth rate $\mu$ in response to different cultivation volumes exposed to a shaking frequency of 120 rpm (A) or 160 rpm (B). Closed symbols refer to the first cycle and open symbols to the second cycle of serial fermentation. (A) Circles and squares - 15 mL, triangles up and down - 20 mL, stars - 30 mL of working volume. (B) Circles and squares - 10 mL, triangles up and down - 30 mL working volume.

### 4.2.4 Reduction of phosphate concentration in samples for LC-ESI/MS

High amounts of phosphate present in the sample matrix are known to decrease the reliability of LC-ESI/MS due to ion suppression and space charge effects [29]. Lowering the initial amount of $KH_2PO_4$ in the medium composition to 0.25 g/L as done in earlier studies on the I.B.B. [30] turned out to be problematic, due to the necessity of measuring and adjusting the pH value frequently, which also comes along with possible $^{12}C$-contaminations. Therefore, an additional washing-step during the quenching procedure was introduced, to gather similar phosphate concentrations in the final LC-ESI/MS samples as obtained with a low-phosphate cultivation.

In order to test the additional washing-step, the quenching procedure was simulated (see Section 3.3.5) for four cell suspensions with different amounts of $KH_2PO_4$. Duplicate samples were taken in order to determine the phosphate concentration after several steps of the quenching procedure. For a detailed description of the implementation of this study see Section 3.3.4. A standard calibration curve was established ($R^2$=0.995) and using its slope, the phosphate concentrations depicted in Table 23 were calculated. Furthermore, the quantity of phosphate in grams in the remaining liquid on the finally quenched cell pellet was determined.

**Table 23:** Phosphate concentrations after different steps of the quenching procedure. Duplicate measurements are separated by dashed lines.

| Sample number | Pi[a] c [g/L] | refound Pi concentrations [mM] Initial | Quenching | Washing | Pi[b] [µg] Wash. |
|---|---|---|---|---|---|
| 1.1 | 14.1 | 99.24 | 21.67 | 0.050 | 0.84 |
| 1.2 | 14.1 | 99.24 | 21.47 | 0.043 | 0.73 |
| 2.1 | 4.00 | 31.56 | 7.44 | 0.022 | 0.27 |
| 2.2 | 4.00 | 32.02 | 7.19 | 0.022 | 0.26 |
| 3.1 | 1.50 | 13.19 | 2.45 | 0.016 | 0.21 |
| 3.1 | 1.50 | 13.06 | 2.48 | 0.015 | 0.21 |
| 4.1 | 0.25 | 2.89 | 0.41 | 0.010 | 0.14 |
| 4.2 | 0.25 | 1.95 | 0.40 | 0.010 | 0.14 |

[a] Initial phosphate concentration of the cell suspension for simulating the quenching procedure. [b] Phosphate amount in the remaining liquid of the quenched cell pellet. Abbreviations: c, phosphate concentration.

In Table 23 the findings are summarized: By introducing a washing step, the phosphate amount could be diluted down to a concentration not more than 0.05 mM. This concentration is already far beyond the concentration obtained by just lowering the initial $KH_2PO_4$ amount to 0.25 g/L (1.95-2.89 g/L). Coming from a cultivation with 14.1 g/L $KH_2PO_4$, after quenching and washing of the LC-ESI/MS sample, only a quantity of about 0.8 µg phosphate remained in the sample matrix. As introducing a washing step

alone gave already satisfying results, the $KH_2PO_4$ concentration of the culture medium was maintained for providing a stable pH value during the serial fermentation.

### 4.2.5 Long-term storage of final $^{13}$C-enriched cells

An experiment was conducted in order to find an appropriate storage compound for the final $^{13}$C-labelled cells after the implementation of the SFA. Common storage compounds like glycerol were not suitable for this purpose, since *S. stipitis* is able to use glycerol as a substrate, which could lead to a $^{12}$C-contamination of the fianl $^{13}$C-enriched cells again. Three different storage compounds (PEG3350, PEG8000, PEG20000) and storage as sole cell pellet were investigated. Common yeast preparation by glycerol was used as reference. For a detailed description of the methodology of this experiment consult Section 3.1.6.2.

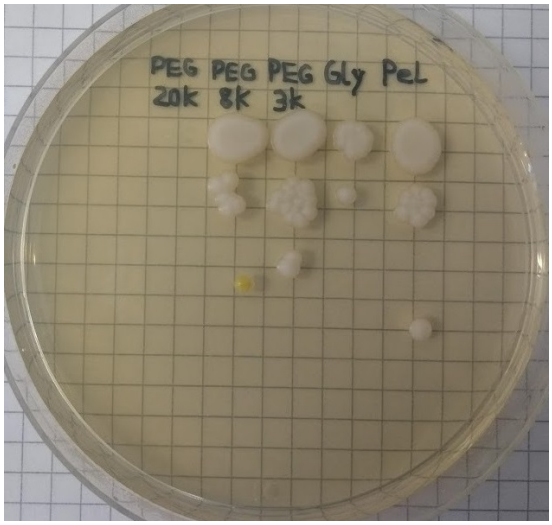


(a) after 1 day

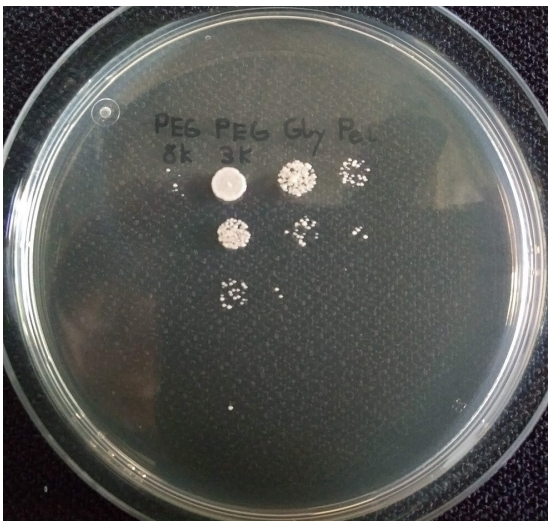


(b) after 1 month

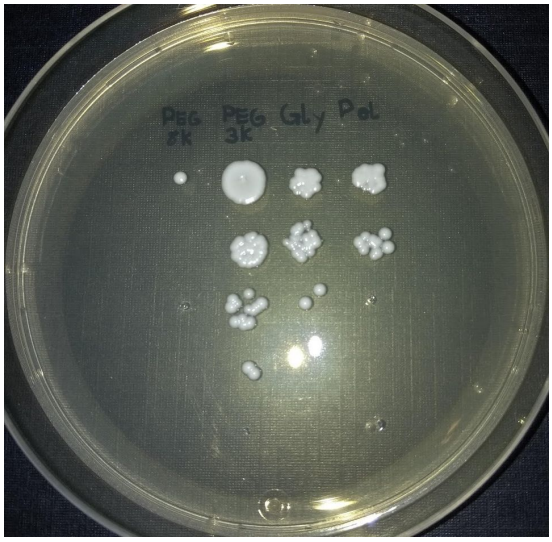


(c) after 4 month


(d) after 6 month

**Figure 17:** Abbreviations: PEG, polyethylene glycol; Gly, glycerol; Pel, pellet. Dilutions from top to bottom: 1:100, 1:10000, 1:100000, 1:1000000 for (A) and 1:10, 1:100, 1:1000, 1:10000, 1:100000 for (B) to (C).

Results are shown in Figure 17: After 1 day of storage, cells prepared with PEG20000 did not show any growth. PEG20000 is therefore not suitable as storage compound. PEG8000 and storage as sole cell pellet showed both growth, even after six month of storage. In general, it was observed, the lower the molecular weight of the applied PEG, the better the viability of *S. stipitis* was preserved. Hence, PEG3350 preserved the viability of cells by far the most, even better than common glycerol. Therefore, PEG3350 was chosen ultimately as storage compound for the final $^{13}$C-enriched cells.

## 4.3 Realization of the SFA

This chapter deals about the results and issues observed during the actual implementation of the SFA, the subsequent LC-ESI/MS measurement as well as the data processing. The SFA was carried out as described in Section 3.2 and in accordance with the schedule shown in Table 10. $OD_{600}$ measurement series for determining the growth rate during the SFA are found in the supplementary excel sheet `supplemental material_preliminary studies`. The resulting data sets after different steps of the data processing procedure are provided in the supplementary excel file `supplemental material_data processing`.

### 4.3.1 Monitoring of the implementation of the two runs of SFA

Tables 24 and 25 comprise the monitoring of the first and the second run, respectively. While in the first run unlabelled $^{12}C$-$Na_2CO_3$ was added, in the second run its $^{13}C$-labelled

**Table 24:** Monitoring of the first run of the SFA, where $^{12}C$-$Na_2CO_3$ was added. Cycles at which samples were withdrawn for LC-ESI/MS analysis are shown in grey. $OD_{600}$ represents the final optical density when cultures were harvested. Coefficients of determination $R^2$ of the growth rate $\mu$ were in a range of 0.994-0.999

| Cycle | no $^{12}C$-$Na_2CO_3$ | | | 0.1 g/L $^{12}C$-$Na_2CO_3$ | | | 1 g/L $^{12}C$-$Na_2CO_3$ | | |
|---|---|---|---|---|---|---|---|---|---|
| | $OD_{600}$ [1] | Gen.[a] | $\mu$ [1/h] | $OD_{600}$ [1] | Gen.[a] | $\mu$ [1/h] | $OD_{600}$ [1] | Gen.[a] | $\mu$ [1/h] |
| 0 | 3.59 | 8.5 | 0.324 | 3.24 | 8.3 | 0.345 | 3.41 | 8.4 | 0.369 |
| 1 | 3.06 | 8.3 | 0.356 | 3.47 | 8.4 | 0.373 | 4.00 | 8.6 | 0.367 |
| 2 | 3.06 | 8.3 | 0.333 | 2.94 | 8.2 | 0.337 | 3.71 | 8.5 | 0.351 |
| 3 | 3.35 | 8.4 | 0.344 | 3.12 | 8.3 | 0.348 | 3.00 | 8.1 | 0.315 |
| 4 | 2.82 | 8.1 | 0.327 | 2.88 | 8.2 | 0.326 | 3.18 | 8.3 | 0.349 |
| 5 | 1.82 | 7.5 | 0.303 | 2.94 | 8.2 | 0.345 | 3.12 | 8.3 | 0.339 |
| 6 | 3.12 | 8.3 | 0.313 | 1.71 | 7.4 | 0.286 | 3.41 | 8.4 | 0.316 |
| 7 | 3.06 | 8.3 | 0.312 | 2.94 | 8.2 | 0.287 | 2.65 | 8.3 | 0.319 |

[a] Generations per cycle - number of doublings of *S. stipitis* per cylce.

**Table 25:** Monitoring of the second run of the SFA, where $^{13}C$-$Na_2CO_3$ was added. Cycles at which samples were withdrawn for LC-ESI/MS analysis are shown in grey. $OD_{600}$ represents the final optical density when cultures were harvested. Coefficients of determination $R^2$ of the growth rate $\mu$ were in a range of 0.985-0.999

| Cycle | no $^{13}C$-$Na_2CO_3$ | | | 0.1 g/L $^{13}C$-$Na_2CO_3$ | | | 1 g/L $^{13}C$-$Na_2CO_3$ | | |
|---|---|---|---|---|---|---|---|---|---|
| | $OD_{600}$ [1] | Gen.[a] | $\mu$ [1/h] | $OD_{600}$ [1] | Gen.[a] | $\mu$ [1/h] | $OD_{600}$ [1] | Gen.[a] | $\mu$ [1/h] |
| 0 | 3.18 | 8.5 | 0.316 | 3.71 | 8.5 | 0.333 | 4.18 | 8.7 | 0.331 |
| 1 | 2.94 | 8.2 | 0.341 | 3.18 | 8.3 | 0.344 | 3.06 | 8.3 | 0.354 |
| 2 | 2.82 | 8.1 | 0.255 | 2.29 | 7.8 | 0.242 | 2.59 | 8.0 | 0.319 |
| 3 | 2.47 | 7.9 | 0.237 | 2.53 | 8.0 | 0.263 | 3.12 | 8.3 | 0.270 |
| 4* | 3.00 | 8.2 | 0.251 | 3.94 | 8.6 | 0.263 | 4.06 | 8.7 | 0.271 |
| 5 | 2.82 | 8.1 | 0.302 | 3.00 | 8.2 | 0.304 | 3.94 | 8.6 | 0.324 |
| 6 | 2.59 | 8.0 | 0.261 | 2.82 | 8.1 | 0.250 | 3.06 | 8.3 | 0.265 |
| 7* | 3.00 | 8.2 | 0.166 | 3.18 | 8.3 | 0.236 | 3.67 | 8.6 | 0.270 |

[a] Generations - number of doublings of *S. stipitis* per cylce. * Addition of 20 µL TE.

equivalent was applied. In both runs a cultivation without any $Na_2CO_3$ added served as reference. Growth rates were determined with at least three $OD_{600}$ measurements and used as readout parameter in order to evaluate the physiological condition of *S. stipitis* during the serial fermentation.

In Figure 18 the obtained growth rates as a function of the fermentation cycles for the first (A) and the second (B) run of the SFA are illustrated. During the first run, the growth rate declined slightly but noticeable over time by about 10 %. However, a drastic decrease which could seriously impede the time management, was never observed.

In contrast, during the second run of the SFA the growth rate dropped two times (during cycles 3 and 7) to a critical level, which could impair the time management of experiments substantially. For this reason, in cycles 4 and 7 20 µL of TE stock solution were spiked to all cultures (indicated by dashed line in panel B). After TE addition all cultures recovered their growth rates within two hours. Note that growth rates depicted in Table 25 and Figure 18 (B) were determined before addition of TE. An influence of the $Na_2CO_3$ addition was not observed, since all three cultures of both runs showed nearly the same growth behaviour.

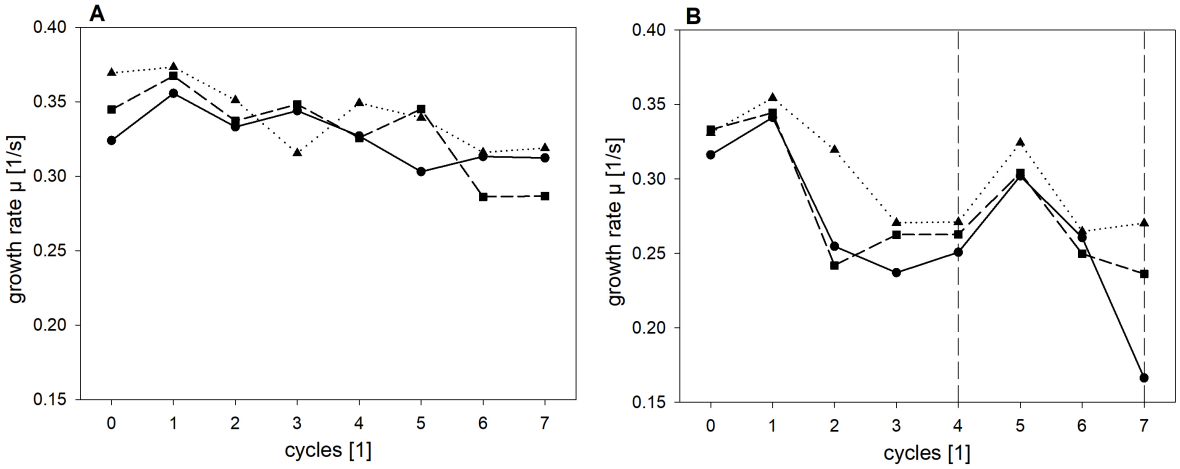


**Figure 18:** Growth rate $\mu$ during the course of serial fermentation. (A) Experiments with addition of $^{12}C$-$Na_2CO_3$. (B) Experiments with addition of $^{13}C$-labelled $Na_2CO_3$. Circles - no addition of $Na_2CO_3$. Squares - addition of 0.1 g/L $^{12}C/^{13}C$-labelled $Na_2CO_3$. Triangles - addition of 1 g/L $^{12}C/^{13}C$-labelled $Na_2CO_3$. The dashed line in (B) indicates the moment of TE spiking.

### 4.3.2 Sampling for LC-ESI/MS during the SFA

Table 26 summarizes all observed final optical densities when samples were taken and the respective sampling volume of both runs of the SFA. It was attempted to take samples when the cultures reached an $OD_{600}$ in a range of 3-3.5. For some samples this could not be fulfilled due to time-management reasons. In theses cases, the sampling volume was adapted in order to ensure the same amount of biomass in all samples (see equation 3, Section 3.3.1).

**Table 26:** Overview of all LC-ESI/MS samples taken during both runs of the SFA. $OD_{600}$ represents the final optical density when samples were taken.

| SFA | Sample | Cycle | no $Na_2CO_3$ | | 0.1 g/L $Na_2CO_3$ | | 1 g/L $Na_2CO_3$ | |
|---|---|---|---|---|---|---|---|---|
| | | | $OD_{600}$ [1] | SV [µL] | $OD_{600}$ [1] | SV [µL] | $OD_{600}$ [1] | SV[µL] |
| first run | 1 | 0 | 3.59 | 836 | 3.24 | 936 | 3.41 | 880 |
| | 2 | 7 | 3.06 | 981 | 2.94 | 1020 | 3.06 | 981 |
| second run | 1 | 0 | 3.18 | 945 | 3.71 | 718 | 4.18 | 810 |
| | 2 | 3 | 2.47 | 1215 | 2.53 | 962 | 3.12 | 1186 |
| | 3 | 7 | 3.00 | 1000 | 3.18 | 797 | 3.67 | 944 |

Abbreviations: SFA, serial fermentation approach; SV, sampling volume.

### 4.3.3 LC-ESI/MS measurement

Prior to the LC-ESI/MS measurement samples were dried by lyophilization (see Section 3.3.5). For seven replicates drying overnight remained incomplete (leftover ES in falcon tubes) at the first attempt and was therefore repeated for these replicates. As these replicates did not show remarkably decreased metabolite levels after data processing, they were not excluded from further calculations.

During the measurement of batch 1 (after analysis of 16 globally randomized replicates) issues with the methodology arose and the LC-ESI/MS system had to be restarted completely. It is assumed that this incident was caused by clogging of the injection needle. Figure 19 provides a view on the overall quality of the LC-ESI/MS measurement. In (A) the sum of all metabolite signals (areas) obtained for all QC samples, whereas in (B) the corresponding averages are shown. White dashed bars represent the first fraction of batch 1 before restarting the LC-ESI/MS system, while the pure white bars refer to the second fraction of batch 1 after restart. QC 4 was measured two times - before and after restart (QC 4 and QC 4.2).

A comparison of the averaged batches in (B) demonstrates that the quality of LC-ESI/MS instruments increased with time: Both, signal levels as well as accuracy of measurement (reduced standard deviations, see error bars in (B)) significantly increased from batch 1 to batch 3. As the QCs of the first fraction of batch 1 differed significantly from each other (compare with error bars in panel B) and showed low signal levels in general, the first 12 replicates of batch 1 were completely excluded from further calculations. Since every LC-ESI/MS sample was underpinned by four replicates, evaluation was still possible but with decreased accuracy. Additionally, replicates measured before QC 4.2 were also excluded due to the low signal level after restart of the LC-ESI/MS system.

Although the dried metabolites were re-suspended to similar concentrations as in earlier studies [30], the LC-ESI/MS measurement gave in general rather low signals. For many metabolites signals were to low to distinguish them from noise level. Compared to earlier studies that were performed by I.B.B. at JOANNEUM RESEARCH, signal yield was in average about 2-3 magnitudes lower. Reasons for this decrease are so far unknown.

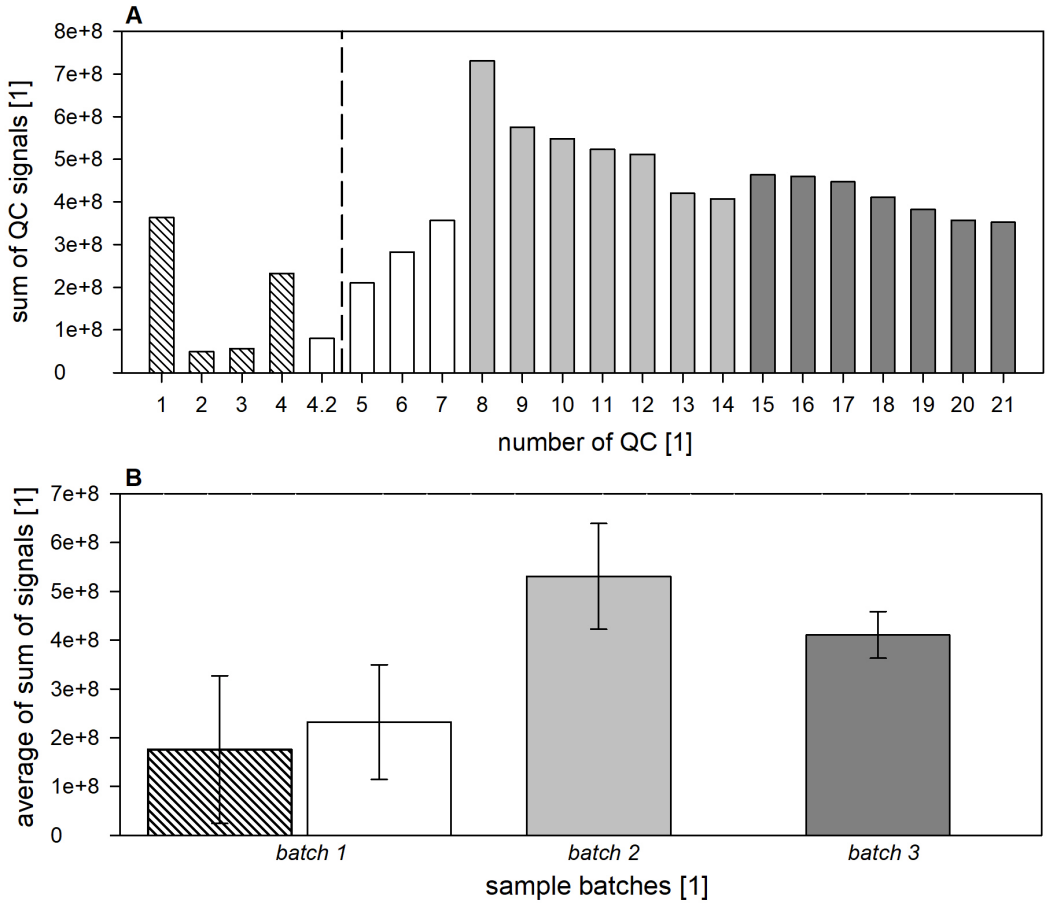


**Figure 19:** Evaluation of the overall quality of data obtained from LC-ESI/MS analysis. (A) Sum of all QC areas over all metabolite signals. White bars and white dashed bars - batch 1; Grey bars - batch 2; Dark grey bars - batch 3. The dashed line indicates the proportion of replicates which were excluded. (B) - Bars represent the average of the sum of the QC signals. Error bars indicate the corresponding standard deviations.

### 4.3.4 Metabolite exclusion due to blank loading

After the three batches of raw data were cleaned for negative values and merged, the areas of the QCs were compared with the areas of the blanks in order to detect blank loading as described in Section 3.3.7. Out of the 231 metabolites for which peaks were found, 60 (45 $^{12}$C- and 15 $^{13}$C-components) were removed due to high blank loading. 44 of these excluded metabolites were acids. Also in earlier studies on the I.B.B. acids were found to be problematic with the deployed LC-ESI/MS setup.

### 4.3.5 Outlier removal and averaging of replicates

Metabolite-wise outlier removal and averaging of replicates were performed as elucidated in Section 3.3.7. Some samples were determined by less than four replicates, since eleven of the replicates had to be excluded due to the above mentioned restart of the LC-ESI/MS system. From the 15 samples in total, 7 and 6 were underpinned by four or three replicates, respectively, and 2 samples by only one or two replicates (sample of cycle 7 with addition of 1 g/L $^{12}$C-$Na_2CO_3$ and sample of cycle 3 with addition of 0.1 g/L $^{13}$C-$Na_2CO_3$).

### 4.3.6 Trend correction and normalization

Trend correction and normalization steps were introduced in order to compensate for trend effects and to make batches comparable for metabolite level determination.
In total, in each batch for about half of the detected metabolites, trend correction led to a significant reduction of the RSE. Figure 20 illustrates an example of the trend correction: For capric acid ($^{12}$C) a linear metabolite degradation over time was detected (indicated by the linear regression over squares). After trend correction (filled circles) no trend appeared any more.

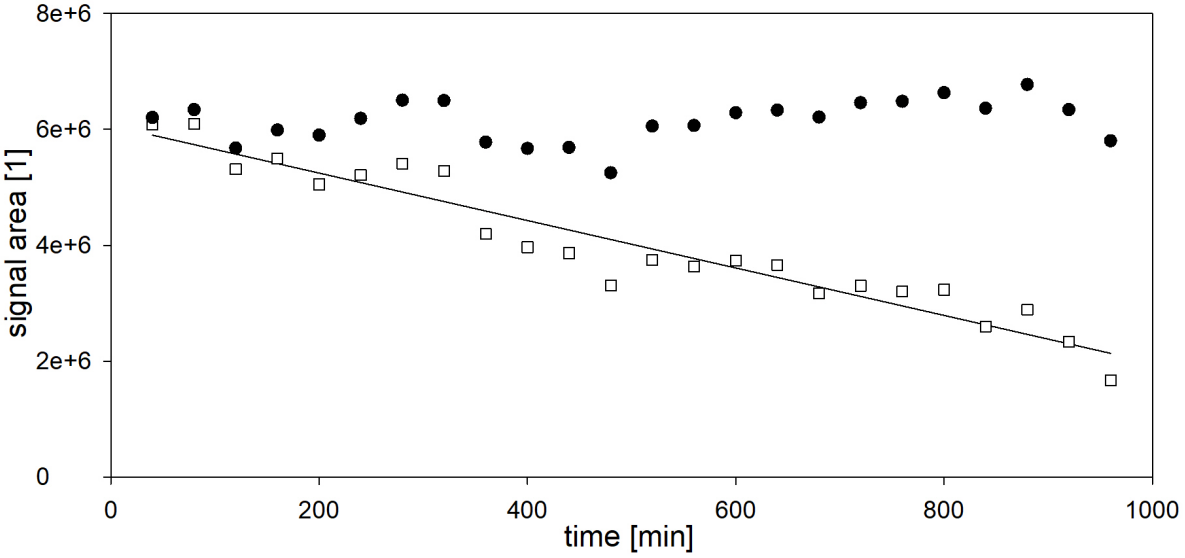


**Figure 20:** Trend correction illustrated with the example of capric acid $^{12}$C. Open squares - before trend correction. Filled circles - after trend correction. Solid line indicates linear regression before trend correction.

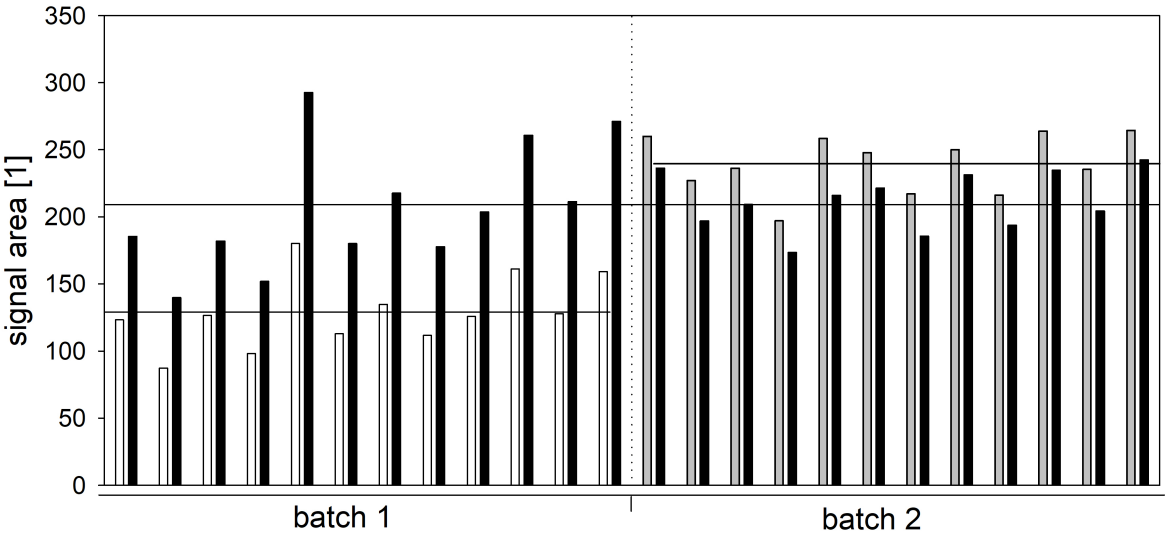


**Figure 21:** Example of the normalization step. White and grey bars represent the sum of signal areas of batch 1 and batch 2, respectively. Black bars constitute the sum of signal areas after normalization. The dotted line separates batch 1 from batch 2. The filled lines represent the averaged sums of signals before and after the normalization step.

In Figure 21 the normalization of batch 1 (white bars) and batch 2 (grey bars) is exemplarily depicted. Before the normalization, sums of signal areas were almost twice as high as for batch 2 compared to batch 1 (see solid lines of each batch in Figure 21). After normalization (black bars) sums of signals were increased for batch 1 and decreased slightly for batch 2. On average (continuous line) signal areas of both batches were the same now.

## 4.4 Metabolomics

In this chapter all findings regarding the $^{13}$C-labelling effectiveness of the introduced hypothesis will be presented. Data processing and data evaluation steps were performed as described in Section 3.3.7 and 3.3.8, respectively. A complete data set containing all findings of the metabolomics study can be found in the supplementary excel sheet `supplemental material_LCMS`.

### 4.4.1 $^{13}$C-ER depending on the number of fermentation cycles

This section includes the metabolite-specific $^{13}$C-ER as a function of the number of fermentation cycles. Table 27 provides a summary of the $^{13}$C-ER of the three sub-experiments (no $Na_2CO_3$, addition of 0.1 and 1 g/L $Na_2cO_3$) of the second run of the SFA.

**Table 27:** Distribution of the 127 metabolites according to their labelling behaviour during serial fermentation.

| | $^{13}$C-ER | Number of metabolites | | |
|---|---|---|---|---|
| | | no $^{13}$C-$Na_2CO_3$ | 0.1 g/L $^{13}$C-$Na_2CO_3$ | 1 g/L $^{13}$C-$Na_2CO_3$ |
| constantly labelled | 100% | 71 (53[a]/18[c]) | 71 (53[a]/18[c]) | 71 (53[a]/18[c]) |
| | >90% | 12 | 14 | 14 |
| | 10%<x<90% | 8 | 8 | 7 |
| | <10% | 4 | 4 | 5 |
| | 0% | 18 (12[b]/6[c]) | 18 (12[b]/6[c]) | 18 (12[b]/6[c]) |
| other | effects | 12 | 12 | 12 |
| | excluded | 2 | – | – |
| | sum | 127 | 127 | 127 |

[a] Missing $^{12}$C-signal. [b] Missing $^{13}$C-signal. [c] Blankload too high.

In total, a $^{13}$C-ER could be calculated for 127 metabolites. Among these 127 metabolites, in all experiments for 71 and 18 metabolites the $^{13}$C-ER was determined to be 100% and 0%, respectively, since either the corresponding $^{12}$C- or $^{13}$C-signal peaks were not found or the corresponding $^{12}$C- or $^{13}$C-metabolite was excluded priorly due to high blankloading. Out of the remaining 38 metabolites, 26 had a confirmed constant labelling between 0 and 100 %, whereby approximately half of them revealed a $^{13}$C-ER greater 90 % and fewer than one fifth below 10 %. In the experiment without addition of $Na_2CO_3$ 2 metabolites were excluded due to inconsistencies in the underlying data.
For all three experiments 12 metabolites were found that exhibit effects (increase or decrease of $^{13}$C-ER) depending on the number of fermentation cycles. Labelling profiles of these metabolites will be presented on the following pages. A full list of all metabolites and their corresponding $^{13}$C-ER can be found in the supplemental material (see Section 7, Table 31).

### $^{13}$C-ER without addition of $Na_2CO_3$

For 12 metabolites effects in the $^{13}$C-ER as a function of the number of serial fermentation cycles were observed (see Figure 22). For 10 of these metabolites the $^{13}$C-ER increased significantly (PI 34:1, PI 34:2, PI 36:3, PI 36:4, panthotenic acid, mannitol/sorbitol, trehalose, succinic acid, lysine, acetylglycine), for 2 contradictory results were obtained (ascorbic acid, histidinol).

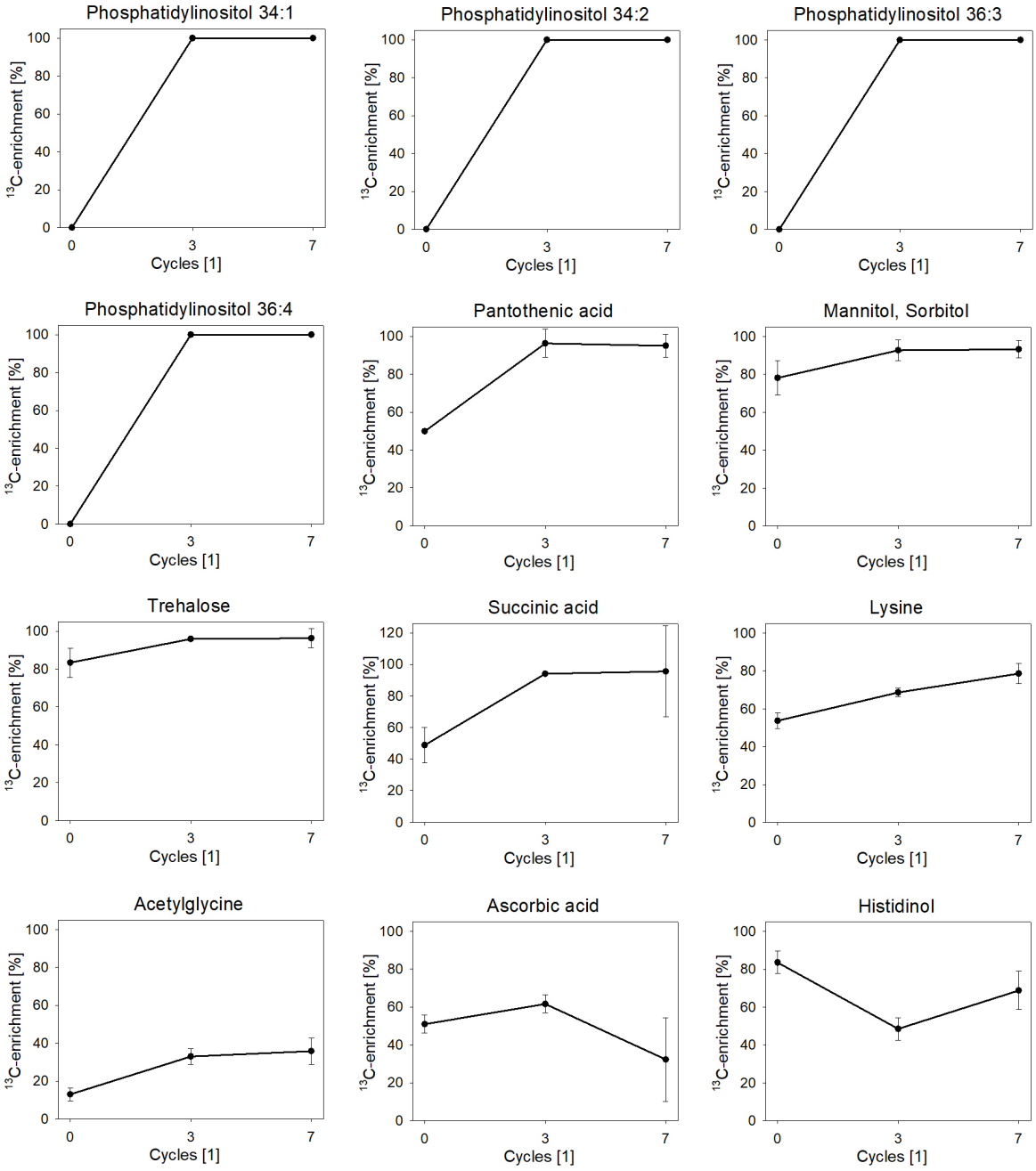


**Figure 22:** Metabolites of the experiment without $Na_2CO_3$ where effects in the $^{13}$C-ER with increasing number of fermentation cycles were observed. Error bars refer to the standard deviation of replicate measurements. When no bars are depicted the corresponding $^{12}$C-signal could be not detected or bars are too small to be depicted (trehalose and succinic acid).

### $^{13}$C-ER during co-cultivation with 0.1 g/L $^{13}$C-$Na_2CO_3$

In Figure 23, metabolites which showed effects in the $^{13}$C-ER depending on the number of fermentations cycles are depicted. Also in this experiment phosphatidylinositols (PI) and pantothenic acid revealed a striking $^{13}$C-ER effect over time. For the remaining metabolites contradictory effects were observed: For 5 metabolites the $^{13}$C-ER increased within the first 3 cycles of serial fermentation but decreased again after 7 cycles (mannitol/sorbitol, trehalose, succinic acid, lysine, acetylglycine). For 2 metabolites the opposite effect was observed (mevalonic acid, histidinol).

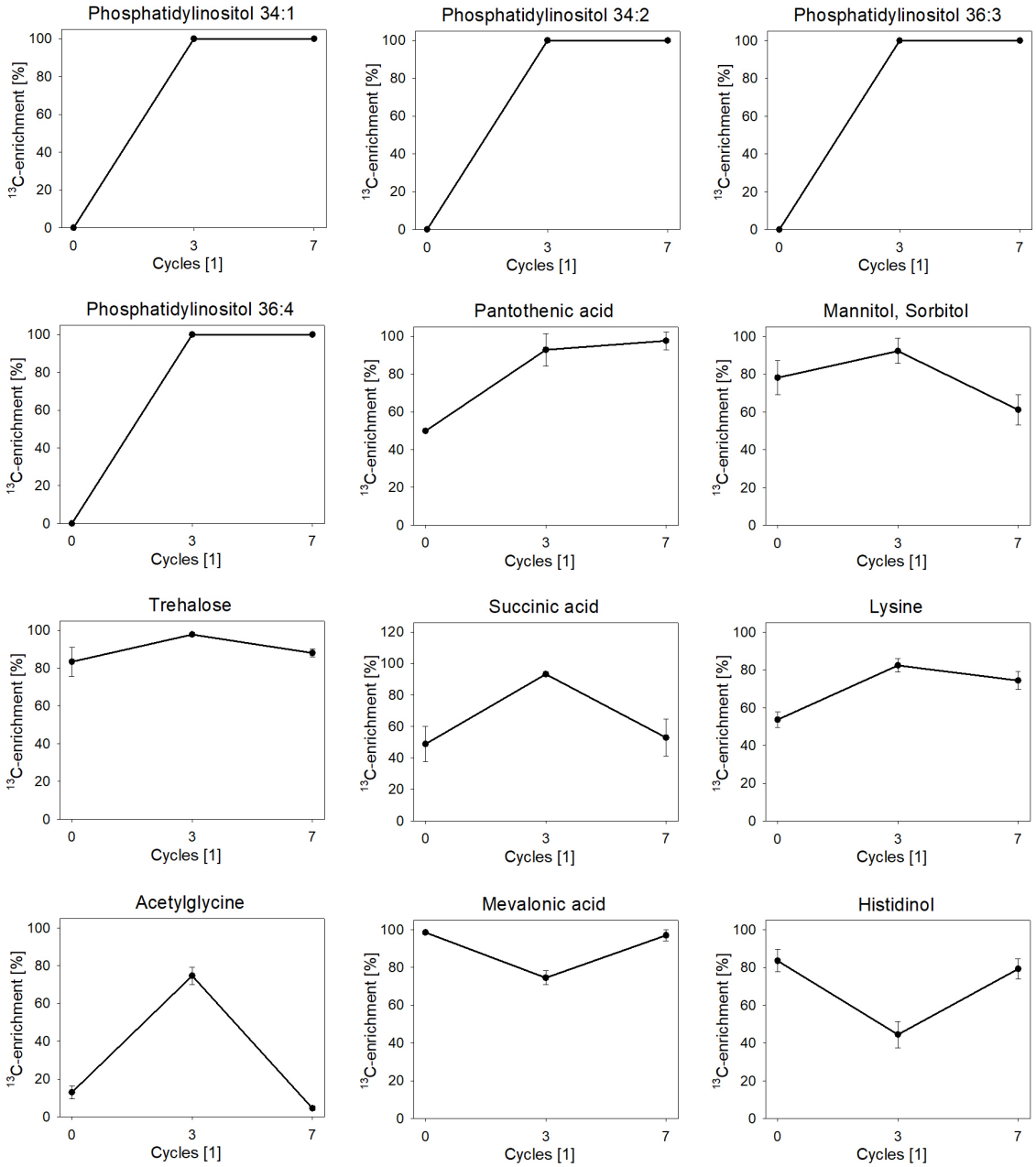


**Figure 23:** Metabolites which showed effects in the $^{13}$C-ER during the experiment with addition of 0.1 g/L $^{13}$C-$Na_2CO_3$. Error bars refer to the standard deviation of replicate measurements. When no bars are depicted the corresponding $^{12}$C-signal could be not detected or bars are too small to be depicted (trehalose, succinic acid, mevalonic acid).

### $^{13}$C-ER during co-cultivation with 1 g/L $^{13}$C-$Na_2CO_3$

During the experiment with 1 g/L $^{13}$C-labelled $Na_2CO_3$, in addition to PIs and pantothenic acid, also the labelling of cytidine diphosphat was enhanced (see Figure 24). For 6 metabolites again contradictory results were obtained: While for mannitol/sorbitol, trehalose, succinic acid, deoxyuridine and acetylglycine the $^{13}$C-ER was increased after 3 cycles but dropped after 7 cycles, for lysine it dropped after 3 cycles but increased again after 7 cycles of serial fermentation.

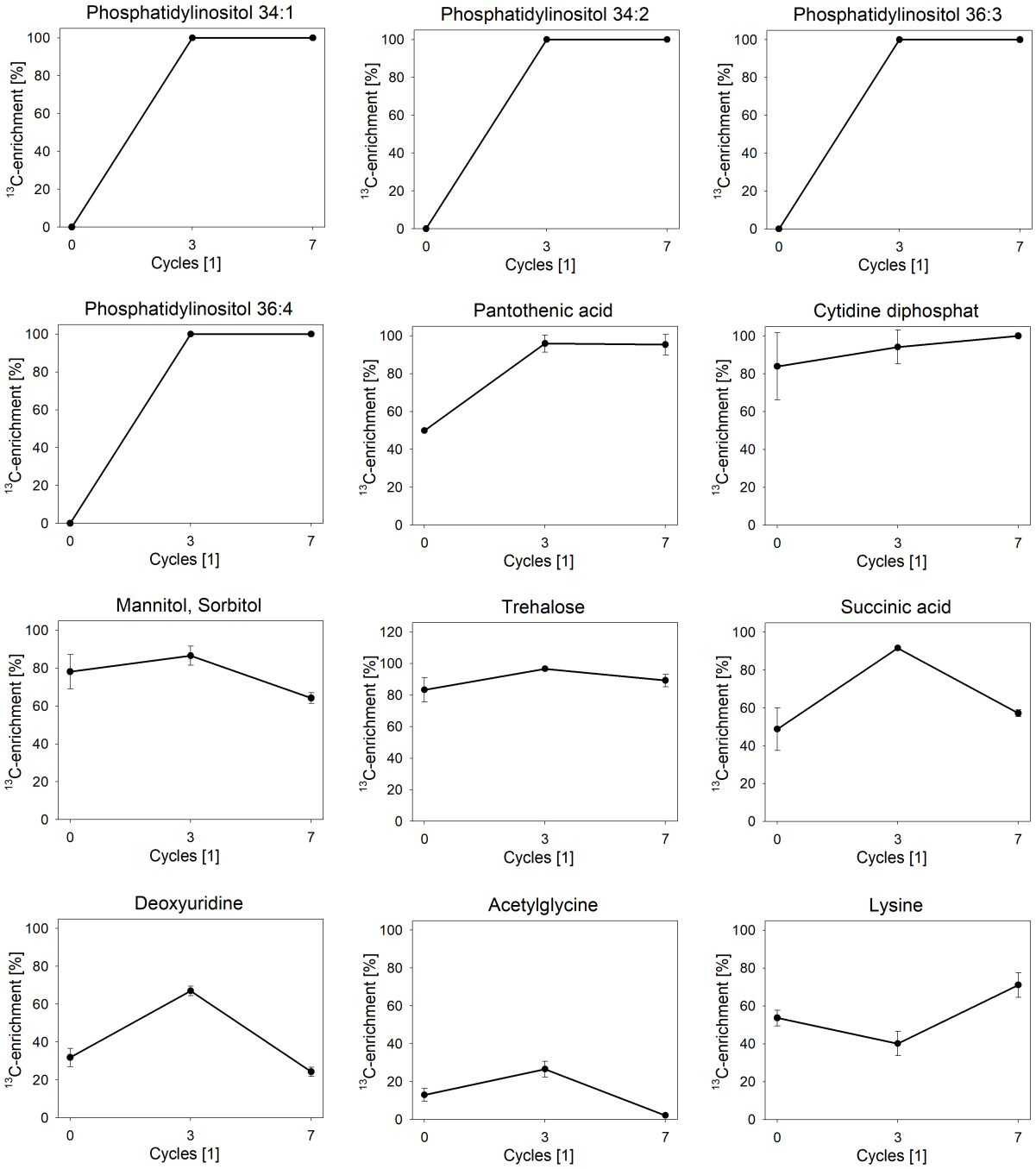


**Figure 24:** Metabolites of the experiment with addition of 1 g/L $^{13}$C-$Na_2CO_3$ where effects in the $^{13}$C-ER with increasing number of fermentation cycles were observed. Error bars refer to the standard deviation of replicate measurements. When no bars are depicted the corresponding $^{12}$C-signal could be not detected or bars are too small to be depicted.

### 4.4.2 Effects of $^{13}C$-$Na_2CO_3$ addition on the $^{13}C$-ER

It was investigated if the addition of $^{13}C$-$Na_2CO_3$ contributed to a higher $^{13}C$-ER of metabolites present in $CO_2$-consuming pathways. For this purpose the experiments in which $^{12}C$-$Na_2CO_3$ was added, were compared with the experiments where $^{13}C$-labelled $Na_2CO_3$ was used. For both comparisons (0.1 and 1 g/L), samples of cycle 7 were evaluated. Effects were determined as described in Section 3.3.8.
In Tabular 28 finding are summarized: Out of 127 metabolites in total, only 4 metabolites were found where the addition of 0.1 g/L $^{13}C$-$Na_2CO_3$ showed effects. For the experiment with addition of 1 g/L $^{13}C$-$Na_2CO_3$ 5 metabolites were found.

**Table 28:** Metabolites where the addition of $^{13}C$-labelled $Na_2CO_3$ showed effects regarding the $^{13}C$-ER. Metabolites where the $^{13}C$-ER increased and decreased, respectively, are separated by dashed lines. The quoted uncertainty corresponds to the standard deviation.

| Comparison | Metabolite name | $^{13}C$-ER [%] | |
|---|---|---|---|
| | | $^{12}C$-$Na_2CO_3$ | $^{13}C$-$Na_2CO_3$ |
| 0.1 g/L $^{12}C$- vs. 0.1 g/L $^{13}C$-$Na_2CO_3$ | Glycine | 0.039 ± 0.000 | 0.117 ± 0.022 |
| | Acetylglycine | 0.216 ± 0.049 | 0.045 ± 0.011 |
| | 3-Methyl-2-oxovaleric acid | 0.071 ± 0.007 | 0.024 ± 0.002 |
| | Succinic acid | 0.928 ± 0.007 | 0.529 ± 0.118 |
| 1 g/L $^{12}C$- vs. 1 g/L $^{13}C$-$Na_2CO_3$ | 1,5-Anhydrosorbitol | 0.279 ± 0.116 | 0.459 ± 0.047 |
| | Glycine | 0.056 ± 0.015 | 0.120 ± 0.037 |
| | Histidine | 0.058 ± 0.014 | 0.258 ± 0.011 |
| | Palmitolinoleic acid | 0.059 ± 0.014 | 0.111 ± 0.029 |
| | 3-Methyl-2-oxovaleric acid | 0.106 ± 0.051 | 0.012 ± 0.003 |

For both comparisons the $^{13}C$-ER was slightly increased for glycine, but decreased for 3-methyl-2-oxovaleric acid. While with the addition of 0.1 g/L $^{13}C$-$Na_2CO_3$ the $^{13}C$-ER decreased slightly but significant for acetylglycine, it decreased drastically for succinic acid. In the experiment with addition of 1 g/L $^{13}C$-$Na_2CO_3$, beside glycine, the $^{13}C$-ER could also be increased for 1,5-anhydrosorbitol, histidine as well as palmitolinoleic acid.
A direct comparison between 0.1 g/L and 1 g/L $Na_2CO_3$ has been rejected, since comparisons presented in this section gave already only few effects with poor reliability.

### 4.4.3 Metabolite levels

It was attempted to gain information about the metabolite levels (labelled and unlabelled) during the SFA. For the calculation of metabolite levels (see Section 3.3.7), the trend-corrected and normalized data sets were consulted.
It was tried to determine changes in the metabolite levels depending on the number of fermentation cycles for the experiment without addition of any $Na_2CO_3$. From 231

metabolites in total, 105 were already excluded since their QCs gave no reproducible results. Further, 18 metabolites were excluded due to high blank loading. From the remaining 87 metabolites, again 44 metabolites were excluded because metabolite levels of samples arising from cycle 1 and 7 were not reproducible. For 10 of the few remaining 43 metabolites, an increase or decrease of metabolite levels as a function of number of fermentation cycles were found. However, none of this effects had a clear trend or could biologically be explained.
In general, no consistent results could be obtained for metabolite levels. Although outliers were removed, trend correction and normalization was performed, the resulting data set was still to erroneous to gather conclusive information. It is assumed, that the inconsistency in the dataset was mainly caused by the overall poor quality of the LC-ESI/MS measurement (see Section 4.3.3). The necessary steps of trend correction and normalization in the data processing might have further increased errors of results. Further evaluations of metabolite levels have therefore been rejected.

### 4.4.4 Partial labelling of selected metabolites

In order to verify found effects in the $^{13}$C-ER, for some metabolites additionally the partial labelling patterns were investigated. For each investigated metabolite, the fraction of isotopologue $m_x$ in % (where m is the molecular mass and x is the number of labelled carbon atoms) was calculated as described in Section 3.3.7. The metabolites selected for this examination, are either known to get $CO_2$ incorporated during biosynthesis or constitute precursors or endproducts of vitamin biosynthesis pathways. Furthermore, lysine was investigated to compare the quality of analytics with earlier studies on the I.B.B.
Table 29 includes all metabolites investigated for partial labelling and the corresponding pathways of their appearance. Additionally, their fraction of the isotopologue with the highest number of $^{13}$C-labelled C-atoms possible ($m+_{max}$), as well as the $^{13}$C-ER (see Section 4.4.1) are depicted. Data presented in this table originates exclusively of cycle 3 from the experiment with addition of 1 g/L $^{13}$C-$Na_2CO_3$, since in this data set the most effects are thought to be found. A complete list containing all data of the partial labelling evaluation is provided by Table 32 in the appendix.
A comparison between the $^{13}$C-ER and the isotopological fraction with the maximum number of C-atoms labelled reveals, that the $^{13}$C-labelling of most metabolites remains still incomplete after 3 cycles of serial fermentation, since there are isotopological fractions below $m+_{max}$ left. There could be no significant difference observed between the experiments with addition of 1 g/L and no addition of $^{13}$C-labelled $Na_2CO_3$ (compare with Table 32).
In Figures 25 to 27 the partial labelling patterns of examined metabolites over all cycles of the SFA are depicted. In the following the labelling patterns will be pathway-wise explained.

**Table 29:** Selected metabolites originating from cycle 3 of the experiment with addition of 1 g/L $^{13}C$-$Na_2CO_3$ for the investigation of the partial labelling, their corresponding $^{13}C$-ER and fraction of isotopological fraction $m+_{max}$. Metabolites are grouped by the pathway of their appearance (separated by dashed lines). Some metabolites are listed multiple times for the sake of clearness, since they occur in several pathways. For fumaric, malic and succinic acid, the fraction with zero C-atoms labelled was excluded from the calculation of partial labelling; since these metabolites are known to cause disproportionally high signals.

| Metabolite name | Formula | Pathway of investigation | Reason of investigation | $^{13}C$-ER [%] | $m+_{max}$ [%] |
|---|---|---|---|---|---|
| PI 34:1 | $C_{43}H_{81}O_{13}P$ | PI biosynthesis | Myo-inositol | 100.00 | 89.98 |
| PI 34:2 | $C_{43}H_{81}O_{13}P$ | | | 100.00 | 87.71 |
| PI 36:3 | $C_{43}H_{81}O_{13}P$ | | | 100.00 | 94.73 |
| PI 36:4 | $C_{43}H_{81}O_{13}P$ | | | 100.00 | 100.00 |
| NAD+ | $C_{21}H_{27}N_7O_{14}P_2$ | NAD salvage pathway | Niacin | 100.00 | 80.33 |
| Niacin | $C_6H_5NO_2$ | | | – | 100.00 |
| Acetyl-CoA | $C_{23}H_{38}N_7O_{17}P_3S$ | Pantothenic acid and Coenzyme A biosynthesis | Pantothenic acid | 100.00 | 23.64 |
| AMP | $C_{10}H_{14}N_5O_7P$ | | | 100.00 | 78.99 |
| Pantothenic acid | $C_9H_{17}NO_5$ | | | 100.00 | 87.82 |
| Acetyl-CoA | $C_{23}H_{38}N_7O_{17}P_3S$ | Citric acid cycle | $CO_2$-incorporation | 100.00 | 23.64 |
| Aspartic acid | $C_4H_7NO_4$ | | | 99.87 | 89.35 |
| Fumaric acid | $C_4H_4O_4$ | | | 100.00 | 85.04 |
| Glutamine | $C_5H_{10}N_2O_3$ | | | 100.00 | 92.68 |
| Lysine | $C_6H_{14}N_2O_2$ | | | 40.16 | 4.52 |
| Malic acid | $C_4H_6O_5$ | | | 100.00 | 85.94 |
| Proline | $C_5H_9NO_2$ | | | 96.30 | 100.00 |
| Succinic acid | $C_4H_6O_4$ | | | 91.58 | 98.02 |
| AMP | $C_{10}H_{14}N_5O_7P$ | Purine biosynthesis | $CO_2$-incorporation | 100.00 | 78.99 |
| GMP | $C_{10}H_{14}N_5O_8P$ | | | – | 77.66 |
| Histidine | $C_6H_9N_3O_2$ | | | 20.40 | 22.54 |
| IMP | $C_{10}H_{13}N_4O_8P$ | | | – | 80.85 |
| Glutamine | $C_5H_{10}N_2O_3$ | Pyrimidine biosynthesis | $CO_2$-incorporation | 100.00 | 92.68 |
| UMP | $C_9H_{13}N_2O_9P$ | | | 100.00 | 65.14 |
| Lysine | $C_6H_{14}N_2O_2$ | – | QC | 40.16 | 4.52 |

Abbreviations: AMP, adenosine monophosphate; CoA, coenzyme A; GMP, guanosine monophosphate; IMP, inosine monophosphate; NAD+/NADH, nicotinamide adenine dinucleotide; UMP, uridine monophosphate; PA, pantothenic acid; PI, phosphatidylinositol

#### 4.4.4.1 Partial labelling patterns of vitamins

The partial labelling of the four PIs states the findings of the $^{13}C$-ER: While the isotopological fractions $m+_{37}$ (for PI 34:1 and PI 34:2) and $m+_{39}$ (for PI 36:3 and 36:4) were decreasing until cycle 3, the fractions of maximum C-atoms labelled were increasing. PIs consist of a fatty acid with a chain length of 37 (for PI 34:1 and PI 34:2) and 39 (for PI 36:3 and 36:4), respectively, C-atoms and an attached inositol ring with six C-atoms

(compare with (a) in Figure 28, Section 5.4.1). It is supposed that the fatty acids are already completely labelled within the first hours, while the inositol rings are successively labelled during the serial fermentation.
Considering the NAD+ (Nicotinamide adenine dinucleotide+) salvage pathway, for niacin only the highest fraction $m+_{max}$ was found. It's high enrichment is underpinned by the partial labelling of NAD+: For NAD+ the two highest isotopological fractions $m+_{21}$ and $m+_{20}$ both together constitute 95 % in average. However, while niacin was already completely enriched at cylce 0, NAD+ showed a trend to higher isotopological fractions with increasing number of fermentation cycles.
For pantothenic acid, $m+_{max}$ increased from 53 % to 88 % after three cycles, while the isotopological fraction with zero C-atoms labelled ($m+_{00}$) decreased to virtually 0 % in the same time. This is underpinned by the partial labelling pattern of acetyl-CoA: Acetyl-CoA consists of 23 C-atoms originating from adenosine monophosphate (AMP; 10 C), pantothenic acid (9 C), mercaptoethanol (2 C) and acetyl (2 C). Whereas the four highest isotopological fractions of acetyl-CoA were increasing ($m+_{20}$, $m+_{21}$, $m+_{22}$ and $m+_{23}$) fractions with nine C-atoms less (originating from pantothenic acid) than the four highest fractions ($m+_{11}$, $m+_{12}$, $m+_{13}$ and $m+_{14}$) disappeared completely after cycle 3 (see Figure 25). But still, after cycle 7 the most dominant fraction of acetyl-CoA was $m+_{21}$. Since the two highest fractions of AMP constituted 99 % from the beginning, it is supposed that acetyl remain unlabelled.

#### 4.4.4.2 Partial labelling of metabolites from $CO_2$-consuming pathways

Several metabolites of the citric acid cycle (TCA) were examined, as for one key metabolite (oxaloacetic acid), $CO_2$ gets incorporated during biosynthesis of pyruvate. Oxaloacetic acid (4 C) constitutes a pre-cursor for aspartate (4 C) and succinic acid (4 C). Succinic acid itself is subsequently converted to fumaric (4 C) and malic acid (4 C), which in turn is converted to oxaloacetic acid and pyruvate, respectively, again. While for aspartic acid $m+_{max}$ was already almost 95 % from the beginning, $m+_{max}$ of succinic acid rose from 59 % to 98 % until cycle 3. The partial labelling patterns of fumaric and malic acid, were almost identical: both increased $m_{max}$ from 79 % to 85 % until cycle 3 by shifting lower isotopological fractions to higher isotopological fractions. Additionally, the partial labelling of one side branch of the TCA – the formation of the amino acids glutamine, lysine and proline was investigated. Lysine (6 C) is formed by the C-atoms of $\alpha$-ketoglutarate (5 C) and acetyl (2 C), minus one C-atom which is dissociated in form of $CO_2$. $\alpha$-ketoglutarate itself is build up by oxaloacetic acid (4 C) and acetyl (2 C) minus one C-atom of a dissociating $CO_2$. $\alpha$-ketoglutarate (5 C) also constitutes a pre-cursor for glutamine (5 C), which itself provides the C-atoms for proline (5 C). Glutamine and proline both were found almost completely enriched from the beginning ($\geq$ 93 % for glutamine and 100 % for proline), which suggests that also $\alpha$-ketoglutarate was labelled al-

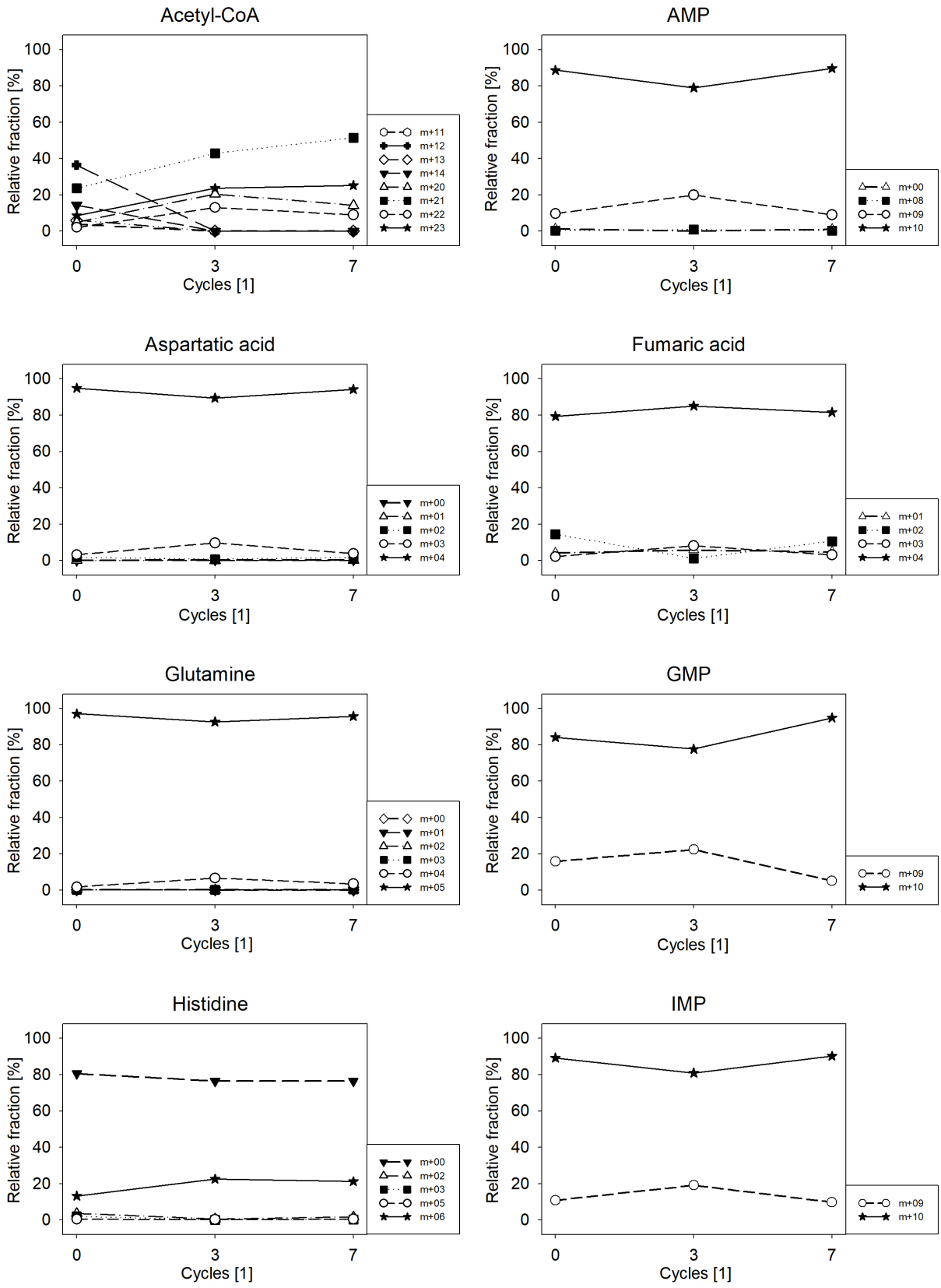


**Figure 25:** Partial labelling patterns of metabolites A-I. Filled stars represent the maximum possible C-atoms labelled. Abbreviations refer to: CoA, coenzyme A; AMP, adenosine monophosphate; GMP, guanosine monophosphate; IMP, inosine monophosphate.

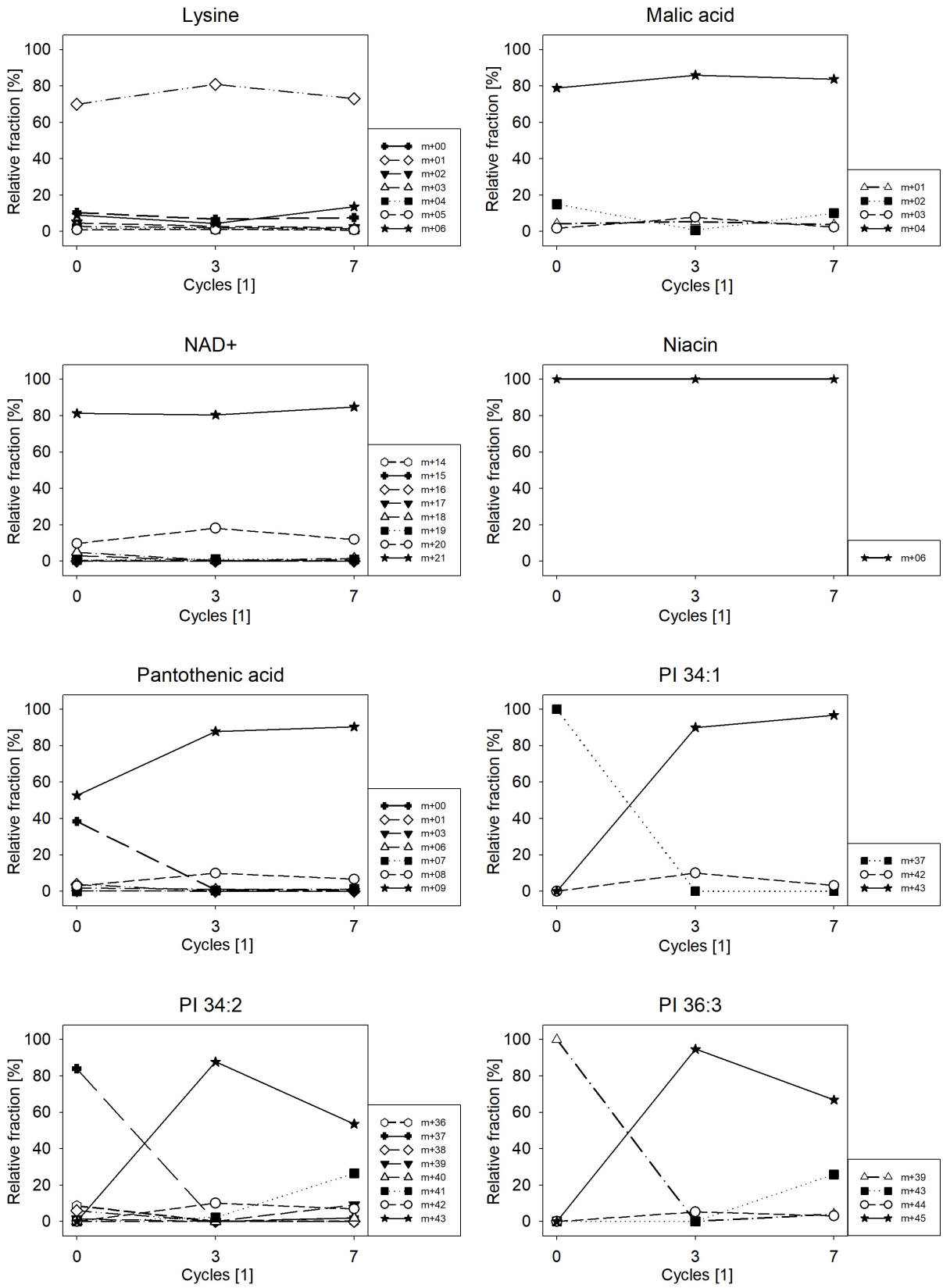


**Figure 26:** Partial labelling patterns of metabolites L-P. Filled stars represent the maximum possible C-atoms labelled. Abbreviations refer to: NAD+, nicotinamide adenine dinucleotide; PI, phosphatidylinositol.

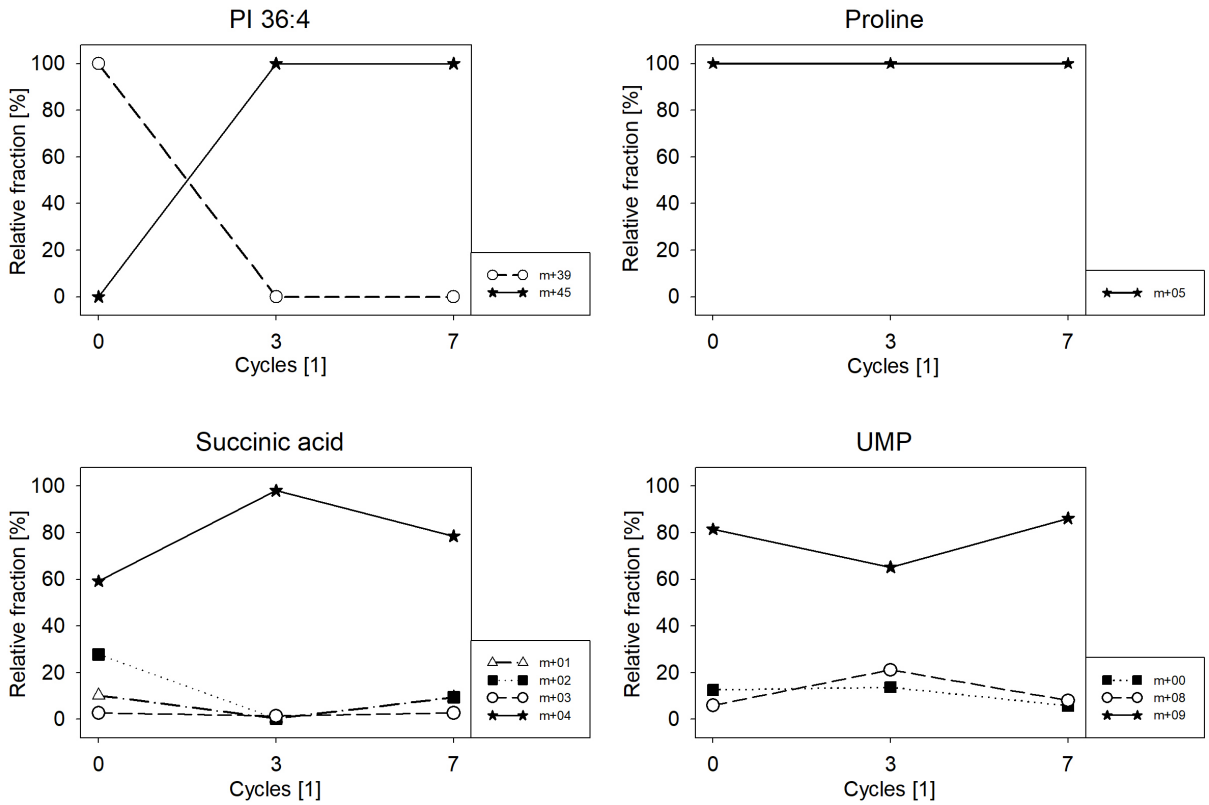


**Figure 27:** Partial labelling patterns of metabolites P-U. Filled stars represent the maximum possible C-atoms labelled. Abbreviations: PI, phosphatidylinositol; UMP, uridine monophosphate.

most completely. For lysine, $m+_{01}$ was found to be by far the most dominant fraction (~75 %) over all serial fermentation cycles. However, a small trend to higher isotopological fractions with increasing number of serial fermentation cycles was observed for lysine.
The purine biosynthesis starts with phosphoribosyl pyrophosphat (PRPP, 5 C), which gets under certain biosynthesis steps glycine (2 C), two formyl molecules (2 C) and $CO_2$ incorporated, resulting in inosine monophosphate (IMP; 10 C). Since the two highest isotopological fractions of IMP ($m+_{09}$ and $m+_{10}$) constitute 100 % of the partial labelling, it is supposed that PRPP, glycine, formyl as well as the incorporated $CO_2$ are also labelled to almost 100 %. As IMP is a pre-cursor for AMP and GMP, their partial labelling profiles are almost identical (compare with Figure 25). The amino acid histidine (6 C) is synthesized by C-atoms arising from PRPP (5 C) and ATP (10 C) (minus 9 C-atoms – AICAR biosynthesis). In contrast to the findings that PRPP and ATP should be labelled almost completely to the highest isotopological fractions, for histidine the fraction with zero C-atoms labelled remained dominant (76 %), followed by $m+_{max}$ (22 %).
In the pyrimidine biosynthesis pathway, UMP was used to investigate the partial labelling. UMP (9 C) is build up by $CO_2$, aspartate (4 C) and PRPP (5 C) minus one C-atom which is dissociated in form of $CO_2$. For UMP $m+_{max}$ was 78 % and $m+_{08}$ was 12 % in average, which underpins the labelling of PRPP and the amino acid aspartate.

# 5 Discussion

## 5.1 Improvement of the medium composition for the SFA

Currently available commercial internal standards suffer from three major drawbacks: Beside the rather high acquisition costs, they do not cover the full spectrum of metabolites and furthermore, the labelling of several metabolites remains incomplete. The applied LC-ESI/MS system in this thesis, is known to be sensitive to ion suppression by divalent salts arising from the sample matrix [29]. With respect to the drawbacks of commercial internal standards, as well as the problem of high divalent salts present in the sample matrix, the medium composition was improved. In this section all findings regarding the improvement of the medium composition will be discussed. A detailed description as well as the corresponding results of these studies can be found in Section 4.1.

### 5.1.1 Reduction of matrix effects for more reliable LC-ESI/MS analysis

Phosphate, sulfate and other divalent salts of the sample matrix are known to co-elute with analytes of interest and therefore compete for charge or space in the ionisiation process in the applied LC-ESI/MS. As a result, due to saturation some analytes could be completely masked by the matrix or lead to non-linear calibration curves [29, 53]. To this end, Trausinger et al. established a protocol, where concentrations of these compounds were lowered to a minimum in biofermentor. Phosphate and sulfate were lowered to a concentration of 0.23 mM and 0.04 mM, respectively. Both still sufficient enough to support a cell growth to a cell density of $OD_{600} \sim 3$ [30, 48]. Due to the usage of Erlenmeyer flasks instead of a bioreactors in this thesis, which lack the opportunity of automated pH-adjustment, it was not possible to apply the protocol of Trausinger et al. without any alterations. In the following, measures for reducing concentrations of phosphate, magnesium, sulfate and TE in the final samples for LC-ESI/MS measurement will be discussed. As expected, magnesium can not be omitted completely, as this reduced the growth rate in the observed time period already by a factor of approximately 2 (see experiment of Section 4.1.2). However, the experiment of Section 4.1.3 stated, that the magnesium concentration can be lowered to a minimum amount without affecting the growth rate. Hence, the magnesium concentration was lowered to 0.05 g/L - a reduction by a factor of 50 in comparison to the standard medium – which still provides enough magnesium and sulfate for physiological growth of *S. stipitis*.
In order to avoid sulfate in the sample matrix, the sulfate-containing nitrogen source ammonium sulfate ($[NH_4]_2SO_4$) was replaced by ammonium chloride ($NH_4Cl$). An influence on the growth behaviour by this substitution was not furhter examined, as this was already investigated and rejected by previous studies on the I.B.B. [30].
An early attempt to lower the phosphate amount in the sample matrix, was done by reducing the concentration of phosphate in the mineral medium to 0.25 g/L and in return,

adjusting the pH-value every 2 hours by addition of 1 M KOH (data of this experiment is not presented in this thesis). However, this approach - which in principle worked - was eventually not deployed for two reasons: Firstly, because of the high experimental effort (preparation of a control flask for pH-measurement, necessity to measure and/or adjust pH-value at least every two hours) and secondly, because of the unsatisfactory possibilities to measure the pH-value without contamination of the experimental flasks with $^{12}$C. Hence, the phosphate concentration was kept at 14.1 g/L (standard medium) and an additional washing step during the sample preparation was introduced. By washing each sample with 40 mL of ice-cold saline, the phosphate concentration could be lowered by a factor of more than 400, without the drawbacks mentioned above. In the final samples phosphate concentrations less than 10 µM can be expected, which is far below concentrations strongly effecting LC-ESI/MS measurements (>1 mM) [30].
For the TE, the situation is so far not clear. Further studies must be carried out to investigate, firstly, if the TE can lead to ion suppression at all and secondly, if they can be omitted entirely.

### 5.1.2 Preparation of SMYE for substituting vitamins and TE

In order to substitute $^{12}$C-containing vitamins and TE, four different methods for preparing a SMYE were investigated. For the purpose of serial fermentation, a growth rate of 0.3 1/h was set as lowest sufficient growth rate, as lower growth rates could have disturbed the time management (contraint: 1 cycle of serial fermentation $\leq 0.75$ days). As the growth rate is depending on the concentration of the SMYE, the cell suspension for preparation of the SMYE was always concentrated to $OD_{600} \sim 10$ ($1\ OD_{600} \sim 8 \times 10^8\ \frac{\text{cells}}{\text{mL}}$) and SMYE was added in a volume fraction of 3.3 % to the medium.
In total, all of the growth rates observed during the experiments were in a range of 0.3 to 0.4 1/h. For the positive controls (prepared with vitamins) growth rates in a range of 0.4 up to 0.5 1/h were observed, which are in concordance to growth rates found in literature (e.g. 0.47 1/h, observed by Papini et al. [54]).
Considering the growth rate of *S. stipitis* when substituting vitamins by SMYE, all four tested methods (boiling for either 30 or 60 min in hot water bath, autoclaving for 20 min and bead beating 7.5 min) provided a SMYE of satisfying quality. Each of the discussed methods gave a yeast extract of hundred percent sterility (see Figure 14 in Section 4.2.2). In the most experiments for improving the medium composition autoclaving method was deployed. Autoclaving benefited from the shorter pre-heating times and the inherent sterility of the prepared $\text{SMYE}_{\text{aut}}$. Later autoclaving was replaced by a combined method of bead beating and thermal inactivation due to the following reasons: With respect to the effort and the flexibility of the investigated production methods, bead beating has proven to be superior. It does not suffer from long pre-heating times of the devices or cooling times of the yeast extract itself. While the methods of boiling in hot water bath and au-

toclaving take at least 45 minutes up to 1 hours to the finished SMYE, bead beating can be performed below ten minutes. And flexibility in the time management constitutes a critical feature, when growing three cultures in parallel. Another reason for choosing bead beating eventually as SMYE production method, constitutes the rather low application temperature (70 °C for bead beating vs. 99 °C for boiling and 120 °C for autoclaving). As some vitamins (especially thiamine, pyridoxine and pantothenic acid [50, 51, 52]) are sensitive to thermal degradation, bead beating should provide a yeast extract of higher quality regarding the availabilty of thermal unstable vitamins. Furthermore, it is not possible to reproduce the time course of autoclaving method, therefore leading to SMYE of different qualities. However, none of the tested methods could supply a yeast extract, which enabled a serial fermentation over more than 1 cycle without addition of biotin. It is not clear whether biotin is depleted or biotin is degraded during the SMYE production methods. Biotin in general, is known as a comparatively stable vitamin [55]. A possible explanation for this could be co-degradation of biotin during bead beating, when attached to carboxylases. Biotin-dependent carboxylases are a functional diverse group of enzymes including six members. Each consists of biotin carboxylase, carboxyltransferase and biotin carboxyl protein components [56]. However, the minimal contamination of 0.05 g/L $^{12}$C-biotin is negligible, since the biotin is not further metabolized.
During the first experiments for improving the medium composition for the SFA, it was observed that the turbidity of the SMYE falsifies $OD_{600}$ measurements. Hence, it was attempted to clarify the yeast extract for more reliable cell density measurements. The clarification of the SMYE by centrifugation has proven to be an easy method to obtain more accurate $OD_{600}$ measurements: Beside the striking reduction of scattering, $OD_{600}$ offsets observed with unclarified SMYE have been reduced significantly (see Figure 11 in Section 4.1.3).

### 5.1.3 Comparison of the final mineral medium with media from literature

In conclusion, Table 30 provides a comparison between the applied medium of this thesis and two media from literature [24, 30]. While in this master thesis *S. stipitis* was labelled in Erlenmeyer flasks, in the two studies from literature *S. cerevisiae* was deployed and labelled in biofermentors.
In addition to $^{13}$C-glucose, $^{13}$C-$Na_2CO_3$ was consulted as additional $^{13}$C-substrate to further increase the $^{13}$C-ER of $CO_2$-consuming pathways. Wu et al. additionally fed $^{13}$C-labelled enthanol for increasing the $^{13}$C-ER, due to the application of a crabtree positive yeast. While Trausinger et al. decreased the concentration of phosphate to a minimum but kept the concentration of magnesium at standard level, in this thesis it was vice versa: The magnesium concentration was lowered to a minimum, but the phosphate concentration was kept at a standard level. The high amount of phosphate in the sample matrix was lowered by introducing an additional washing step during the sample preparation.

Wu et al. did not lower phosphate, magnesium or sulfate concentrations in the media, due to application of different LC-MS analytics. In order to keep $^{12}$C-contaminations as low as possible, vitamins and TE were substituted completely by a SMYE in this thesis. Nevertheless, still biotin had to be added for sufficient growth of *S. stipitis*. While Trausinger et al. did not account for issue, Wu et al. supplemented only essential vitamins (biotin, thiamine).

**Table 30:** Comparison of applied media for the production of $^{13}$C-labelled internal standards.

| | Component | MMf6 | Trausinger et al. | Wu et al. |
|---|---|---|---|---|
| | | Concentration [g/L][a] | | |
| $^{13}$C-source | $^{13}C_6$-glucose | 5.00 | 5.00 | 56.80 |
| | $^{13}C_2$-ethanol | – | – | 3.00 |
| | $^{13}$C-$Na_2CO_3$ | 1.00 | – | – |
| Salts | KCl | – | 1.50 | – |
| | $KH_2PO_4$ | 14.10 | 0.25 | 10.10 |
| | $MgSO_4 \cdot 7\,H_2O$ | 0.05 | 0.50 | 1.70 |
| | $[NH_4]Cl$ | 4.05 | 4.00 | – |
| | $[NH_4]_2SO_4$ | – | – | 16.70 |
| TE and vitamins | TE[b] | – | 0.10 % | 0.33̇% |
| | Vitamins[b] | – | 0.10 % | – |
| | Yeast extract[bd] | 3.33̇% | – | – |
| | Biotin | 0.05 | – | 0.05 |
| | Thiamin | – | – | 1.00 |

[a] Values refer to final concentrations. [b] Values refer to (*v/v*). [d] Clarified by centrifugation and prepared by bead beating (see Section 3.1.5).

## 5.2 Preliminary studies for the SFA

After improving the medium composition for the task of serial fermentation, it was attempted to establish a protocol which allows *S. stipitis* to grow over more than 1 cycle of serial fermentation. The most crucial step here was, to obtain a growth rate which is sufficiently high enough to ensure a timed serial fermentation over one week, even when three experiments are run in parallel. The time management was designed in the sense that 1 cycle of serial fermentation should not excess 18 hours (1 cycle $\leq$ 0.75 days). Furthermore, an appropriate storage condition for the inoculum during the preparation of SMYE had to be found. Additionally, a suitable long-term storage compound for freezing the final $^{13}$C-enriched cells after the realization of the SFA was searched for. Finally, the cultivation volume and shaking frequency were adapted for the purpose of serial fermentation.

### 5.2.1 Establishment of a protocol for the purpose of serial fermentation

First of all, an appropriate inoculum storage condition during the timespan between harvesting the ECs and inoculation of the next cultures was investigated. The storage condition should firstly, prevent *S. stipitis* from growth during storage and secondly, maintain the yeasts viability as good as possible. Storage at 4 °C in the cooling room prevented yeast from growth satisfyingly in all tested cases. From the three storage conditions investigated, only storage as cell suspension with glucose gave an insufficient growth rate. It is assumed, that this loss of growth performance after storage might be caused by the restricted ability of *S. stiptis* to adapt to cold temperatures when glycolysis remains active. However, this issue was not examined in more detail. Storage as sole cell pellet or as concentrated cell suspension both gave sufficient growth. Since storage as cell pellet requires an additional centrifugation and dilution step, storage as cell suspension was eventually introduced as inoculum storage condition.
The SFA itself was performed as depicted in Figure 4. The first attempts to cultivate the yeast for more than 1 cycle of serial fermentation always resulted in a virtually complete loss of growth within cycle 2. Indicated by the literature, it was assumed that two essential but thermolabile vitamins of *S. stipitis* (pantothenic acid and thiamine) are degraded during the production process of the SMYE by autoclaving [50, 52]. As a consequence it was investigated to retain cell growth by addition of both of this vitamins. Furthermore, it was attempted to replace autoclaving method by the more gentle method of bead beating. However, both approaches still did not result in a serial fermentation with sufficient cell growth for more than 1 cycle of serial fermentation. Finally, it turned out that the yeast was missing biotin which is essentially for yeast growth [57] (the addition of biotin is discussed in more detail in Section 5.1.2).
The working volume was lowered in order to use the expensive $^{13}$C-labelled glucose substrate more economically, but still providing enough cell suspension to enable the production of $SMYE_{bb}$, to serve as inoculum, to monitor the SFA with $OD_{600}$ measurements and to take samples in quadruplicates, if necessary. 10 g of $^{13}$C-labelled glucose with a purity $\geq 99\,\%$, currently cost about 2200 euro[3]. Furthermore, it was investigated if a possible decrease of growth rate could be compensated by increasing the shaking frequency. The study indicated that the growth rate decreases when lower cultivation volumes are applied ($< 30$ mL). However, it was not possible to compensate this by increasing the shaking frequency from 120 rpm to 160 rpm. As a compromise a working volume of 20 mL was eventually used.

[3] www.sigmaaldrich.com

### 5.2.2 Storage of the final $^{13}$C-enriched cells

For the long-term storage of micro organisms, frozen glycerol stocks are commonly prepared. Since *S. stipitis* is able to metabolize unlabelled glycerol, which could contamine the final $^{13}$C-enriched cells with $^{12}$C again, another appropriate storage compound had to be found. A literature research suggested the usage of PEG as a storage compound, or to freeze the cells as sole cell pellet. Thus, polyethylene glycol with different chain lengths (molecular weight: 3350, 8000 and 20000) was investigated for long-term storage. Although PEG also contains carbon atoms, it can not be utilized as substrate by *S. stipitis*. Alternatively, it was attempted to freeze the final $^{13}$C-enriched cells as sole cell pellet. As depicted in Figure 17 (Section 4.2.5), long-term storage of *S. stipitis* was dependent on the chain length of PEG – the longer the chain length of PEG the shorter the longevity of cells. Although long-term storage as sole cell pellet could also maintain cell viability, PEG3350 preserved *S. stipitis* physiology by far the best. After 6 month storage at −70 °C, cells prepared with PEG3350 still showed the same viability than after 1 day storage. Therefore PEG3350 was chosen to preserve the final $^{13}$C-enriched cells after the realization of the SFA.

## 5.3 Realization of the SFA

After improving the medium composition and establishing a working routine for serial fermentation, two runs of the SFA were performed. In this section all findings, observations and troubles during the implementation of both runs of the SFA and the subsequent LC-ESI/MS measurement at Joanneum Research will be discussed.

### 5.3.1 Implementation of the SFA

The established protocol for serial fermentation was tested two times ($^{12}$C vs. $^{13}$C-$Na_2CO_3$), each with three subexperiments (no $Na_2CO_3$ or 0.1 and 1 g/L $Na_2CO_3$).
It was attempted to harvest or withdraw samples, respectively, the cultures when reaching a final $OD_{600}$ of 3-3.5 (with an average growth rate of 0.3 1/h ~ 8.2 generations). However, it was not possible to harvest and sample all three cultures at the same time. Hence, the sampling volume was adapted to ensure the same amount of biomass in all samples.
Another issue regarding the time management was the slight decrease of growth rate over time (compare with Tables 24 and 25 in Section 4.3): During the first run of the SFA, in all three cultures cells retained their growth rate until cycle 7 without the necessity of interventions. In contrast, during the second run of the SFA growth rates dropped two times below 0.25 1/h (cycles 3 and 7). Thus, leading to problematic time shifts between the three cell cultures. In both cases the growth rate could be recovered entirely by addition of 20 µL of TE solution. This amount of TE solution in relation to cultivation volume of 20 mL can be considered as uncritical regarding a $^{12}$C-contamination (EDTA in

TE solution). This observation suggests, that the initial amount of TE solution (present in the media of cycle 0) as well as the amount of metals in the SMYE are diluted out entirely within several cycles of serial fermentation. However, it is not clear why the growth rate limitation by TE occurred only during the second run of the SFA. Both runs differed only in the type of $Na_2CO_3$ isotope applied, the additional sampling step in run 2 (cycle 3) and showed overall similar growth behaviour. A drop of growth rate caused by the one additional sampling step can be rejected, since the decrease of growth rate occurred already in cycle 2 (1 day before sampling). A possible remedy to this problem could be the addition of uncritical amounts of TE during every cycle of the SFA by default. In future studies, this problem could be circumvented by application of higher initial concentration of TE or by spiking uncritical low amounts of TE during the SFA. However, as unforeseen growth rate limitations constitute a critical problem, especially when cultivating more flasks in parallel, this issue has to be investigated in further studies.
Growth rate shifts between the individual cultures, caused by nutrition limitation or by inaccuracies with the inoculation volume, underline the necessity of a flexible methodology, especially a flexible SMYE production method. The duration of the experiment (7 cycles from $OD_{600}$ 0.01 to $OD_{600}$ 3-3.5 correspond to 65 generations) will be discussed in Section 5.4.

### 5.3.2 LC-ESI/MS measurement and quality of data

The LC-ESI/MS measurement was conducted at Joanneum Researchs Health institute and performed and supervised, respectively, by personnel of Joanneum Research. Samples were randomized globally and subdivided into three batches - each measured on a different day. QCs were introduced between each four replicates in order to make batches comparable and to achieve an overall quality evaluation of the analysis. Problems arose with the LC-ESI/MS measurement and their implications onto the data evaluation will be discussed in the following.
In general, the used LC-ESI/MS system needs a lead time (several hours to days) until the applied method runs stable on the system. Since batch 1 was measured during this time, signals of batch 1 were at least two magnitudes lower than for batch 2 and 3 and hence, also manifested with a higher standard deviation (see Figure 19, Section 4.3.3). Furthermore, during the measurement of batch 1 the system had to be restarted completely due to clogging of the injection needle. Because of the resulting high RSEs the first half of the replicates of batch 1 had to be excluded from data evaluation. Since all samples were determined with four replicates and randomized globally, still all samples could be determined by averaging the replicates. Nevertheless, replicates were lost and therefore some samples were less reliably determined than others.
Obtained signal yield was about two to three magnitudes lower compared to earlier LC-ESI/MS experiments performed at the I.B.B. Dried samples (harvested at $OD_{600}$

3-3.5) were re-suspended in 300 µL HPLC grade water. 45 $^{12}$C-metabolites and 15 $^{13}$C-metabolites had a signal to noise ratio too low in order to distinguish the wanted metabolite signal from background noises and were therefore excluded. In earlier studies on the I.B.B., units of 1 $OD_{600}$ were sampled and re-suspended after drying with 100 µL [30], resulting approximately in the same range of metabolite concentrations as in this thesis. In order to decrease the error of results an algorithm for outlier exclusion was introduced (for a description see Section 3.3.7). Especially with the more erroneous replicates of the second part of batch 1 (the first part was excluded), it was possible to reduce RSEs significantly.
Furthermore, to investigate metabolite levels, a trend correction as well as a normalization processing step was introduced. Without these additional processing steps, a comparison of metabolite levels between batches would not be reliable, due to the distinct signal yields. However, although both data processing steps worked, the processed data was still to erroneous for a conclusive data evaluation of metabolite levels.
Effects in the $^{13}$C-ER of metabolites were evaluated using LSD and Scheffe test. While the a-priori LSD test is known to be very sensitive, the post-hoc Scheffe test in contrast, is by far more conservative. All effects presented in this thesis were found by LSD test. Note that in general, the application of LSD test allows only 1.5 comparisons per definition. In this thesis, LSD test was applied making 2 comparisons. Hence, Scheffe test was applied to verify found effects of LSD test.

## 5.4 Metabolomics

A metabolomics study was carried out in order to investigate if the stated three hypothesis of this thesis could help to increase the $^{13}$C-ER and the spectrum of labelled metabolites. In this section all findings regarding the effectiveness of serial fermentation, the substitution of vitamins and TE by SMYE as well as the further addition of $^{13}$C-$Na_2CO_3$ and their contribution for achieving the goals will be discussed.

### 5.4.1 General consideration of the $^{13}$C-ER during the SFA

Mashego et al. reported, that four hours of cultivating yeast on $^{13}$C-labelled glucose substrate are too short for a complete labelling of several metabolites. The incomplete labelling was especially observed for conserved metabolite storage pools with a slow turnover rate [43]. Therefore a protocol for serial fermentation was developed, which, in theory, allows a multiple of processing time for $^{13}$C-ER without any further $^{12}$C-contamination except $^{12}$C-$CO_2$ arising from the air and the negligible biotin addition.
Both runs of the SFA were performed for seven cycles. With an average growth rate $\mu$ of 0.33 1/h and an average final $OD_{600}$ of 3.07 (data shown relates to the first run of the SFA), seven cycles of serial fermentation time correspond to 121.5 hours of cultivation time or virtually 66 generations of *S. stipitis*. Since a similar approach was not tried

before, it was unclear in advance, if 1 cycles of serial fermentation would be too few for a complete $^{13}$C-ER or would already constitute an unnecessary excess of cultivation time. Among the 127 metabolites for which an $^{13}$C-ER could be calculated, 18 metabolites never showed any $^{13}$C-ER. These metabolites are mostly fatty acids, which are known to give insufficient signals with the LC-ESI/MS method applied. An appropriate measurement of fatty acids using LC/ESI-MS requires additional derivatization steps [58]. 71 metabolites were already labelled to 100 % with $^{13}$C after cycle 0 (~17 hours cultivation time). It should be kept in mind, that for these 89 metabolites in total, the corresponding $^{12}$C- or $^{13}$C-signal, respectively, could not be detected or was excluded due to high blankloading. These findings are masked by the errors of the methodology – they do not represent the actual $^{13}$C-ER but at least indicate the tendency. However, it was shown that in total 85 out of 127 metabolites revealed a $^{13}$C-ER greater than 90 % over all cycles.
Although for most of the metabolites the highest isotopological fraction $m+_{max}$ constituted more than 80 %, for several metabolites still a certain amount of $^{13}$C remains in isotopological fractions below $m+_{max}$. This demonstrates, that even with the application of the SFA a specific amount of valuable $^{13}$C-labelled glucose substrate is lost, as for internal standardization fully $^{13}$C-labelled metabolites are preferred. In future studies it should be investigated how lower isotopological fractions, especially $m+_{max-1}$ (compare with Table 32 in the supplemental), can be $^{13}$C-enriched completely to $m+_{max}$, since overcoming this issue could help to decrease the production costs of SIL internal standards.
26 metabolites (24 for the experiment without addition of $^{13}$C-$Na_2CO_3$) showed a constant labelling between 0 % and 100 % during all 7 cycles of serial fermentation. This result illustrates, that the SFA constitutes a tool, which is rather useful for labelling specific conserved metabolite pools than the majority of metabolites. This is in concordance with the findings of Mashego et al. Although they used a short labelling time of 4 h (121.5 h in total for 7 cycles of the SFA) they demonstrated that already 80 % of investigated metabolites were entirely $^{13}$C-labelled after this time. Furthermore, they speculated that the fractions of unlabelled metabolites that remained, originated from mobilized unlabelled storage sugars like glycogen or trehalose [43]. Metabolites that showed an increase of their $^{13}$C-ER over time will be discussed in the following.

### Increasing $^{13}$C-ER of vitamins with rising number of fermentation cycles

The most striking effect in the $^{13}$C-ER depending on the number of serial fermentation cycles was found for four phophatidylinositols (PI 34:1, PI 34:2, PI 36:3 and PI 36:4). In all experiments the $^{13}$C-ER of PIs increased drastically from 0 to 100 % within two cycles. As described in Section 4.4.4, this is also underpinned by the data of partial labelling: In the beginning, at cycle 0 only the fatty acid tails of PIs are completely $^{13}$C-labelled. Though, with increasing number of cycles and the resulting longer cultivation time, the attached inositol head group (compare with Figure 28, (a)) is successively labelled. PIs

represent a family of minority acidic phospholipids present in the cell membranes, where they act as key regulators of several cellular processes [59, 60]. They constitute key membrane signals responsible for activating and regulating intrinsic membrane proteins and serve as loose anchor points for peripheral membrane proteins [59, 61].

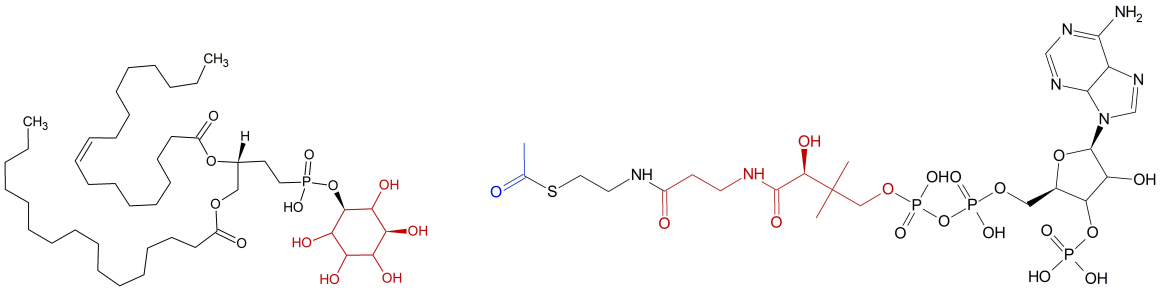

(a) PI 34:1 (b) Acetyl-CoA

**Figure 28:** Structural formula of PI and acetyl-CoA, respectively. Inositol and pantothenic acid are depicted in red. Acetyl group is depicted in blue.

Inositol (vitamin B8) itself, constitutes, beside its role in phophatidylinositols, an important growth factor for several micro organisms [62].
Further on, it was possible to increase the $^{13}$C-labelling of pantothenic acid from an initial $^{13}$C-ER of about 50 % to virtually 100 % until cycle 3. The partial labelling states this result, since a substantial shift from lower isotopological fractions to higher ones within 3 cycles of serial fermentation was observed (compare with Figure 26). Since pantothenic acid is a major constituent of Acetyl-CoA (see Figure 28, (b)), this observation is also validated by the partial labelling pattern of Acetyl-CoA (see Section 4.4.4). Pantothenic acid, commonly known as vitamin B5, serves in the metabolism as essential precursor for coenzyme A (CoA) and as acyl carrier protein (ACP). CoA and ACP, in turn, function as carriers of acyl groups and activators of carbonyl groups in a broad range of pathways, e.g. the TCA and the metabolism of fatty acids. While acyl CoA constitutes an essential cofactor for at least 100 enzymes, ACP is one of several componentes of the multienzyme complex fatty acid synthase [63].
The third vitamin investigated was niacin (vitamin B3). In contrast to the other examined vitamins, niacin was already $^{13}$C-labelled entirely from the beginning. Other fractions than the maximum isotopological fraction $m+_{max}$ were not found. Thus, application of the SFA for $^{13}$C-labelling niacin is, by considering these results, not necessary.

The gradually $^{13}$C-labelling of vitamins proofs the concept of serial fermentation: A substitution of vitamins by SMYE enabled a virtually complete $^{13}$C-ER of observed vitamins which are synthesized by *S. stipitis*. However, to achieve this, serial fermentation over several cycles, each with an appropriate cultivation time, for diluting out remaining $^{12}$C-components, is indispensable. Nevertheless, in future studies the LC-ESI/MS methodology should be adapted in order to investigate the $^{13}$C-ER of other essential vitamins like thiamine or pyridoxine.

**Further metabolites where the SFA influenced the $^{13}$C-ER**

In all three experiments, the $^{13}$C-ER of the sugars mannitol or sorbitol (not distinguishable by mass) could be slightly increased (~10 %) until cycle 3. Both metabolites are known to be produced by yeasts under environmental stressful conditions, such as heat or salt [64, 65]. Lysine and succinic acid, both components of the TCA, as well as acetylglycine also showed an increase in the $^{13}$C-ER during cycles 0 to 3, but independent from the addition of $^{13}$C-$Na_2Co_3$ (see Section 5.4.2). A few metabolites showed a significant decrease of the $^{13}$C-ER between cycles 0 and 3 (mevalonic acid and histidinol) or cycles 3 and 7 (deoxyuridine, succinic acid and acetylglycine). Beside the incomplete purity of the applied $^{13}$C-labelled glucose substrate (≥ 99 %) and the twofold spiking of 20 µL of TE solution in the second run of the SFA, any further sources of $^{12}$C-contamination (air, media) can be excluded. A $^{12}$C-contamination by natural $CO_2$ proportion occurring in the air (~0.04 %) of the flasks can be rejected, since an effect would have been observed in the experiments with addition of $^{13}$C-$Na_2CO_3$. A study of the partial labelling patterns of mentioned metabolites could contribute to find an explanation for this issue. In contrast, found effects for ascorbic acid and cytidine diphosphate are more likely false positive. They are caused by the comparatively bad quality of LC-ESI/MS analysis and the resulting bad reproducibility of replicates, as indicated by the high RSEs of underlying data.
However, as indicated by the findings, it turned out that three cycles of serial fermentation (~28 generations) are sufficient for labelling the majority of metabolites. A further benefit of four additional cycles of serial fermentation could not be observed.

### 5.4.2 No observable effects with $^{13}$C-$Na_2CO_3$

The hypothesis was, that the addition of $^{13}$C-labelled $Na_2CO_3$ to the culture medium would support the $^{13}$C-ER of metabolites of the $CO_2$-consuming pathways. In order to investigate this assumption, in two experiments of the second run of the SFA 0.1 or 1 g/L of $^{13}$C-$Na_2CO_3$ were supplemented to the cultivation medium.
There was no significant effect observed in the $^{13}$C-ER of metabolites (succinic acid, acetylglycine and lysine) of $CO_2$-consuming pathways (compare metabolites of Figures 22 to 24). On the contrary, for lysine the $^{13}$C-ER even decreased until cycle 3 in the experiment with addition of 1 g/L $Na_2CO_3$. A comparison between the experiments with addition of $^{12}$C-$Na_2CO_3$ and $^{13}$C-$Na_2CO_3$ also did not indicate a benefit of $^{13}$C-$Na_2Co_3$ addition. For a deeper insight, the partial labelling of metabolites of three $CO_2$-consuming pathways (TCA, purine and pyrimidine biosynthesis) was examined. With respect to the comparatively low quality of the LC-ESI/MS measurement, no substantial difference between the partial labelling patterns of the experiments with or without addition of 1 g/L $^{13}$C-$Na_2Co_3$ was investigated (compare with Table 32 in the appendix).
In summary, it can ascertained that the supplementary addition of $^{13}$C-$Na_2CO_3$ does not give any beneficial effect to the limited quality of the $^{13}$C-ER of internal standards.

# 6 Conclusion

In this master thesis a protocol for the production of SIL internal standards by *in vivo* labelling of yeast has been successfully established. It was demonstrated, that the SFA constitutes a tool particularly suitable for labelling metabolite pools like vitamins or storage sugars. In comparison to the current production method for internal standards (cycle 0) no adverse effects regarding the quality were observed. Especially the successive labelling of inositol and pantothenic acid demonstrate the necessity of serial fermentation for at least three cycles. In contrast, no benefits of the supplemental addition of $^{13}C$-$Na_2CO_3$ could be observed. Furthermore, divalent salts and ions, which are known to impede the ionization efficiency of the MS, could be successfully reduced to a minimum by introducing an additional washing step during the sample preparation. The validity of results was limited by the rather poor quality of the LC-ESI/MS measurement. It remains to be clarified, if observed decreases in the $^{13}C$-enrichment were caused by the established protocol itself or if they reflect solely the comparatively low quality of the LC-ESI/MS measurement.

# 7 Supplemental material

## 7.1 Digital supplemental material

In addition to the two supplementary tables in this section, three supplementary excel files are added to this master thesis. The file `supplemental material_preliminary studies` includes all $OD_{600}$ measurement series for determination of the growth rate of the preliminary experiments for improving the medium composition, the preliminary studies for the SFA, as well as the monitoring during the implementation of the SFA. The excel sheet `supplemental material_data processing` contains the LC-ES-MS raw data and results regarding the data processing. In the file `supplemental material_LCMS` all final results corresponding to the metabolome study can be found.

## 7.2 Supplementary tables

**Table 31:** Complete list of the $^{13}$C-ER depending on the number of fermentation cycles of all metabolites. Grey marks represent metabolites for which effects over number of fermentation cycles were found. The quoted uncertainty corresponds to the standard deviation.

| Metabolite name | $^{13}$C-ER as a function of fermentation cycles [%] $^{13}$C-$Na_2CO_3$ addition | | |
|---|---|---|---|
| | – | 0.1 g/L | 1 g/L |
| 1,5-Anhydrosorbitol | 42.36 ± 6.796 | 51.53 ± 5.652 | 49.3 ± 4.902 |
| 2.3-Bisphosphoglyceric acid | 100.00$^{a}$ ± 0.000 | 100.00$^{a}$ ± 0.000 | 100.00$^{a}$ ± 0.000 |
| 2'-IMP (Inosine 2'-phosphate) | 100.00$^{a}$ ± 0.000 | 100.00$^{a}$ ± 0.000 | 100.00$^{a}$ ± 0.000 |
| 2-Isopropylmalic acid | 99.67 ± 0.149 | 99.58 ± 0.262 | 99.64 ± 0.143 |
| 2-Oxovaleric acid, Oxoisovaleric acid | 100.00$^{a}$ ± 0.000 | 100.00$^{a}$ ± 0.000 | 100.00$^{a}$ ± 0.000 |
| 3-Hydroxyphenylacetic acid | 100.00$^{a}$ ± 0.000 | 100.00$^{a}$ ± 0.000 | 100.00$^{a}$ ± 0.000 |
| 3-Methyl-2-oxovaleric acid | 4.49 ± 0.389 | 3.85 ± 0.297 | 5.24 ± 0.672 |
| 3-Phosphoglyceric acid | 100.00$^{c}$ ± 0.000 | 100.00$^{c}$ ± 0.000 | 100.00$^{c}$ ± 0.000 |
| 4-Hydroxy-benzoic acid | 0.00$^{b}$ ± 0.000 | 0.00$^{b}$ ± 0.000 | 0.00$^{b}$ ± 0.000 |
| 4-Hydroxyproline | 100.00$^{a}$ ± 0.000 | 100.00$^{a}$ ± 0.000 | 100.00$^{a}$ ± 0.000 |
| 5,10-Methenyl-tetrahydrofolic acid | 100.00$^{a}$ ± 0.000 | 100.00$^{a}$ ± 0.000 | 100.00$^{a}$ ± 0.000 |
| 6-Phosphogluconic acid | 100.00$^{a}$ ± 0.000 | 100.00$^{a}$ ± 0.000 | 100.00$^{a}$ ± 0.000 |
| 6-Phosphoglucono-D-lactone | 100.00$^{a}$ ± 0.000 | 100.00$^{a}$ ± 0.000 | 100.00$^{a}$ ± 0.000 |
| Acetolactic acid | 100.00$^{a}$ ± 0.000 | 100.00$^{a}$ ± 0.000 | 100.00$^{a}$ ± 0.000 |
| Acetyl-CoA | 100.00$^{a}$ ± 0.000 | 100.00$^{a}$ ± 0.000 | 100.00$^{a}$ ± 0.000 |
| Acetylglycine | effect | effect | effect |
| Acetyllysine | 100.00$^{a}$ ± 0.000 | 100.00$^{a}$ ± 0.000 | 100.00$^{a}$ ± 0.000 |
| Acetylphosphate | 100.00$^{a}$ ± 0.000 | 100.00$^{a}$ ± 0.000 | 100.00$^{a}$ ± 0.000 |
| Adenine | 100.00$^{c}$ ± 0.000 | 100.00$^{c}$ ± 0.000 | 100.00$^{c}$ ± 0.000 |
| Adenosylhomocysteine | 100.00$^{a}$ ± 0.000 | 100.00$^{a}$ ± 0.000 | 100.00$^{a}$ ± 0.000 |
| ADP | 100.00$^{c}$ ± 0.000 | 100.00$^{c}$ ± 0.000 | 100.00$^{c}$ ± 0.000 |
| Allantoin | 0.00$^{b}$ ± 0.000 | 0.00$^{b}$ ± 0.000 | 0.00$^{b}$ ± 0.000 |
| Aminoadipic acid | 100.00$^{a}$ ± 0.000 | 100.00$^{a}$ ± 0.000 | 100.00$^{a}$ ± 0.000 |
| AMP | 100.00$^{c}$ ± 0.000 | 100.00$^{c}$ ± 0.000 | 100.00$^{c}$ ± 0.000 |
| Ampicillin | 0.00$^{b}$ ± 0.000 | 0.00$^{b}$ ± 0.000 | 0.00$^{b}$ ± 0.000 |
| Arginine | 100.00$^{a}$ ± 0.000 | 100.00$^{a}$ ± 0.000 | 100.00$^{a}$ ± 0.000 |
| Ascorbic acid | effect | 48.88 ± 10.108 | 47.94 ± 6.7 |
| Asparagine | 100.00$^{a}$ ± 0.000 | 100.00$^{a}$ ± 0.000 | 100.00$^{a}$ ± 0.000 |
| Aspartic acid | 99.36 ± 0.694 | 99.71 ± 0.193 | 99.87 ± 0.11 |
| ATP | 100.00$^{a}$ ± 0.000 | 100.00$^{a}$ ± 0.000 | 100.00$^{a}$ ± 0.000 |
| CDP | excluded | 90.72 ± 12.572 | effect |
| CDP-Ethanolamine | 100.00$^{a}$ ± 0.000 | 100.00$^{a}$ ± 0.000 | 100.00$^{a}$ ± 0.000 |
| Citraconic acid | 100.00$^{c}$ ± 0.000 | 100.00$^{c}$ ± 0.000 | 100.00$^{c}$ ± 0.000 |
| Citramalic acid | 100.00$^{c}$ ± 0.000 | 100.00$^{c}$ ± 0.000 | 100.00$^{c}$ ± 0.000 |
| Citric acid / Isocitric acid | 100.00$^{c}$ ± 0.000 | 100.00$^{c}$ ± 0.000 | 100.00$^{c}$ ± 0.000 |
| Citrulline | 100.00$^{c}$ ± 0.000 | 100.00$^{c}$ ± 0.000 | 100.00$^{c}$ ± 0.000 |

| | | | |
|---|---|---|---|
| Coenzyme A | excluded | excluded | 100.00[a] ± 0.000 |
| CTP | 100.00[a] ± 0.000 | 100.00[a] ± 0.000 | 100.00[a] ± 0.000 |
| Deoxyinosine | 0.00[b] ± 0.000 | 0.00[b] ± 0.000 | 0.00[b] ± 0.000 |
| Deoxyuridine | 28.23 ± 1.872 | 27.76 ± 7.103 | effect |
| diFA C12:0 (Dodecanedioic acid) | 100.00[c] ± 0.000 | 100.00[c] ± 0.000 | 100.00[c] ± 0.000 |
| Dihydroorotic acid | 100.00[a] ± 0.000 | 100.00[a] ± 0.000 | 100.00[a] ± 0.000 |
| dTDP | 100.00[a] ± 0.000 | 100.00[a] ± 0.000 | 100.00[a] ± 0.000 |
| FAD | 100.00[a] ± 0.000 | 100.00[a] ± 0.000 | 100.00[a] ± 0.000 |
| FFA C12:1 (Lauroleic acid) | 0.00[c] ± 0.000 | 0.00[c] ± 0.000 | 0.00[c] ± 0.000 |
| FFA C12:2 (Dodecadienoic acid) | 0.00[c] ± 0.000 | 0.00[c] ± 0.000 | 0.00[c] ± 0.000 |
| FFA C13:1 (Tridecenoic acid) | 0.00[c] ± 0.000 | 0.00[c] ± 0.000 | 0.00[c] ± 0.000 |
| FFA C13:2 (Tridecadienoic acid) | 0.00[c] ± 0.000 | 0.00[c] ± 0.000 | 0.00[c] ± 0.000 |
| FFA C14:0 (Myristic acid) | 0.00[b] ± 0.000 | 0.00[b] ± 0.000 | 0.00[b] ± 0.000 |
| FFA C14:3 (Tetradecatrienoic acid) | 10.49 ± 2.451 | 9.11 ± 1.472 | 11.05 ± 2.67 |
| FFA C15:2 (Pentadedienoic acid) | 4.12 ± 0.708 | 4.65 ± 0.913 | 4.57 ± 1.099 |
| FFA C16:0 (Palmitic acid) | 0.00[b] ± 0.000 | 0.00[b] ± 0.000 | 0.00[b] ± 0.000 |
| FFA C16:2 (Palmitolinoleic acid) | 10.02 ± 1.481 | 11.6 ± 2.213 | 10.68 ± 2.187 |
| FFA C16:3 (Hiragonic acid) | 14.60 ± 1.556 | 9.81 ± 0.893 | 14.05 ± 1.821 |
| FFA C18:0 (Stearic acid) | 0.00[b] ± 0.000 | 0.00[b] ± 0.000 | 0.00[b] ± 0.000 |
| FFA C18:1 (Oleic acid) | 100.00[c] ± 0.000 | 100.00[c] ± 0.000 | 100.00[c] ± 0.000 |
| FFA C5:0 (Valeric acid) | 100.00[a] ± 0.000 | 100.00[a] ± 0.000 | 100.00[a] ± 0.000 |
| FFA C7:0 (Heptylic acid) | 0.00[b] ± 0.000 | 0.00[b] ± 0.000 | 0.00[b] ± 0.000 |
| FFA C9:0 (Pelargonic acid) | 0.00[b] ± 0.000 | 0.00[b] ± 0.000 | 0.00[b] ± 0.000 |
| Fructose 1.6-bisphosphate | 100.00[a] ± 0.000 | 100.00[a] ± 0.000 | 100.00[a] ± 0.000 |
| Fumaric acid | 100.00[c] ± 0.000 | 100.00[c] ± 0.000 | 100.00[c] ± 0.000 |
| GDP | 100.00[a] ± 0.000 | 100.00[a] ± 0.000 | 100.00[a] ± 0.000 |
| Gluconic acid | 87.46 ± 9.274 | 89.92 ± 9.93 | 90.36 ± 10.648 |
| Glutamic acid | 99.98 ± 0.009 | 99.97 ± 0.009 | 99.98 ± 0.005 |
| Glutamine | 100.00[c] ± 0.000 | 100.00[c] ± 0.000 | 100.00[c] ± 0.000 |
| Glutathione | 100.00[a] ± 0.000 | 100.00[a] ± 0.000 | 100.00[a] ± 0.000 |
| Glyceric acid | 100.00[a] ± 0.000 | 100.00[a] ± 0.000 | 100.00[a] ± 0.000 |
| Glycine | 5.09 ± 0.99 | 9.67 ± 1.495 | 9.05 ± 2.102 |
| Glyoxilic acid | 100.00[c] ± 0.000 | 100.00[c] ± 0.000 | 100.00[c] ± 0.000 |
| GMP | 100.00[a] ± 0.000 | 100.00[a] ± 0.000 | 100.00[a] ± 0.000 |
| GTP | 100.00[a] ± 0.000 | 100.00[a] ± 0.000 | 100.00[a] ± 0.000 |
| Guanine | 100.00[a] ± 0.000 | 100.00[a] ± 0.000 | 100.00[a] ± 0.000 |
| Guanosine | 100.00[a] ± 0.000 | 100.00[a] ± 0.000 | 100.00[a] ± 0.000 |
| Hexose mono-phosphate | 100.00[a] ± 0.000 | 100.00[a] ± 0.000 | 100.00[a] ± 0.000 |
| Histidine | 12.71 ± 2.191 | 18.98 ± 4.154 | 20.40 ± 1.239 |
| Histidinol | effect | effect | 77.97 ± 4.128 |
| Homocysteine | 69.27 ± 2.738 | 70.24 ± 5.945 | 69.65 ± 5.199 |
| Hypoxanthine | 100.00[a] ± 0.000 | 100.00[a] ± 0.000 | 100.00[a] ± 0.000 |
| Indole-3-carboxylic acid | 100.00[a] ± 0.000 | 100.00[a] ± 0.000 | 100.00[a] ± 0.000 |
| Inosine | 100.00[a] ± 0.000 | 100.00[a] ± 0.000 | 100.00[a] ± 0.000 |
| Leucine, Isoleucine | 98.42 ± 0.663 | 98.30 ± 0.809 | 98.54 ± 0.688 |
| Lysine | effect | effect | effect |
| Malic acid | 100.00[c] ± 0.000 | 100.00[c] ± 0.000 | 100.00[c] ± 0.000 |
| Mannitol, Sorbitol | effect | effect | effect |
| Methionine | 99.71 ± 0.357 | 99.38 ± 0.999 | 99.81 ± 0.233 |
| Mevalonic acid | 95.09 ± 3.625 | effect | 96.96 ± 1.084 |
| N-Acetyl-glutamic acid | 100.00[a] ± 0.000 | 100.00[a] ± 0.000 | 100.00[a] ± 0.000 |
| N-acetyl-glutamine | 0.00[b] ± 0.000 | 0.00[b] ± 0.000 | 0.00[b] ± 0.000 |
| N-acetyl-l-ornithine | 100.00[a] ± 0.000 | 100.00[a] ± 0.000 | 100.00[a] ± 0.000 |
| NAD+ | 100.00[a] ± 0.000 | 100.00[a] ± 0.000 | 100.00[a] ± 0.000 |
| NADH | 100.00[a] ± 0.000 | 100.00[a] ± 0.000 | 100.00[a] ± 0.000 |
| NADP+ | 100.00[a] ± 0.000 | 100.00[a] ± 0.000 | 100.00[a] ± 0.000 |
| NADPH | 100.00[a] ± 0.000 | 100.00[a] ± 0.000 | 100.00[a] ± 0.000 |
| Ornithine | 100.00[a] ± 0.000 | 100.00[a] ± 0.000 | 100.00[a] ± 0.000 |
| Orotic acid | 100.00[c] ± 0.000 | 100.00[c] ± 0.000 | 100.00[c] ± 0.000 |
| Oxalic acid | 0.00[b] ± 0.000 | 0.00[b] ± 0.000 | 0.00[b] ± 0.000 |
| Oxidized-glutathione | 100.00[a] ± 0.000 | 100.00[a] ± 0.000 | 100.00[a] ± 0.000 |
| p-Aminobenzoic acid | 0.09 ± 0.015 | 0.06 ± 0.015 | 0.07 ± 0.014 |
| Pantothenic acid | effect | effect | effect |
| Pentose | excluded | 94.63 ± 4.286 | 95.04 ± 4.412 |
| Phenylalanine | 98.14 ± 1.38 | 98.49 ± 1.353 | 98.42 ± 1.058 |
| Phenylpyruvic acid | 0.00[c] ± 0.000 | 0.00[c] ± 0.000 | 0.00[c] ± 0.000 |
| Phosphoenolpyruvic acid | 100.00[c] ± 0.000 | 100.00[c] ± 0.000 | 100.00[c] ± 0.000 |
| Phosphoribosyl pyrophosphate | 100.00[a] ± 0.000 | 100.00[a] ± 0.000 | 100.00[a] ± 0.000 |
| Phthalic acid | 0.00[b] ± 0.000 | 0.00[b] ± 0.000 | 0.00[b] ± 0.000 |
| PI 34:1 | effect | effect | effect |
| PI 34:2 | effect | effect | effect |

| | | | |
|---|---|---|---|
| PI 36:3 | effect | effect | effect |
| PI 36:4 | effect | effect | effect |
| Proline | 96.80 ± 1.588 | 97.29 ± 1.376 | 96.30 ± 1.508 |
| Pyroglutamic acid | 95.85 ± 3.173 | 94.96 ± 3.423 | 95.85 ± 2.03 |
| Sedoheptulose 7-phosphate | 100.00[a] ± 0.000 | 100.00[a] ± 0.000 | 100.00[a] ± 0.000 |
| Sedoheptulose-1-7-bisphosphate | 100.00[c] ± 0.000 | 100.00[c] ± 0.000 | 100.00[c] ± 0.000 |
| Serine | 100.00[a] ± 0.000 | 100.00[a] ± 0.000 | 100.00[a] ± 0.000 |
| Succinic acid | effect | effect | effect |
| Threonine, Homoserine | 100.00[a] ± 0.000 | 100.00[a] ± 0.000 | 100.00[a] ± 0.000 |
| TMP | 100.00[a] ± 0.000 | 100.00[a] ± 0.000 | 100.00[a] ± 0.000 |
| Trehalose | effect | effect | effect |
| Trehalose 6 phosphate | 100.00[a] ± 0.000 | 100.00[a] ± 0.000 | 100.00[a] ± 0.000 |
| Tyrosine | 98.53 ± 0.861 | 98.79 ± 0.847 | 98.88 ± 1.056 |
| UDP | 100.00[a] ± 0.000 | 100.00[a] ± 0.000 | 100.00[a] ± 0.000 |
| UDP-D-Glucose | 100.00[a] ± 0.000 | 100.00[a] ± 0.000 | 100.00[a] ± 0.000 |
| UDP-N-acetyl-glucosamine | 100.00[a] ± 0.000 | 100.00[a] ± 0.000 | 100.00[a] ± 0.000 |
| Uridine | 98.67 ± 0.879 | 98.60 ± 1.409 | 98.80 ± 1.225 |
| Uridine monophosphate (UMP) | 100.00[c] ± 0.000 | 100.00[c] ± 0.000 | 100.00[c] ± 0.000 |
| UTP | 100.00[a] ± 0.000 | 100.00[a] ± 0.000 | 100.00[a] ± 0.000 |
| Valerenic acid | 0.00[c] ± 0.000 | 0.00[c] ± 0.000 | 0.00[c] ± 0.000 |
| Valine | 99.62 ± 0.201 | 99.67 ± 0.169 | 99.77 ± 0.155 |

[a] No $^{12}$C-signal. [b] No $^{13}$C-signal. [c] Blankload too high.

**Table 32:** Partial labelling of selected metabolites over all cycles of the serial fermentation approach. Only masses where signals were found are presented. Note that for fumaric, malic and succinic acid, the fraction with zero C-atoms labelled was excluded from the calculation of partial labelling (marked in grey). Furthermore, the mass m+01 of lysine is known to be a fake signals from previous studies on the I.B.B. [30].

| | | | Fraction of isotopologue [%] | | | | | |
|---|---|---|---|---|---|---|---|---|
| Metabolite | C-atoms | m/z | Experiment 1 g/L | | | Experiment -g/L | | |
| name | labelled | $[\frac{kg}{C}]$ | Cycle 0 | Cycle 3 | Cycle 7 | Cycle 0 | Cycle 3 | Cycle 7 |
| Acetyl-CoA | m+11 | 819.16 | 3.79 | 0.00 | 0.00 | 6.75 | 0.00 | 0.00 |
| Acetyl-CoA | m+12 | 820.16 | 36.34 | 0.00 | 0.00 | 36.43 | 0.00 | 0.00 |
| Acetyl-CoA | m+13 | 821.16 | 6.09 | 0.00 | 0.00 | 7.34 | 0.00 | 0.00 |
| Acetyl-CoA | m+14 | 822.17 | 14.38 | 0.00 | 0.00 | 15.49 | 0.00 | 0.00 |
| Acetyl-CoA | m+20 | 828.19 | 4.99 | 20.47 | 14.27 | 5.58 | 16.88 | 17.15 |
| Acetyl-CoA | m+21 | 829.19 | 23.65 | 42.87 | 51.47 | 18.21 | 37.04 | 49.18 |
| Acetyl-CoA | m+22 | 830.19 | 2.15 | 13.03 | 9.00 | 2.81 | 15.35 | 9.79 |
| Acetyl-CoA | m+23 | 831.20 | 8.59 | 23.64 | 25.25 | 7.40 | 30.73 | 23.89 |
| AMP | m+00 | 346.06 | 1.22 | 0.10 | 0.99 | 0.39 | 2.33 | 0.18 |
| AMP | m+08 | 354.08 | 0.41 | 0.95 | 0.38 | 0.80 | 2.04 | 0.63 |
| AMP | m+09 | 355.09 | 9.69 | 19.95 | 9.05 | 14.81 | 24.30 | 12.78 |
| AMP | m+10 | 356.09 | 88.67 | 78.99 | 89.58 | 84.00 | 71.32 | 86.42 |
| Aspartic acid | m+00 | 132.03 | 0.06 | 0.26 | 0.15 | 0.60 | 1.05 | 0.30 |
| Aspartic acid | m+01 | 133.03 | 0.10 | 0.04 | 0.12 | 0.20 | 0.03 | 0.10 |
| Aspartic acid | m+02 | 134.04 | 1.72 | 0.72 | 1.68 | 1.83 | 0.39 | 1.54 |
| Aspartic acid | m+03 | 135.04 | 3.26 | 9.63 | 3.90 | 3.88 | 4.87 | 3.44 |
| Aspartic acid | m+04 | 136.04 | 94.86 | 89.35 | 94.16 | 93.49 | 93.65 | 94.63 |
| Fumaric acid | m+00 | 115.00 | 31.84 | 59.96 | 42.24 | 28.65 | 43.10 | 29.49 |
| Fumaric acid | m+01 | 116.01 | 4.16 | 5.71 | 4.62 | 4.43 | 3.52 | 3.39 |
| Fumaric acid | m+02 | 117.01 | 14.44 | 1.15 | 10.65 | 16.57 | 0.00 | 11.97 |
| Fumaric acid | m+03 | 118.01 | 2.08 | 8.10 | 3.12 | 2.11 | 5.47 | 2.36 |
| Fumaric acid | m+04 | 119.02 | 79.32 | 85.04 | 81.61 | 76.89 | 91.00 | 82.29 |
| Glutamine | m+00 | 145.06 | 0.24 | 0.20 | 0.15 | 0.22 | 1.15 | 0.22 |
| Glutamine | m+01 | 146.07 | 0.23 | 0.16 | 0.11 | 0.30 | 0.43 | 0.11 |
| Glutamine | m+02 | 147.07 | 0.41 | 0.10 | 0.07 | 0.54 | 0.21 | 0.07 |
| Glutamine | m+03 | 148.07 | 0.21 | 0.19 | 0.53 | 0.23 | 0.21 | 0.22 |
| Glutamine | m+04 | 149.08 | 1.80 | 6.68 | 3.49 | 2.63 | 5.50 | 2.83 |
| Glutamine | m+05 | 150.08 | 97.11 | 92.68 | 95.64 | 96.08 | 92.49 | 96.54 |
| GMP | m+09 | 371.08 | 15.89 | 22.34 | 5.11 | 15.47 | 38.99 | 15.13 |
| GMP | m+10 | 372.08 | 84.11 | 77.66 | 94.89 | 84.53 | 61.01 | 84.87 |
| Histidine | m+00 | 154.06 | 80.54 | 76.48 | 76.32 | 84.88 | 87.88 | 84.45 |

| | | | | | | | | |
|---|---|---|---|---|---|---|---|---|
| Histidine | m+02 | 156.07 | 3.70 | 0.53 | 1.63 | 2.10 | 1.04 | 2.91 |
| Histidine | m+03 | 157.07 | 2.05 | 0.17 | 0.32 | 1.10 | 0.78 | 1.03 |
| Histidine | m+05 | 159.08 | 0.46 | 0.28 | 0.48 | 0.23 | 0.30 | 0.48 |
| Histidine | m+06 | 160.08 | 13.25 | 22.54 | 21.25 | 11.69 | 10.00 | 11.13 |
| IMP | m+09 | 356.07 | 10.79 | 19.15 | 9.76 | 17.50 | 28.38 | 12.07 |
| IMP | m+10 | 357.07 | 89.21 | 80.85 | 90.24 | 82.50 | 71.62 | 87.93 |
| Lysine | m+00 | 145.10 | 10.38 | 6.83 | 7.59 | 9.00 | 11.53 | 6.98 |
| Lysine | m+01 | 146.10 | 69.98 | 80.97 | 73.05 | 73.84 | 58.54 | 60.14 |
| Lysine | m+02 | 147.11 | 4.72 | 2.91 | 2.18 | 4.42 | 3.81 | 3.91 |
| Lysine | m+03 | 148.11 | 2.87 | 2.09 | 1.59 | 2.60 | 2.11 | 2.58 |
| Lysine | m+04 | 149.11 | 1.91 | 1.52 | 1.12 | 1.63 | 1.04 | 1.87 |
| Lysine | m+05 | 150.12 | 1.03 | 1.17 | 0.81 | 1.82 | 1.01 | 2.30 |
| Lysine | m+06 | 151.12 | 9.11 | 4.52 | 13.66 | 6.69 | 21.96 | 22.23 |
| Malic Acid | m+00 | 133.01 | 31.90 | 58.30 | 36.83 | 29.42 | 43.15 | 26.03 |
| Malic Acid | m+01 | 134.02 | 4.23 | 5.46 | 3.76 | 4.67 | 2.89 | 3.07 |
| Malic Acid | m+02 | 135.02 | 15.05 | 0.77 | 10.13 | 16.38 | 0.32 | 12.40 |
| Malic Acid | m+03 | 136.02 | 1.82 | 7.82 | 2.34 | 2.13 | 4.56 | 2.36 |
| Malic Acid | m+04 | 137.03 | 78.90 | 85.94 | 83.77 | 76.82 | 92.24 | 82.17 |
| NAD+ | m+14 | 676.15 | 0.28 | 0.00 | 0.09 | 2.15 | 0.00 | 0.03 |
| NAD+ | m+15 | 677.15 | 2.95 | 0.10 | 0.68 | 12.84 | 0.00 | 0.34 |
| NAD+ | m+16 | 678.16 | 0.11 | 0.00 | 0.00 | 0.84 | 0.00 | 0.10 |
| NAD+ | m+17 | 679.16 | 0.12 | 0.00 | 0.00 | 1.40 | 0.00 | 0.07 |
| NAD+ | m+18 | 680.16 | 4.86 | 0.36 | 1.52 | 14.07 | 0.11 | 0.83 |
| NAD+ | m+19 | 681.17 | 0.76 | 1.08 | 1.00 | 1.54 | 2.01 | 1.40 |
| NAD+ | m+20 | 682.17 | 9.71 | 18.13 | 11.89 | 10.00 | 23.55 | 14.52 |
| NAD+ | m+21 | 683.17 | 81.21 | 80.33 | 84.82 | 57.16 | 74.33 | 82.70 |
| Niacin | m+06 | 128.05 | 100.00 | 100.00 | 100.00 | 100.00 | 100.00 | 100.00 |
| Pantothenic acid | m+00 | 218.10 | 38.41 | 0.76 | 0.61 | 45.68 | 2.15 | 0.26 |
| Pantothenic acid | m+01 | 219.11 | 3.73 | 0.00 | 0.00 | 3.72 | 0.00 | 0.00 |
| Pantothenic acid | m+03 | 221.11 | 0.34 | 0.00 | 0.00 | 0.38 | 0.00 | 0.00 |
| Pantothenic acid | m+06 | 224.12 | 1.86 | 1.04 | 1.12 | 1.91 | 1.32 | 1.53 |
| Pantothenic acid | m+07 | 225.13 | 0.11 | 0.43 | 1.26 | 0.11 | 0.46 | 1.03 |
| Pantothenic acid | m+08 | 226.13 | 2.92 | 9.95 | 6.67 | 2.75 | 9.64 | 6.91 |
| Pantothenic acid | m+09 | 227.13 | 52.63 | 87.82 | 90.34 | 45.45 | 86.43 | 90.27 |
| PI 34:1 | m+37 | 872.66 | 100.00 | 0.00 | 0.00 | 100.00 | 0.00 | 0.00 |
| PI 34:1 | m+42 | 877.68 | 0.00 | 10.02 | 3.16 | 0.00 | 10.59 | 4.114 |
| PI 34:1 | m+43 | 878.68 | 0.00 | 89.98 | 96.84 | 0.00 | 89.41 | 95.89 |
| PI 34:2 | m+36 | 869.64 | 8.68 | 0.00 | 0.00 | 8.73 | 0.00 | 0.00 |
| PI 34:2 | m+37 | 870.64 | 83.95 | 0.00 | 2.01 | 83.67 | 0.00 | 0.00 |
| PI 34:2 | m+38 | 871.65 | 5.91 | 0.00 | 0.00 | 5.98 | 0.00 | 0.00 |
| PI 34:2 | m+39 | 872.65 | 1.46 | 0.00 | 9.15 | 1.63 | 0.00 | 0.00 |
| PI 34:2 | m+40 | 873.65 | 0.00 | 0.00 | 1.91 | 0.00 | 0.22 | 0.00 |
| PI 34:2 | m+41 | 874.66 | 0.00 | 2.21 | 26.50 | 0.00 | 3.64 | 4.05 |
| PI 34:2 | m+42 | 875.66 | 0.00 | 10.08 | 6.87 | 0.00 | 10.24 | 10.28 |
| PI 34:2 | m+43 | 876.66 | 0.00 | 87.71 | 53.56 | 0.00 | 85.90 | 85.67 |
| PI 36:3 | m+39 | 898.67 | 100.00 | 0.00 | 4.07 | 100.00 | 0.00 | 0.00 |
| PI 36:3 | m+43 | 902.68 | 0.00 | 0.00 | 25.90 | 0.00 | 3.05 | 0.00 |
| PI 36:3 | m+44 | 903.68 | 0.00 | 5.27 | 3.19 | 0.00 | 7.67 | 6.99 |
| PI 36:3 | m+45 | 904.69 | 0.00 | 94.73 | 66.83 | 0.00 | 89.27 | 93.01 |
| PI 36:4 | m+39 | 896.65 | 100.00 | 0.00 | 0.00 | 100.00 | 0.00 | 0.00 |
| PI 36:4 | m+45 | 902.67 | 0.00 | 100.00 | 100.00 | 0.00 | 0.00 | 100.00 |
| Proline | m+05 | 119.07 | 100.00 | 100.00 | 100.00 | 100.00 | 100.00 | 100.00 |
| Succinic acid | m+00 | 117.02 | 60.37 | 8.18 | 40.93 | 22.81 | 5.09 | 49.71 |
| Succinic acid | m+01 | 118.02 | 10.23 | 0.34 | 9.36 | 4.57 | 0.18 | 0.00 |
| Succinic acid | m+02 | 119.03 | 27.84 | 0.24 | 9.45 | 23.31 | 0.33 | 11.35 |
| Succinic acid | m+03 | 120.03 | 2.72 | 1.41 | 2.71 | 2.26 | 1.15 | 1.84 |
| Succinic acid | m+04 | 121.03 | 59.20 | 98.02 | 78.48 | 69.85 | 98.34 | 80.42 |
| UMP | m+00 | 323.03 | 12.56 | 13.72 | 5.76 | 11.60 | 16.68 | 6.26 |
| UMP | m+08 | 331.06 | 5.99 | 21.14 | 8.05 | 9.20 | 18.30 | 7.88 |
| UMP | m+09 | 332.06 | 81.45 | 65.14 | 86.18 | 79.22 | 65.02 | 85.86 |

Abbreviations: AMP, adenosine monophosphate; CoA, coenzyme A; GMP, guanosine monophosphate; IMP, inosine monophosphate; NAD+/NADH, nicotinamide adenine dinucleotide; UMP, uridine monophosphate; PA, pantothenic acid; PI, phosphatidylinositol.

# References


[1] A. H. Zhang, H. Sun, P. Wang, Y. Han, and X.-J. Wang, "Modern analytical techniques in metabolomics analysis," *The Analyst*, vol. 137, pp. 293 – 300, 2011.

[2] G. Harrigan and R. Goodacre, *Metabolic Profiling: Its Role in Biomarker Discovery and Gene Function Analysis*, vol. 17. Springer, 2002.

[3] S. G. Oliver, M. K. Winson, D. B. Kell, and F. Baganz, "Systematic functional analysis of the yeast genome," *Trends Biotechnol.*, vol. 16, no. 9, pp. 373 – 378, 1998.

[4] J. Förster, I. Famili, P. fu, B. Ø Palsson, and J. Nielsen, "Genome-scale reconstruction of the saccharomyces cerevisiae metabolic network," *Genome research*, vol. 13, pp. 244 – 53, 2003.

[5] O. Fiehn, "Metabolomics - the link between genotypes and phenotypes," *Plant Molecular Biology*, vol. 48, no. 1 - 2, pp. 155 – 171, 2002.

[6] W. B. Dunn and D. I. Ellis, "Metabolomics: Current analytical platforms and methodologies," *TrAC Trends in Analytical Chemistry*, vol. 24, no. 4, pp. 285 – 294, 2005.

[7] S. Putri, Y. Nakayama, F. Matsuda, T. Uchikata, S. Kobayashi, A. Matsubara, and E. Fukusaki, "Current metabolomics: Practical applications," *Journal of bioscience and bioengineering*, vol. 115, 2013.

[8] L. D. Roberts, A. L. Souza, R. E. Gerszten, and C. B. Clish, "Targeted metabolomics," *Current Protocols in Molecular Biology*, vol. 98, no. 1, pp. 30.2.1 – 30.2.24, 2012.

[9] J. C Lindon, J. Nicholson, E. Holmes, H. Antti, M. E Bollard, H. Keun, O. Beckonert, T. Ebbels, M. D Reily, D. Robertson, G. Stevens, P. Luke, A. P Breau, G. H Cantor, R. H Bible, U. Niederhauser, H. Senn, G. Schlotterbeck, U. G Sidelmann, and C. Thomas, "Contemporary issues in toxicology the role of metabonomics in toxicology and its evaluation by the comet project," *Toxicology and applied pharmacology*, pp. 137–46, 04 2003.

[10] S. Yang, M. Sadilek, and M. E Lidstrom, "Streamlined pentafluorophenylpropyl column liquid chromatography-tandem quadrupole mass spectrometry and global (13)c-labeled internal standards improve performance for quantitative metabolomics in bacteria," *Journal of chromatography. A*, vol. 1217, pp. 7401 – 10, 2010.

[11] S. J. Jol, A. Kümmel, M. Terzer, J. Stelling, and M. Heinemann, "System-level insights into yeast metabolism by thermodynamic analysis of elementary flux modes," *PLOS Computational Biology*, vol. 8, pp. 1–9, 03 2012.

[12] M. R. Mashego, K. Rumbold, M. De Mey, E. Vandamme, W. Soetaert, and J. J. Heijnen, "Microbial metabolomics: past, present and future methodologies," *BIOTECHNOLOGY LETTERS*, vol. 29, no. 1, pp. 1 – 16, 2007.

[13] R. Beger, "A review of applications of metabolomics in cancer," *Metabolites*, vol. 3, pp. 552 – 74, 2013.

[14] R. Hall, M. Beale, O. Fiehn, N. Hardy, L. Sumner, and R. Bino, "Plant metabolomics," *The Plant Cell*, vol. 14, no. 7, pp. 1437 – 1440, 2002.

[15] J. Hong, L. Yang, D. Zhang, and J. Shi, "Plant metabolomics: An indispensable system biology tool for plant science," *International Journal of Molecular Sciences*, vol. 17, no. 6, 2016.

[16] C. Birkemeyer, A. Luedemann, C. Wagner, A. Erban, and J. Kopka, "Metabolome analysis: The potential of in vivo labeling with stable isotopes for metabolite profiling," *Trends in biotechnology*, vol. 23, pp. 28 – 33, 2005.

[17] A. B. Canelas, C. Ras, A. ten Pierick, J. C. van Dam, J. J. Heijnen, and W. M. van Gulik, "Leakage-free rapid quenching technique for yeast metabolomics," *Metabolomics*, vol. 4, no. 3, 2008.

[18] A. Chokkathukalam, D.-H. Kim, M. Barrett, R. Breitling, and D. Creek, "Stable isotope-labeling studies in metabolomics: New insights into structure and dynamics of metabolic networks," *Bioanalysis*, vol. 6, pp. 511 – 24, 2014.

[19] G. J. Patti, O. Yanes, and G. Siuzdak, "Innovation: Metabolomics: the apogee of the omics trilogy," *Nat. Rev. Mol. Cell Biol.*, vol. 13, no. 4, pp. 263 – 269, 2012.

[20] M. Brown, W. B. Dunn, D. I. Ellis, R. Goodacre, J. Handl, J. D. Knowles, S. O'Hagan, I. Spasić, and D. B. Kell, "A metabolome pipeline: from concept to data to knowledge," *Metabolomics*, vol. 1, no. 1, pp. 39 – 51, 2005.

[21] A. A. Caudy, M. Mulleder, and M. Ralser, "Metabolomics in Yeast," *Cold Spring Harb Protoc*, vol. 2017, no. 9, p. pdb.top083576, 2017.

[22] J. Boccard, J.-L. Veuthey, and S. Rudaz, "Knowledge discovery in metabolomics: An overview of ms data handling," *Journal of Separation Science*, vol. 33, no. 3, pp. 290 – 304, 2009.

[23] A. Alonso, S. Marsal, and A. Julià, "Analytical methods in untargeted metabolomics: State of the art in 2015," *Frontiers in bioengineering and biotechnology*, vol. 3, p. 23, 2015.

[24] L. Wu, M. R. Mashego, J. C. van Dam, A. M. Proell, J. L. Vinke, C. Ras, W. A. van Winden, W. M. van Gulik, and J. J. Heijnen, "Quantitative analysis of the microbial metabolome by isotope dilution mass spectrometry using uniformly 13C-labeled cell extracts as internal standards," *Anal. Biochem.*, vol. 336, no. 2, pp. 164 – 171, 2005.

[25] C. Bueschl, R. Krska, B. Kluger, and R. Schuhmacher, "Isotopic labeling-assisted metabolomics using LC-MS," *Anal Bioanal Chem*, vol. 405, no. 1, pp. 27 – 33, 2013.

[26] C. A Crutchfield, W. Lu, E. Melamud, and J. D Rabinowitz, "Mass spectrometry-based metabolomics of yeast," *Methods in enzymology*, vol. 470, pp. 393 – 426, 2010.

[27] H. Faccin, C. VIANA, P. do Nascimento, D. Bohrer, and L. Carvalho, "Study of ion suppression for phenolic compounds in medicinal plant extracts using liquid chromatography electrospray tandem mass spectrometry," *Journal of Chromatography A*, vol. 1427, p. 111, 2016.

[28] Q. Liu, F. Jiang, J. Zhu, G.-p. Zhong, and M. Huang, "Development, validation and application of a new method to correct the nonlinearity problem in lc-ms/ms quantification using stable isotope labeled internal standards," *Analytical Chemistry*, 2019.

[29] W. Lu, M. F. Clasquin, E. Melamud, D. Amador-Noguez, A. A. Caudy, and J. D. Rabinowitz, "Metabolomic analysis via reversed-phase ion-pairing liquid chromatography coupled to a stand alone orbitrap mass spectrometer," *Analytical Chemistry*, vol. 82, no. 8, pp. 3212 – 3221, 2010.

[30] G. Trausinger, "Mass spectrometry based quantitative analysis of intracellular metabolites of yeasts converting xylose to ethanol.," *Master thesis*, 2015.

[31] M. Berg, M. Vanaerschot, A. Jankevics, B. Cuypers, R. Breitling, and J.-C. Dujardin, "Lc-ms metabolomics from study design to data-analysis – using a versatile pathogen as a test case," *Computational and structural biotechnology journal*, p. e201301002, 2013.

[32] S. Neubauer, C. Troyer, K. Klavins, H. Rußmayer, M. Steiger, B. Gasser, M. Sauer, D. Mattanovich, S. Hann, and G. Koellensperger, "U13c cell extract of pichia pastoris - a powerful tool for evaluation of sample preparation in metabolomics," *Journal of separation science*, vol. 35, 2012.

[33] F. Pinu, S. Villas-Bôas, and R. Aggio, "Analysis of intracellular metabolites from microorganisms: Quenching and extraction protocols," *Metabolites*, vol. 7, p. 53, 2017.

[34] C. Chassagnole, N. Noisommit-Rizzi, J. W. Schmid, K. Mauch, and M. Reuss, "Dynamic modeling of the central carbon metabolism of escherichia coli," *Biotechnology and Bioengineering*, vol. 79, no. 1, pp. 53 – 73, 2002.

[35] W. de Koning and K. van Dam, "A method for the determination of changes of glycolytic metabolites in yeast on a subsecond time scale using extraction at neutral ph," *Analytical biochemistry*, vol. 204, pp. 118 – 23, 1992.

[36] S. Villas-Bôas and P. Bruheim, "Cold glycerol-saline: The promising quenching solution for accurate intracellular metabolite analysis of microbial cells," *Analytical biochemistry*, vol. 370, pp. 87 – 97, 2007.

[37] C. J. Bolten, P. Kiefer, F. Letisse, J.-C. Portais, and C. Wittmann, "Sampling for metabolome analysis of microorganisms," *Analytical Chemistry*, vol. 79, no. 10, pp. 3843 – 3849, 2007.

[38] B. Gonzalez, J. Francois, and M. Renaud, "A rapid and reliable method for metabolite extraction in yeast using boiling buffered ethanol," *Yeast (Chichester, England)*, vol. 13, pp. 1347 – 55, 1997.

[39] S. G. Villas-Boas, J. H?jer-Pedersen, M. Akesson, J. Smedsgaard, and J. Nielsen, "Global metabolite analysis of yeast: evaluation of sample preparation methods," *Yeast*, vol. 22, no. 14, pp. 1155 – 1169, 2005.

[40] R. P. Maharjan and T. Ferenci, "Global metabolite analysis: the influence of extraction methodology on metabolome profiles of Escherichia coli," *Anal. Biochem.*, vol. 313, no. 1, pp. 145 – 154, 2003.

[41] J. D. Rabinowitz and E. Kimball, "Acidic acetonitrile for cellular metabolome extraction from Escherichia coli," *Anal. Chem.*, vol. 79, no. 16, pp. 6167 – 6173, 2007.

[42] E. Oliveira, E. Muller, F. Abad, J. Dallarosa, and C. Adriano, "Internal standard versus external standard calibration: an uncertainty case study of a liquid chromatography analysis," *Quimica Nova - QUIM NOVA*, vol. 33, 2010.

[43] M. R. Mashego, L. Wu, J. C. Van Dam, C. Ras, J. L. Vinke, W. A. Van Winden, W. M. Van Gulik, and J. J. Heijnen, "MIRACLE: mass isotopomer ratio analysis of U-13C-labeled extracts. A new method for accurate quantification of changes in concentrations of intracellular metabolites," *Biotechnol. Bioeng.*, vol. 85, no. 6, pp. 620 – 628, 2004.

[44] M. R. Antoniewicz, "Tandem mass spectrometry for measuring stable-isotope labeling," *Current Opinion in Biotechnology*, vol. 24, no. 1, pp. 48 – 53, 2013.

[45] G. Hermann, M. Schwaiger-Haber, P. Volejnik, and G. Koellensperger, ""13c-labelled yeast as internal standard for lc–ms/ms and lc high resolution ms based amino acid quantification in human plasma"," *"Journal of Pharmaceutical and Biomedical Analysis"*, vol. "155", pp. "329 – 334", "2018".

[46] M. Jeppsson, O. Bengtsson, K. Franke, H. Lee, B. Hahn-Hägerdal, and M. Gorwa-Grauslund, "The expression of a pichia stipitis xylose reductase mutant with higher km for nadph increases ethanol production from xylose in recombinant saccharomyces cerevisiae," *Biotechnology and bioengineering*, vol. 93, pp. 665 – 73, 2006.

[47] S. Saheki, A. Takeda, and T. Shimazu, "Assay of inorganic phosphate in the mild ph range, suitable for measurement of glycogen phosphorylase activity," *Analytical biochemistry*, vol. 148, pp. 277 – 81, 1985.

[48] G. Trausinger, C. Gruber, S. Krahulec, C. Magnes, B. Nidetzky, and M. Klimacek, "Identification of novel metabolic interactions controlling carbon flux from xylose to ethanol in natural and recombinant yeasts," *Biotechnology for Biofuels*, 2015.

[49] J. M. Buescher, S. Moco, U. Sauer, and N. Zamboni, "Ultrahigh performance liquid chromatography–tandem mass spectrometry method for fast and robust quantification of anionic and aromatic metabolites," *Analytical Chemistry*, vol. 82, no. 11, pp. 4403 – 4412, 2010.

[50] C. Kadakal, T. Duman, and R. Ekinci, "Thermal degradation kinetics of ascorbic acid, thiamine and riboflavin in rosehip (rosa canina l) nectar," *Ciencia e Tecnologia de Alimentos*, vol. 38, 2017.

[51] N. Muhamad, M. M. Yusoff, and J. Gimbun, "Thermal degradation kinetics of nicotinic acid, pantothenic acid and catechin derived from averrhoa bilimbi fruits," *RSC Adv.*, vol. 5, pp. 74132 – 74137, 2015.

[52] S. Navankasattusas and D. B. Lund, "Thermal destruction of vitamin b6 vitamers in buffer solution and cauliflower puree," *Journal of Food Science*, vol. 47, no. 5, pp. 1512 – 1518, 1982.

[53] T. M. Annesley, "Ion suppression in mass spectrometry," *Clinical Chemistry*, vol. 49, no. 7, pp. 1041 – 1044, 2003.

[54] M. Papini, I. Nookaew, M. Uhlén, and J. Nielsen, "Scheffersomyces stipitis: a comparative systems biology study with the crabtree positive yeast saccharomyces cerevisiae," *Microbial Cell Factories*, vol. 11, no. 1, p. 136, 2012.

[55] P. B. "Ottaway, *"Stability of vitamins in food"*, pp. "90 – 113". "Springer US", "1993".

[56] L. Tong, "Structure and function of biotin-dependent carboxylases," *Cellular and molecular life sciences : CMLS*, vol. 70, 2012.

[57] S. Zhang, I. Sanyal, G. Bulboaca, A. Rich, and D. Flint, "The gene for biotin synthase from saccharomyces cerevisiae: Cloning, sequencing, and complementation of escherichia coli strains lacking biotin synthase," *Archives of Biochemistry and Biophysics*, vol. 309, no. 1, pp. 29 – 35, 1994.

[58] W.-C. Yang, J. Adamec, and F. E. Regnier, "Enhancement of the lc/ms analysis of fatty acids through derivatization and stable isotope coding," *Analytical Chemistry*, vol. 79, no. 14, pp. 5150 – 5157, 2007.

[59] B. Falkenburger, J. Jensen, E. Dickson, B. Suh, and B. Hille, "Phosphoinositides: Lipid regulators of membrane proteins," *Journal of Physiology*, vol. 588, no. 17, pp. 3179 – 3185, 2010.

[60] G. Odorizzi, M. Babst, and S. D. Emr, "Phosphoinositide signaling and the regulation of membrane trafficking in yeast," *Trends in Biochemical Sciences*, vol. 25, no. 5, pp. 229 – 235, 2000.

[61] B. Hille, "Diversity of phosphoinositide signaling," *Biochemistry (Moscow) Supplement Series A: Membrane and Cell Biology*, vol. 6, no. 2, pp. 113 – 119, 2012.

[62] P. R. Burkholder, "Vitamin deficiencies in yeasts," *American Journal of Botany*, vol. 30, no. 3, pp. 206 – 211, 1943.

[63] G. F. Combs and J. P. McClung, "Chapter 16 - pantothenic acid," in *The Vitamins (Fifth Edition)*, pp. 387 – 398, Elsevier, 2017.

[64] Q. Liu, S.-H. Ying, M.-G. Feng, and X.-H. Jiang, "Physiological implication of intracellular trehalose and mannitol changes in response of entomopathogenic fungus beauveria bassiana to thermal stress," *Antonie van Leeuwenhoek*, vol. 95, no. 1, p. 65, 2008.

[65] J. R. Managbanag and A. P. Torzilli, "An analysis of trehalose, glycerol, and mannitol accumulation during heat and salt stress in a salt marsh isolate of aureobasidium pullulans," *Mycologia*, vol. 94, no. 3, pp. 384 – 391, 2002.